AEROSOL; CYCLE AND INFLUENCE ON THE RADIATION BALANCE

MEMORA: Measurement and Modeling of the reduction of Radiation by Aerosol

H.M. ten Brink et al.

AEROSOL; CYCLE AND INFLUENCE ON THE RADIATION BALANCE

also known as

MEMORA: MEasurement and MOdeling of the reduction of Radiation by Aerosol

Cluster-project in the Dutch National Research Program on
Global Air Pollution and Climate Change

COLLABORATING INSTITUTES

.Netherlands Energy Research Foundation ECN
H.M. ten Brink, A. Hensen, A. Khlystov
.Royal Netherlands Meteorological Institute, KNMI
R. van Dorland, A. Jeuken, P. van Velthoven
.University of Utrecht; Institute for Marine and Atmosphere Research IMAU
J. Lelieveld, A. van den Berg
.National Institute of Public Health and Environmental Protection, RIVM
D.P.J. Swart, J.B. Bergwerff, A. Apituley

Co-ordinator: H.M. ten Brink

Duration: 1996 - 1999

The contribution of J.P. Veefkind (FEL-TNO) to the work described in chapter 3 is gratefully acknowledged.

CONTENTS

SAMENVATTING

Deze Nederlandse samenvatting is algemeen van aard en bedoeld voor de minder ingewijde lezer. Het onderwerp wordt daarom ook ingeleid met een kort exposé over stralingsbalans stralingsforcering en aërosolen. Voor detaillering van aanpak en resultaten zij verwezen naar de Engelse samenvatting.

Inleiding in de "Stralingsforcering door aërosolen"

Klimaatverandering door menselijk ingrijpen is het centrale onderwerp binnen het NOP Climate-Change programma. Aan de basis van de klimaatverandering staat de verandering in de stralingsbalans van de aarde. Dit is de balans tussen inkomende zonnestraling en uitgaande aardse straling. Verandering in die balans heeft een verschil in temperatuur op aarde tot gevolg. Voor de verandering in de stralingsbalans gebruikt IPCC het begrip forcering (forcing). De forcering van de stralingsbalans door aërosoldeeltjes is zeer eenvoudig te begrijpen. Aërosolen weerkaatsen zonlicht, zodat de aarde minder licht ontvangt, wat tot afkoeling leidt. Aërosolen zijn zeer kleine deeltjes, die in de atmosfeer zweven. De meeste aërosolen reflecteren het zonlicht goed omdat de deeltjes dezelfde grootte afmeting hebben als de golflengte van het zonlicht. Roet absorbeert zonlicht, wat een lokaal verwarmend effect kan hebben.

Volgens IPCC is de stralingsforcering door aërosolen sterk negatief en compenseert hiermee een aanzienlijk deel van de positieve stralingsforcering door de toenemende concentraties broeikasgassen. Bovendien is de onzekerheid in de stralingsforcering door aërosolen veel groter dan die van alle broeikasgassen tezamen. Dit komt doordat de aërosolconcentratie over de aarde niet bekend is. De relatief korte verblijftijd in de lucht heeft tot gevolg dat de deeltjes slechts over afstanden van enkele duizenden kilometers worden verspreid. De forcering door aërosolen is derhalve een typisch regionaal verschijnsel. IPCC schat dat in Europa de negatieve stralings-forcering door de aërosolen wel eens even groot of zelfs groter kan zijn dan de positieve forcering door de toenemende concentraties broeikasgassen. Het probleem is dat relevante metingen ontbreken. Door het regionale karakter van aërosolen is er behoefte aan regionale metingen en modellering.

Van (politiek) belang is niet alleen hoe groot het effect nu is maar ook hoe het effect in de toekomst zal zijn. Om scenario's te kunnen maken moeten de bronnen van de aërosolen bekend zijn. Dit is een probleem: ook uit het huidige onderzoek blijkt weer dat de forcering door aërosolen wordt veroorzaakt door aërosolcomponenten die niet direct worden geëmitteerd door bronnen. De twee veruit belangrijkste componenten, sulfaat en nitraat, ontstaan in de lucht uit het gasvormige zwaveldioxide en stikstofoxide. Scenario's voor de complexe cyclus van vorming en verwijdering kunnen alleen met complexe modellen worden gemaakt. De modelontwikkeling was daarom ook een onderdeel van deze studie.

De onzekerheid in de forcering door aërosolen, het sterke vermoeden dat het effect in Nederland groot is en expertise uit eerder onderzoek aan de stralingseigenschappen van aërosolen waren de redenen om onderzoek naar de forcering door aërosolen in Nederland uit te voeren. Een belangrijke onzekerheid komt voort uit een gebrek aan aërosolgegevens op de juiste tijd, n.l. als de zon schijnt. In de studie werd met name op dit punt nieuw vernieuwend onderzoek verricht, gebruik makend van de gezamenlijke expertise van de betrokken instituten.

Doelstelling en aanpak

Het doel van het onderzoek was het kwantificeren van het effect van antropogene aërosolen op de stralingsbalans in Europa en vooral vaststellen welke componenten dominant bijdragen. Nederland gold daarbij als referentiepunt vanwege de speciaal uit te voeren aërosolmetingen. Het continu meten van "nitraat" aërosol en het berekenen van het aandeel van deze component aan de stralingsforcering door aërosolen was nieuw.

De cluster die het onderzoek uitvoerde was opgedeeld in drie groepen met een eigen specialisme en taak, te weten.

- Experimenten:

  .karakteriseren van het aandeel antropogene aërosolcomponenten

.bepalen van de hoogte waarop aerosolen in de lucht voorkomen
.extrapolatie van de experimentele gegevens naar een lokale forcering door aerosolen.

- Modellering van de mondiale forcering door aerosolen, inclusief gevoeligheidstudie

- Ontwikkelen van een model dat de aërosolcyclus in Europa beschrijft, met toetsing van het model aan de experimentele gegevens uit het onderzoek. FEL-TNO heeft hieraan meegewerkt middels gegevens van satelliet-observaties van aerosolen.

Resultaten en conclusies

De gecombineerde aanpak van experimenteren en modelleren bleek zeer effectief. Experimentele gegevens konden direct na validatie in de modellen worden gebruikt en de modelontwikkeling gaf aan welke aërosolkarakteristieken speciaal moesten worden gemeten.

Het belangrijkste resultaat is dat werd vastgesteld dat nitraat een belangrijke component is in Nederland in de regionale stralingsforcering door aërosol, een gegeven dat uitgebreid wordt vermeld in het binnenkort uit te komen Third Assessment Report (TAR) van het IPCC . Het nitraat neemt vocht op waardoor de deeltjes druppels worden die tot twee keer meer licht zonlicht weerkaatsen dan droge deeltjes.

Op de meest relevante dagen voor de stalingsforcering, n.l. de heldere dagen, komen aerosolen ook voor in luchtlagen die niet in verbinding staan met de grond. De samenstelling en optische eigenschappen van die aerosolen kunnen niet worden gemeten en alleen met een betrouwbaar model worden beschreven. Dat model is ontwikkeld (TM3-inzoomversie) en de berekende concentraties zijn vergeleken met concentraties gemeten aan de grond. Ook is de stralingsmodule, die werd ontwikkeld in het mondiale model, ingebracht in dit regionale model. Daarmee is de vermindering in zonnestraling op de heldere meetdagen berekend en vergeleken met metingen.

In de modellering ontbreekt momenteel de component koolstof, waarvan experimenteel werd vastgesteld dat het ca. 25% kan bijdragen aan de stralingsforcering van de antropogene aerosolen in Nederland. Koolstof is een complex van duizenden verbindingen die gemakshalve in twee categorieën worden opgesplitst: “organisch” en “roet-zwart”. Roet-zwart absorbeert zonlicht. De pionier van de stralingsforcering (Hansen) beschouwt roet derhalve als broeikascomponent. Hij raadt aan eerst vermindering van deze component te realiseren bij de aanpak van het broeikasprobleem, zoals hij in interviews in september 2000 in de nationale bladen aangaf. De absorptie door roet is een centraal aspect in een vervolgproject op de huidige studie.

Landelijke presentaties

Maart 1998 werd een nationaal symposium georganiseerd, bijgewoond door 46 personen, waarop de tussenresultaten werden gepresenteerd.

Van het onderzoek is een verslag uitgekomen, waarvan de samenvatting op het NOP-symposium van oktober 1998 is gepresenteerd; de samenvatting staat in de proceedings.

Stuurgroep

Het project had een stuurgroep, bestaande uit dr. R. Guicherit. en dr. G. de Leeuw en ir. G.J. Heij. De voortgang werd jaarlikjks aan deze groep gepresenteerd en zij bepaalde mede de wetenschappelijke koers in het onderzoek.

Noot: indirect effect

Aërosoldeeltjes beïnvloeden de stralingsbalans van de aarde op twee manieren. Direct, door weerkaatsing van inkomende zonnestraling, en indirect via het proces van wolkenvorming. In het *huidige onderzoek* werd de *directe* invloed onderzocht. Het directe effect is niet significant als wolken de zon afschermen Het directe effect moet en kan daarom apart onderzocht worden. Het indirecte effect is in een eerder NOP-project door ons onderzocht.

ABSTRACT

In this project experiments were performed and models were developed and implemented to come to a better assessment of the forcing of the radiation balance by the anthropogenic aerosol. Aerosols exert a forcing because they reflect solar radiation. IPCC estimates that this effect is large, but it also indicates a high uncertainty factor which is mostly due to the short lifetime of the relevant aerosol component in the atmosphere. As a result, the aerosol forcing is a regional phenomenon. The approach followed here was to assess the magnitude of this uncertainty for Europe and quantify the contribution of the various anthropogenic components to the forcing at a representative site. With the help of the chemical speciation the anthropogenic aerosols could be identified. The aim of the study was to provide the tools required for optimized scenario projections of the future aerosol forcing.

The major outcome was the large contribution of nitrate to the aerosol radiative forcing in the Netherlands. Other results and accomplishments are discussed in detail below.

EXTENDED SUMMARY

BACKGROUND

Anthropogenic aerosols scatter solar radiation back into space and therefore act as a cooling agent. The perturbation ("forcing") of the radiation balance is so large that, according to estimates by IPCC, it could off-set the long-wave radiative forcing by the manmade greenhouse gases in areas like Europe. IPCC reports that the uncertainty in the globally averaged aerosol forcing is of the order of **3 Wm^{-2}**. This uncertainty exceeds the magnitude of the long-wave forcing by the manmade greenhouse gases. Of national interest is the fact that the aerosol forcing is a **regional** phenomenon because of the limited lifetime and transport distance of aerosol. The claim in IPCC-95 that sulfate is the only relevant manmade aerosol component in Europe is highly questionable in view of the high nitrate concentrations measured in the national monitoring network for aerosol.

Whereas the value of the aerosol effect is uncertain, predictions of the coming trend are even more problematic. This is due to the fact that the cycle of the most important anthropogenic

ingredients of the aerosol are complex: sulfate and nitrate are not directly emitted by sources, but made in the atmosphere from the precursor gases. A linear relation between emission of precursors and aerosol seems highly unlikely given the non-linear historical trend found in the present study. Therefore models which properly describe the cycle of formation and removal of the mentioned components are needed. Such models should use input of and be checked with relevant data. This approach was followed in the present study and should provide the tools for **reliable scenarios** for the aerosol radiative forcing effect.

OBJECTIVES

Improvement of the current large uncertainty in the forcing of the radiation balance by anthropogenic aerosol in Europe and development of tools for reliable regional scenario's.

APPROACH

Given the highly variable character of aerosols, a dense network of monitoring stations would be required to assess their concentration fields and reflective properties. In practice, in the European domain not a single station of this kind was in operation at the start of this project and measurements were initiated in the Netherlands, a location which is very well situated for this purpose: on the one hand it is the starting point for "clean" air-masses entering Europe from the arctic, on the other hand it is the end point of continental air-masses from the east, which have large anthropogenic aerosol loadings, as confirmed in the present study.

The estimates of the aerosol radiative forcing which are being made, also in the study performed here, are based on very coarse-grid models in which monthly averaged weather patterns are used to describe the aerosol-sulfate field. Such results can not be experimentally verified. A model was therefore developed with a greater resolution to especially model the nitrate cycle and nitrate field in Europe, using actual meteorological data and thus amenable for comparison with data obtained in this project. The reduction in the direct solar radiation, as expressed in the aerosol optical depth (AOD), was calculated and compared with measured AOD. The radiation scheme, used off-line in the global model, was included into the regional model to calculate the aerosol radiative forcing on measuring days.

CHAPTER 1. MEASUREMENTS

In summary the following experimental work was performed

- Year-round automated measurements, providing a climatological database on sulfate and nitrate concentrations and aerosol light-scattering, including its dependence on relative humidity.

  Detailed measurement of composition and size of the aerosol in situations which are most relevant for anthropogenic aerosol forcing, i.e. in cloudless continental air.

- On a stand-by basis, detailed aerosol characterization and solar radiation measurements, combined with vertical profiling of the aerosol.

Section 1.1

Automated instruments were used to ***continuously*** follow the concentration of the two dominant manmade aerosol components in the Netherlands, ammonium sulfate and ammonium nitrate. The contribution of these compounds to the aerosol light-scattering was established by performing detailed measurements of the composition of the aerosol at times of high solar flux. It was found that nitrate is as important for the light-scattering as sulfate.

In *measuring-**campaigns*** the aerosol was characterized with respect to concentration, size, composition and optical properties. Also the amount of anthropogenic versus natural aerosol was assessed. It was concluded that sulfate, the only chemical aerosol component considered by IPCC, is not the dominant aerosol constituent in the Netherlands. **Nitrate** is as important. Work is in progress at the moment to assess the area in Europe were this is the case.
From more indirect evidence it was concluded that the concentration of **carbonaceous** material might be similar to that of sulfate and nitrate. However, its aerosol light-scattering is smaller than that by the other two compounds because the carbon is not as hygroscopic. Artefacts in the sampling that have not yet been resolved result into an uncertainty of (at least) a factor of two in directly measured concentrations of carbon.

The light-scattering by aerosol as measured at ground level was extrapolated over the vertical and the associated aerosol radiative forcing was calculated, taking into account sunshine duration, average cloud coverage, RH and surface albedo. We arrive at a value of –3 Wm^{-2} with an uncertainty of a factor of two because of a combined uncertainty in the height of the boundary layer over which the extrapolation is performed and uncertainty in the relative humidity. It should be emphasized that this is an annually averaged forcing, thus including night-time hours and daytime periods with clouds.

Section 1.2 Radiative column closure tests

The assumptions made in the extrapolation of ground level data were checked on cloudless days. Use was made of a detailed ***radiative transfer*** model (MODTRAN-3.5) to obtain the relevant optical parameters. Experience with this model was gained from data-evaluation in the Atmospheric Radiation Measurement (AR M) program in the US, **see section 1.3**.

The extrapolated reduction in solar radiation level over the height of the layer in direct contact with the surface, the boundary layer, was compared with the actually measured attenuation. Radiative column closure, i.e. consistency between extrapolated and experimentally determined reduction in solar radiation, was observed in winter time, giving confidence in the extrapolation method. In such situations the aerosol is confined to the boundary layer. In summer, aerosol in layer(s) above the boundary layer contribute to the aerosol forcing. Evidence for this was also provided by the lidar-profiling. The properties of the aerosol in layers above the boundary layer can not be monitored measured and must be thus be derived from modeling.

In **section 1.4** the trend in sulfate aerosol in Europe is reported. The decrease by a factor of two over the period analysed must have led to an increase in soalr irradiance. However, such a trend is not seen and it argued that an increase in other aerosol components might have compensated the decrease in sulfate. The observed non-linear relation between the emission of the primary SO_2 and the product sulfate is not reproduced by the models. This mismatch for historic trend contains a warning with respect to the reliability of models for prediction of future trends.

MODELING

The work performed in the modeling area was subdivided according to the two subjects described in chapter 2 and 3. These are identified with the same numbering here.

CHAPTER 2. RADIATION FORCING OF TROPOSPHERIC AEROSOL

The IS92a emission scenario of IPCC-92 and ***parameterized*** optical characteristics were used to calculate the ***Global*** sulfate radiative forcing for 1990. This was compared to a similarly modeled (natural) forcing in the pre-industrial year 1850. The increase in the forcing between the two years is -0.36 Wm-2. In July a large (negative) forcing of -5.5 Wm-2 is calculated over Europe and the eastern United States. With an assumed emission scenario, as described in detail in section 2.1 of the full report an increase in the radiative forcing in 2050 by ozone by another 70% was calculated, while the direct cooling effect of sulfate aerosols is estimated to increase with 150%, with a southward shift towards countries with emerging economies.

The effect of relative humidity on the aerosol optical parameters, and on the sulfate forcing has been studied. It appears that globally differences forcing computed with fixed relative humidity and that with an RH- dependence is 10%. Regionally, differences up to 5 Wm^{-2} (!) were found.

An analytical fit was developed for the sulfate forcing as a function of surface albedo, solar zenith angle and day fraction. The new analytical expression matches the detailed radiation computations much better than the commonly used "Charlson" relationship as used in the present experimental part of the subproject. On-line computations of the radiative forcing were performed using the new expression in the TM3 model, see below under the heading integration.

Also the first approach ever was made to describe the global aerosol nitrate fields and the resulting forcing by this component. The optical properties of ammonium nitrate were used as deduced from the results in the experimental part of the program. It seems that the directly

measured concentrations and forcing by nitrate are higher than the values modeled for the Netherlands. This can be due to the coarse resolution of the model used (MOGUNTIA). In the more detailed model the nitrate concentrations are higher and thus its forcing larger, as described next.

CHAPTER 3. AEROSOL CYCLE IN EUROPE

3.1 Modeling the ammonium sulfate and nitrate aerosol distributions over Europe with the chemical tracer transport model TM3

A zoom- version of the transport model TM3 was developed to model in detail the sulphate and nitrate fields in Europe. Nitrate, in the form of the relevant component ammonium nitrate, is semi-volatile and the partitioning of nitrate over gas phase and aerosol phase, which depends on temperature and humidity was calculated with a special sub-module. The model uses ***real-time*** meteorology and thus provides a detailed description of the nitrate aerosol life-***cycle***.

Model output was compared with measurements. The main result was that sulfate aerosol distributions are well simulated, both the absolute magnitude of the concentrations and the seasonal day-to-day variability. In contrast, the SO_2 concentrations as modeled were higher than the measured concentration; this, incidentally, appears to be a general phenomenon in sulfur modeling. With surface measurements alone, the complex mechanisms and feedbacks in the sulfur cycle cannot be fully understood. Both model outcome and a limited number of measured profiles show that a major fraction of sulfate and SO_2 resides above the boundary layer.

Simulated sulfate and nitrate patterns for Europe were translated to Aerosol Optical Depth. The AOD-fields correlated well with the AOD-patterns analyzed with satellite retrieval of ATSR-2 data.

3.2 Aerosol-cloud interactions and heterogeneous chemistry

A ***mechanistic*** transformation module was developed with a detailed chemistry scheme of the ***formation*** of sulfate in clouds. It was found that this must have been the dominant route for formation of sulfate from sulfur dioxide in the NW-European region. The model was

evaluated with data from field campaigns over the ocean, a situation which is the simplest to evaluate with such a highly complex model. Implementation of the module in the TM3 transport model is foreseen.

INTEGRATION

The TM3-model was used in combination with the radiation transfer scheme developed in part 2 to calculate the aerosol radiative forcing for given days. On-line computations of the forcing were performed using the mentioned analytical fit for the sulfate and nitrate radiative forcing. It was found that the height at which the sulfate and nitrate aerosols are present in the atmosphere is of utmost importance, due to the fact that the aerosol scattering so strongly depends on relative humidity. And, as evidenced in section 1.2.5, the boundary layer is usually much more humid than the layers above it. For three summer days on which also column closure tests were made (section 1.2.5) the forcing over Europe was calculated. It was –1.5 Wm^{-2} on average. The examples show the power of the zoom-version of TM3 to obtain real-time values for the aerosol radiative forcing.

ACCOMPLISHMENTS AND NOVELTIES

- Sixteen peer-reviewed papers were published and three have been recently submitted. More than twenty conference presentations were held and these appeared as (reviewed) extended abstracts in proceedings
- Three Ph.D. theses were completed and defended. A fourth thesis is in preparation.

The following novelties were developed:

- Automated instrumentation for continuous measurement of ammonium sulfate
- Similar instrumentation for ammonium nitrate
- Radiative column closure tests on a stand-by basis
- Global patterns of radiative forcing by the mix of anthropogenic sulfate, nitrate and ozone
- Parameterization of the interaction of nitrate aerosol and solar radiation using the empirically determined optical properties of nitrate in the experimental part
- A regional aerosol chemistry/transport model for nitrate driven by actual meteorology

- A mechanistic module describing the formation of sulfate in clouds
- On-line calculation of the aerosol forcing

GENERAL CONCLUSIONS, SHORTCOMINGS AND RECOMMENDATIONS

The present measurements and modeling efforts quantified the contribution of the various anthropogenic aerosol components to the aerosol light-scattering in the Netherlands. The large value of the local aerosol forcing of the radiation balance, obtained by extrapolation measured aerosol light-scattering, supports the large value obtained by modeling. The uncertainty in the extrapolated value is as large as that estimated from modeling because of uncertainties in the vertical extension of the aerosol and the RH profile. These uncertainties can be reduced by aircraft monitoring of these parameters.

The importance of light-absorbing, carbonaceous, aerosol was not addressed in detail. This omission is being made up for in a new study.

DETAILED REPORT

In this part of the report those technical and scientific aspects are discussed in detail which were not described in the progress report, published as report NOP/410-200-025 in 1999, or in the peer-reviewed publications mentioned in the reference lists.

1. MEASUREMENTS

H.M. ten Brink, A. Hensen, A. Khlystov, G.P.A. Kos; ECN
D.P.J. Swart, J.B. Bergwerff, A. Apituley; RIVM

1.1 Long-term measurements and extrapolated aerosol forcing

Automated instruments were used to ***continuously*** follow the concentration of the two dominant manmade aerosol components in the Netherlands, ammonium sulfate and ammonium nitrate. The long-term data, in combination, with the composition and size-distribution as determined in the campaigns, were used to estimate the annually averaged local aerosol radiative forcing.

A selection of data was made in the following sense. The relation between the (midday) aerosol light-scattering and the concentrations of nitrate and sulfate was assessed. Midday was selected because this is the time at which the aerosol at the ground is representative for that in the whole of the boundary layer, as discussed in section 1.2.

The conventional method for assessing the concentration of ammonium nitrate is by sampling of aerosol on a filter with subsequent chemical analysis of the sampled material. It has been established that evaporation of the semi-volatile ammonium nitrate occurs from some type of filters in use in Europe; other filters can suffer from extra absorption of gaseous nitric acid, which is then appreciated as aerosol nitrate [ten Brink et al., 2000a]. The real concentration of ammonium nitrate can be determined with a combination of a gas-denuder in which the nitric acid is stripped, followed by a filter from which the ammonium nitrate does not evaporate because of a special treatment. Denuder/filterpacks are barely sensitive enough for hourly aerosol-measurements and too costly because of the manual handling. At the time the thermodenuder was the only automated and sensitive instrument available [Khlystov et al., 1998; ten Brink et al., 1996]. For this reason an automated “thermodenuder” was developed. The device provides the hourly concentration of the most abundant species, i.e. ammonium sulfate and ammonium nitrate.

The (dry) aerosol light-scattering was measured with an integrating nephelometer described below; the average aerosol light-scattering coefficient, at a wavelength of 525 nm, was $0.71*10^{-4}$ m^{-1}. In arctic marine air the aerosol light-scattering was a factor of ten lower than the average value, in continental air it was up to a factor of ten higher. The ratio of the total aerosol light-scattering to the concentration of sulfate was 20 m^2/g. The contribution of nitrate to the aerosol light-scattering was higher than that of sulfate in winter and of about equal magnitude in summer.

1.1.1 Light-scattering as a function of RH

Measurement of the aerosol light-scattering is a straightforward process. It is performed with "integrating nephelometers" which measure in an absolute sense because they are calibrated against the known light-scattering of an inert gas. The only uncertainty arises from the fact that particles scatter more light in the direction of the test-beam. However, solar light is scattered in a precisely similar way and therefore the scattering (coefficient) as determined with the nephelometers apply for calculating the scattering of solar radiation by aerosol as performed in the next section.

A „humidograph" was built to investigate the uptake of water and its effect on light-scattering of ambient aerosol. In the humidograph the relative humidity can be scanned over a large RH-trajectory. Details can be found in a very recent publication [ten Brink et al., 2000]. Two types of (continental) aerosol were found with respect to their humidity behavior. One type showed a significant increase in light-scattering at the deliquescence points of ammonium nitrate and ammonium sulfate, with that of ammonium nitrate being the most pronounced. The second type of continental aerosol did not show deliquescence, but followed the typical humidity dependence of aerosol in a supersaturated droplet state. In this latter aerosol type, nitrate dominated over sulfate. It was concluded from the study that the aerosol light-scattering in The Netherlands, in particular its humidity dependence, is governed by (ammonium) nitrate.

1.1.2 Detailed aerosol characterization

The size dependent composition was measured on cloudless or nearly cloudless days in the period 1991 to 1995 [ten Brink et al., 1997].

Cascade-impactor measurements

Mass and composition were determined after sampling of the aerosol in size-classes with a cascade impactor. The lower limit of detection (LOD) of the weighing is 3 μg which corresponds to an LOD for the mass concentration of 0.1 μg m^{-3}. More details can be found in ten Brink et al. (1997).

Sampling of the aerosol was performed at Petten, directly on the coast of the North Sea in the north-west of The Netherlands. The site is rural and the nearest large aerosol source is a steel-works complex at a distance of 30 km in a southerly direction. Measurements performed at a relative humidity over 85% were not evaluated. The reason for excluding such data is the fact that ambient aerosols are hygroscopic and that their mass, size and aerodynamic diameter at those high humidities are dominated by (an unknown) amount of water. Also, at high humidities the size increase with RH is large and this parameter becomes therefore so critical that it should be maintained at the same value in the collection lines and inside the aerosol instruments, which is technically not feasible.

The aforementioned semi-volatile nature of ammonium nitrate can lead to an underestimate in the measurement of its concentration. For this reason the nitrate data presented here should be considered as minimum values. Cloud free conditions and situations with little overcast and high aerosol loadings typically occur in persistent continental easterly air flows. In these situations on average 75% of the aerosol mass was in the submicron fraction, see fig. 1.1. The impactor measurements are represented in the usual way here as the mass concentration per size class (impactor stage).

Fig. 1.1 Average mass distribution on cloudless days with easterly to southeasterly winds. Shown is the mass concentration per impactor stage, size class, left scale.
The light-scattering coefficient at 525 nm calculated for the aerosol in the given size-class is given, scale to the right in the appropriate unit.

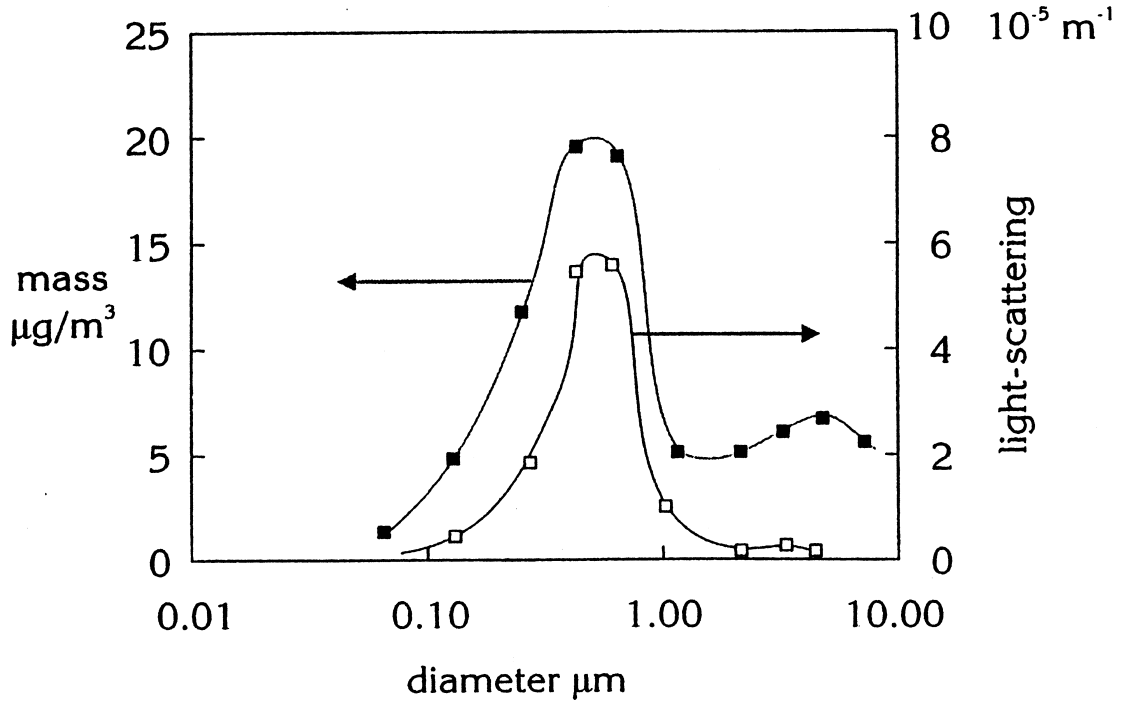

On the x-axis the median size of the respective stage is tabulated. Ammonium nitrate and ammonium sulfate (figure 1.2) were the dominant aerosol species with total concentrations as high as 25 µg m^{-3}. In arctic air the concentrations of these species is negligible and it is thus concluded that they are of a manmade origin in continental air.

Light-absorbing carbon contributes an estimated 5% to the total mass [Berner et al., 1996]. Submicron dust is of a similar magnitude. Almost half of the submicron aerosol in the relevant size range could not be identified. The amount of water associated with the hygroscopic salts is not known but could be as high as 10-20%, according to literature. However we found that it is less by drying some samples to very low RH-values. It was thus concluded by inference that most of this unidentified material must be organic carbon. The amount of submicron organic carbon is derived by subtracting the concentration of the measured components from the total

weight (per stage). Its contribution seems as high as that of ammonium nitrate and ammonium sulfate.

Fig. 1.2 Idem as fig. 1.1. The average concentration of the single two dominating chemical components in the aerosol on those days

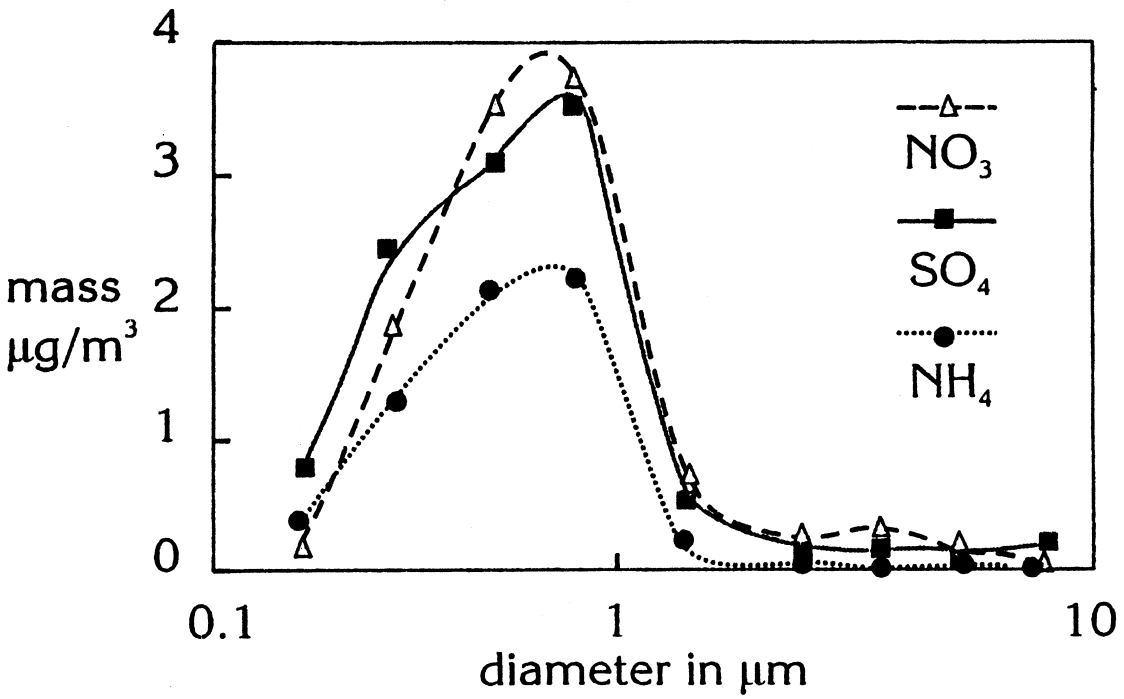

The light-scattering by the aerosol with the average dry mass-distribution as shown in fig. 1.1, was calculated, assuming a refractive index of 1.5 for the short-wave solar light [see, e.g., IPCC-95, pg. 107]. The resulting light-scattering by the dry aerosol in the given size class is also presented in fig. 1.1. It is seen that the aerosol light-scattering is almost exclusively exerted by particles with a diameter between 0.2 and 1.0 µm. The light-scattering is calculated for the aerosol as sampled and weighed which by definition does not include the water associated with the ammonium sulfate and ammonium nitrate in the actual atmosphere.

Contribution of the major aerosol components to the aerosol light-scattering

Ammonium nitrate and ammonium sulfate are the dominant inorganic aerosol species in the aerosol fraction with a size which most effectively scatters radiation (compare fig. 1.2 and fig. 1.1). 1.1). The ammonium nitrate concentrations are as high as or even higher than those of

ammonium sulfate, given the possibility of evaporative losses of this semi-volatile component during collection. The contribution of submicron organic carbon seems as high as that of ammonium nitrate or ammonium sulfate. However, the contribution of the organic material to the aerosol light-scattering in the atmosphere is lower because it is mostly non-hygroscopic, while the ammonium salts are associated with a relatively large amount of aerosol-water which scatters additional light, as shown above.

The contribution of seasalt to the aerosol is quite easily assessed from the concentration of sodium in combination with magnesium which are tracers for this aerosol type. It appears that the seasalt is virtually only present in particles larger than 1 μm. Crustal material, "dust", is another aerosol component. It is also insoluble in water and identified in this way as well as by the calcium content of the aerosol [ten Brink et al., 1997]. It was shown that in continental air almost all of the hypermicron aerosol is made up of crustal material, but the light-scattering by this component is small compared to that by the submicron aerosol (fig. 1.1). Large particles scatter predominantly in the forward direction and thus contribute relatively little to the reflection of solar radiation. Moreover, the dust is mostly of natural origin and thus not a real, i.e. manmade, aerosol forcing factor. These are the (combined) reasons why coarse dust, as well as seasalt, were not further considered.

1.1.3 Extrapolated aerosol radiative forcing

The long-term data, in combination, with the composition and size-distribution as determined in the campaigns, were used to estimate the annually averaged local aerosol radiative forcing. Full details of this approach can be found in the thesis of Khlystov [1998] and Veefkind et al. [1996].

Use was made of the well-known approximation by Charlson [e.g. IPCC-94] to deduce the average direct radiative forcing, ΔF:

$$\Delta F = -0.5\ F\ T^2\ OD\ \beta\ (1-A_c)\ (1-R_s)^2$$

in which the parameters are defined in short as follows:

F is the average solar flux at the top of the atmosphere
T is the fraction of light transmitted through the atmospheric
OD is the fraction of the solar radiation scattered by the aerosol, see also section 1.2.2
β is the fraction of the light which is scattered upwards (away from the earth)
$1\text{-}A_C$ is the fraction of the sky without clouds
R_S is the mean surface albedo (reflectance)

The local climatological values for the various parameters, like cloud cover, were used. OD is obtained from integration of the light-scattering of the aerosol, as measured at the ground, see section 1.1.1, over the height of the boundary layer. The crucial assumption here is that the average height of this layer is 1200 m. An average relative humidity in the boundary layer was assumed so that the actual light-scattering is twice the value of the dry scattering of section 1.1.1. A value for β of 0.3 ± 0.05 was deduced from the average size distribution measured in the campaigns.

The calculated OD amounted to 0.11, with an estimated uncertainty of 40% which is mostly related to uncertainty in the height of the boundary layer and RH.

A best estimate of the local forcing thus obtained is -3 W m^{-2} with an uncertainty of a factor of two. Given the fact that nitrate contributes to the aerosol light-scattering as much as sulfate, it can be assumed that its contribution to the aerosol radiative forcing in the Netherlands is also similar to that of sulfate.

Since aerosol radiative aerosol forcing is a reduction in solar radiation it is in principle a measurable quantity, which could be checked against measurements. However, the reduction as estimated here is an average annual reduction of 2%. Such a small decrease cannot be assessed against the much larger and variable reduction of solar radiation by reflection on clouds. However, verification is possible in cloud-free conditions. Such experiments were performed and described in the next section. The reduction in solar radiation as calculated from ground level measurements, following the approach in this section, was compared with the measured reduction.

References

1996:
A. Berner, S. Sidla, Z. Galambos, C. Kruisz and R. Hitzenberger (1996);
H.M. ten Brink and G.P.A. Kos: "Modal character of black carbon size distributions"
J. Geophys Res. **101,** 19559-19565.

P.G. Dougle, A. Vlasenko, J.P. Veefkind and H.M. ten Brink: "Humidity dependence of the light-scattering by mixtures of ammonium nitrate, ammonium sulfate and soot" *J. Aerosol Sci.* **27**, S513-514.

ten Brink, H.M., J.P. Veefkind, A. Waijers-IJpenlaan, and J.C. van der Hage: “Aerosol light-scattering in the Netherlands”. *Atmos. Environ.*, 30, 4251-4261.

1997:
H.M. ten Brink, C. Kruisz, G.P.A. Kos and A. Berner
"Size/composition of the light-scattering aerosol in the Netherlands"
Atmos. Environ. **31**, 3955-3962.

1998:

Khlystov, A., Thesis, Wageningen University. March 1998.

Khlystov , A., P. Dougle, R. Otjes, P. Jongejan, A. Waijers-IJpelaan and H.M. ten Brink
"Comparison of four techniques for measurement of aerosol ammonium nitrate content"
J. Aerosol Sci. **29**, S151-152.

Pauline G. Dougle, J. Pepijn Veefkind and Harry M. ten Brink*)
"Crystallisation of mixtures of ammonium nitrate, ammonium sulfate and soot"
J. Aerosol Sci. **29**, 375-386

Harry ten Brink, Anita Waijers-IJpelaan and Sjaak Slanina
"Performance of an automated thermodenuder for ammonium nitrate measurements"
J. Aerosol Sci. **29**, S633-S634.

Harry M. ten Brink and Arjan Hensen
"Light-scattering data relevant for aerosol radiative forcing"
J. Aerosol Sci. **29**, S675-S676.

2000:
H. M. ten Brink, A. Khlystov, G. Kos, T. Tuch, C. Roth, W. Kreyling
A high-flow humidograph for testing the water uptake by ambient aerosol
Atmos. Environ. **34**, 4291-4300.

H. ten Brink, M. Schulz, J.-P. Putaud, P. Jongejan, E. Plate
Comparison of the collection of ammonium nitrate by various sampling methods
To be published in Proc. Eurotrac-Symposium 2000.

1.2 Radiative column closure measurements

A. Hensen, H.M. ten Brink / D. Swart, J.B. Bergwerff, A. Apituley

1.2.1 Introduction

“Radiative column closure” is the term used for tests on cloudless days in which the measured reduction in solar radiation is compared with the reduction extrapolated from ground-level aerosol-scattering measurements. “Column” refers to the aerosol in the column of air through which the solar radiation passes. "Radiative column closure" is obtained when calculated and measured reduction agree.

For a proper column closure the characteristic of the aerosol in the vertical column should be the same as that at ground-level. This applies in case of rapid vertical mixing. This indeed occurs on cloudless days, because the heating of the surface leads to strong convections. This theoretical justification is supported by measurements in the past with an aircraft in the Netherlands in which a constant vertical aerosol scattering profile was found on cloudless days. However, in the morning a surface layer was present, often with fog or fog-like conditions. Obviously measurements should be performed after this surface layer has broken up. In the present study Lidar profiling was used to see when this was the case.

1.2.2 Experimental approach

Solar radiation measurements

In a closure study the intensity of the radiation in the direct solar beam is measured. The reduction in solar intensity by aerosol scattering is obtained by comparing the measured intensity with that for a situation without aerosol. This aerosol-free intensity was calculated taking into account the scattering and absorption of radiation by the various trace gas species in the atmosphere. We used the MODTRAN radiation transfer code (version 3.5) and known trace gas concentrations. Calculated Io is typically around 900 W m^{-2}.

Uncertainty analysis

The experimental uncertainty in measuring I is 10 W m^{-2} at most, as discussed in detail in section 1.2.4. Halthore et al. [1997] made a sensitivity test and found that the largest uncertainty in the aerosol-free I stems from uncertainties in the absorption by water vapor. A conservative estimate of its uncertainty translates into an uncertainty of 15 W m^{-2} in I. The combined uncertainty, including calibration errors of the radiometers, is therefore 18 W m^{-2}. The measured reduction in I is at least 100 W m^{-2} and hence the uncertainty is relatively small compared to the uncertainty in other parameters closure parameter tests, as shown below.

Aerosol optical depth

In the further discussion we use the concept of Aerosol Optical Depth (AOD) for description of the reduction of solar radiation by scattering on aerosols. AOD is directly related to the ratio of the intensity of the solar radiation entering the atmosphere and the intensity at the ground. The AOD is defined as the logarithm of this ratio, but then for a reference vertical direction. The AOD pertains to light of a narrow wavelength. In the present study this reference wavelength is that of the instrument used to measure he aerosol light-scattering at the ground operating at 525 nm.

$$AOD = m^{-1} * \ln Io_{525}/I_{525} \qquad (2)$$

in which m^{-1} is the sine of the angle of elevation of the sun (inverse airmass m).

m is the air path or "air mass", a measure for the distance traveled by the solar beam over the slant path through the atmosphere compared to that in the vertical direction.

The AOD at the reference wavelength of 525 nm is obtained from the total reduction in solar radiation via the well-known Angstrom expression for the λ-dependence of the AOD:

$$AOD(\lambda) = \beta \lambda^{-\alpha} \qquad (3)$$

in which β is a measure for the amount of light scattered, while α is for the size of the aerosol. α is usually between 0.5 and 3 with the highest value indicating that the light-scattering

aerosols have a size appreciable smaller than the wavelength of the solar light (around 1 um) and 0.5 indicates that the light-scattering aerosols are mostly of a larger size. β is obtained by integration of equation (3) over the total spectrum and fitting measured and calculated reduction in solar radiation.

α was estimated from the measured aerosol size distributions and light-scattering properties as given in fig. 1.1 in section 1.1.1; the most probable value is 1.45 [Veefkind et al., 1996]. This is close to the average value of 1.5 deduced from recent measurements [Stammes and Henzing, 2000]. Expression (3) is integrated over the total solar spectrum and β is fitted so that calculated total I equals measured I.

The uncertainty in AOD as a result of uncertainty in α was analyzed. α was varied from 1.1 to 1.5, but in every run β was readjusted so that modeled I equaled measured I. It was found that AOD varies by 12% at most. Combined with the above mentioned uncertainty in aerosol-free Io and measured I this amounts to an uncertainty of 15% or less in AOD. This uncertainty value compares favorably with the estimate for the uncertainty in the boundary-layer AOD, described below.

Boundary-layer AOD

The "boundary-layer AOD" is obtained by extrapolation of the aerosol scattering as measured at ground level. This extrapolation or rather integration of the scattering coefficient occurs over the atmospheric layer which is in direct contact with the ground. The layer in contact with the surface is known as the boundary layer. The integration over height of the scattering coefficient gives the total scattering of radiation traveling in a vertical direction in this layer. This is equivalent to an AOD, as the following shows. The light-scattering coefficient, Bsp, is the differential decrease in intensity of a beam of light: $dI/I = Bsp$, in units m^{-1}. Integration of this differential dI over height gives the total reduction in intensity by scattering in the boundary layer. The integrated Bsp is equal to the logarithm of initial to final intensity of the beam, which is by definition an optical depth, as described above. In other words the vertically integrated Bsp is the boundary-layer AOD.

Vertical RH-profile

Even in case of complete vertical mixing of air and aerosol in the boundary layer, the aerosol light-scattering is a function of height because of Relative Humidity (RH) differences. In a well-mixed layer, RH increases with height and aerosol light-scattering also increases due to uptake of water. The RH-dependence of the light-scattering was assessed by measuring the RH-dependence of the light-scattering in the "humidograph", described in section 1.1.1. Balloon-soundings provided the vertical RH-profile. The light-scattering at a given height with its associated RH was taken from the humidity scan, as exemplified in fig. 1.4.

Uncertainty in the boundary-layer AOD

Measurement of the light-scattering coefficient , Bsp, is a rather precise process, see previous section. There is an uncertainty in the extrapolation of the light-scattering over height, partly because of some uncertainty in the measurement of the RH-dependence of the light-scattering. However the main uncertainty lies in the RH data from the balloon-soundings, which is close to 5% RH-units. This uncertainty is specifically important at higher RH, as can be seen from fig. 1.4. At 70% RH the uncertainty corresponds to a relative uncertainty in Bsp of 0.2, while at 85% RH a difference of 10% in RH translates into a difference in Bsp of a factor of two, which is unacceptable. This is the reason for the strict criterion posed here that RH should not exceed 80% anywhere in the boundary layer for a proper column closure test.

Apart from scattering light, aerosols absorb light. The estimated error in the light absorption by the aerosol is a factor of two, but because absorption is typically less than 0.1 of the aerosol scattering in the Netherlands its uncertainty is small in comparison.

The height of the mixing layer is in general uncertain by some 50 m, which translates into 5% to 10% relative uncertainty in the boundary layer height and integrated vertical aerosol scattering. The uncertainty in the extrapolated AOD is in the order of 25%.

General prerequisites for radiative column closure tests

RH

A first rigorous criterion for performing or evaluating a closure test is that the relative humidity in the boundary layer should be less than 80%. This is a stricter criterion than the

requirement that clouds must be absent, which is equivalent to the criterion for RH less than the saturation RH of 100%. Experiments are therefore only performed when visual inspection shows that clouds are absent anywhere in the sky. However, also "sub-visual" cirrus may occur. The absence or presence of these thin high clouds was deduced from the troposphere Lidar signals.

Anthropogenic aerosol

The focus of the project is assessment of the magnitude of the anthropogenic aerosol radiative forcing; therefore days were selected on which the contribution of anthropogenic aerosol to the total aerosol was expected to be high. The continuous monitoring study, see section 1.1.1 showed that this is the case when the air is from an easterly direction.

Selection of days

Measurements were initiated on days that the forecast indicated cloud-free conditions and easterly winds. The absence of clouds and subvisual cirrus was verified. Ground-level RH less than 80% was also checked. Whether the RH was less than that throughout the boundary layer could only be checked afterwards from the balloon-soundings. It is true in general, that it was only afterwards known whether all criteria for a successful test were fulfilled.

Early on in the study it was found that the boundary layer becomes well-mixed at about 11:00 local time and the very costly manual measurements were therefore started at that hour.

1.2.3 Experiments and evaluation

The following gives a brief overview of the key measurements and the analysis procedure in the closure tests:

I. Radiation measurements
   - Radiation transfer model calculations providing the aerosol-free Io.
   - Calculation of the ***total Aerosol Optical Depth*** (AOD) at 525 nm.

II Ground based aerosol scattering measurements as a function of RH

Extrapolation of the scattering coefficient over the height of the boundary layer, providing the ***boundary-layer AOD***.

III *Comparison* of total AOD and boundary-layer AOD

Analysis of contribution by aerosol ***above*** the boundary layer to the total ***AOD***.

1.2.4 Measurement sites and methods

Measurements were made at Bilthoven near Utrecht in the center of the Netherlands and in Petten on the seacoast in the Northwest. In addition, solar radiation data are used from the Royal Dutch Meteorological Office in de Bilt, a site very close to Bilthoven. Balloon soundings of the vertical profile of RH were also provided by this institute.

The reason that measurements were not collocated was the presence of aerosol measurement devices which could not be transported at the time. The reason we prefer the radiation data from the northern site is that they were screened for the presence (or rather absence) of thin cirrus.

Comparability of the aerosol at the two sites seems warranted because in the situation in which closure tests were made the concentrations of the major aerosol components are quite homogeneous over the Netherlands. Nevertheless more recent closure studies were centered at the central site to avoid any problems in comparing parameters obtained at different geographic sites.

We tried to gather as many data as possible by operating on an alert basis.

Measurement Techniques

Lidar

Lidar was applied to assess the height of the boundary layer, the status of mixing in this layer, detection of elevated aerosol-containing layers and estimation of the AOD in these layers. Lidar was also used for detection of interfering (sub)visual cirrus. The two Lidar systems used and described next are those of RIVM, Bilthoven.

The RIVM Boundary layer Lidar

The RIVM boundary layer Lidar operates in the near infrared, at a wavelength of 1064 nanometer, and performs automatic, routine observations of the lowest 4 km of the atmosphere. The vertical resolution in this mode is 50 meters, and the temporal resolution is 5 minutes. Measurements are available for the full research period described in this report.

Boundary layer height

Standard analysis include automatically analyzed hourly values for the boundary layer height. For some days these were supplemented by a more detailed manual analysis, providing boundary layer height values with a typical accuracy of better than 50 meters every 5 minutes. The technique used and its accuracy are described in [Visser et al., 1996].

Mixing status of the boundary layer

Especially during the morning hours, but also in the late afternoon, temperature inversions at the surface preclude homogeneous mixing of the air in the boundary layer. The time at which the boundary layer is “well mixed” is manually deduced from the Lidar signals.

The troposphere Lidar

The RIVM tropospheric Lidar [Apituley et al., 1996], operating in the ultraviolet region, at 299 nm is operator-controlled, has a typical frequency of once per second, and targets the altitude range of 1 to 15 km. The vertical resolution is 30 meters.

Detection of subvisual cirrus and clouds

The presence of low clouds can be assessed by visual inspection or from short-term variations in radiation. Cirrus clouds are often not detected in this way, because they are optically thin and spatially homogeneous. The RIVM tropospheric Lidar is therefore used to assess absence (and unwanted presence) of "subvisual” cirrus.

Elevated aerosol- layers

The tropospheric Lidar “sees” aerosol above the boundary layer. This aerosol can be present in two categories: in so-called residual layers at altitudes of 1 to 3 km and as free tropospheric aerosol above these layers. *”Free tropospheric" aerosol* is present in concentrations which are low. However, since it extends up to tropopauze at 10 km, there is a considerable path-length involved. As a consequence, there might be a significant relevant contribution by this type of aerosol to the total AOD. An effort was made to quantify the AOD in the elevated layers. The technique will be described in a separate technical report. Many assumptions had to be made. The Lidar AOD values for residual layer aerosol and especially those for the free troposphere aerosol, given in the present report should therefore be considered as indicative, not as absolute values.

The AOD in the upper layers was added to the boundary-layer AOD and this gives total AOD. The value should be comparable with the directly determined AOD. As mentioned this information is semi-quantitative.

Solar radiation measurements (DNSI)

Direct Normal Solar Irradiance was measured with pyrheliometers. This type of radiometers measures the intensity of the solar radiation perpendicular to the beam, in a solid angle of 5°. We used two pyrheliometers (CM1, Kipp instruments) in parallel. They were manually operated, because we had the quartz windows removed to eliminate fouling. The use of two pyrheliometers in parallel guarantees that a failure in one of the instruments is immediately noticed. Our meters were calibrated against the national standard, CH1.

Sensitivity analysis

The following four causes for uncertainty were identified in measuring with pyrheliometers:

1. Calibration of the national CH1 standard
2. Comparison of our CM1 with the national standard
3. Response as function of intensity, linearity
4. Emission of heat radiation by the sensor

1: The national standard CH1 was calibrated in October 1995 with intensities in the range of 700-1000 W m^{-2}. On days with a significant aerosol loading the intensity is less than that and especially at low intensities the CH1 value can be off by 0.5-2 %.
2: For an individual measurement (1 minute averaged) there can be a difference of about 5 W m^{-2} between the CM1 and the CH1 value.
3: The corrections for temperature non-linearity can be significant, typically ranging from + 15 to -30 W m^{-2}. At 25 °C it can be 1%, but there are formulae for a proper correction.
4: The detector emits radiation which is apparent from the negative readings at night. KNMI found for the operational CH1 a negative irradiance of 0.5 W m^{-2}. We will assume this to be the average error for this effect.
The combined uncertainties are most likely in the range between 6 and 7 W m^{-2} for the measurements made here.

Light-scattering coefficient

Measurements of the light-scattering coefficient, Bsp, are part of the monitoring described in section 1.1.1, in which also the procedure to determine the RH-dependence of Bsp is described.

1.2.5 Results and Evaluation

An overview of the days on which measurements were made is given in table 1.1. Over the years many data were gathered, but it was found in the evaluation stage that the criteria for a proper closure test had often not been met. Those days are marked in the table and the reason why measurements were not further evaluated is indicated in the caption of the table. Most often the constraint that the RH should not exceed 80% was violated.

Because of the relative paucity of acceptable days also more recent measurements were evaluated. In addition, measurements made via a simplified approach in 1993 and 1994 [Veefkind et al. 1996], were considered. The data from 1994 were not used because of an

interference by an unknown amount of stratospheric aerosol from the Pinatubo volcanic eruption.

Those experiments which met the criteria and were evaluated in detail so far are indicated by "selected" in the table. The measurements and results are reported below by first sketching the local meteorological conditions and the mixing state of the boundary layer. Then the solar radiation measurements and the AOD derived from these measurements are presented, followed by the calculation of the boundary-layer AOD from the ground based measurements. The comparability of the two AOD's is then discussed. Finally estimates of the AOD in layers above the boundary layer are presented. The evaluation procedure of a closure test is illustrated here by describing in more detail experiments performed on two consecutive closure days, viz. 25 and 26 July 1995.

25 July was chosen as the prime example because this is the day on which very pertinent additional information was available, such as AOD for the upper atmospheric layers, AOD from satellite observations and AOD in the UV-region of the solar spectrum. It serves as the best example of a radiative column closure experiment but it does not necessarily mean that it provided optimum results. On the contrary, the detailed evaluation shows that it is the worst case. Nonetheless it exemplifies the structure of the analysis of a column closure study best. The evaluation for this day is followed by evaluation of two more days. For other days, of which two are successful examples of closure, the relevant data and evaluation are only summarized, while a more detailed analysis is currently being made for other days in the list; this is done in the context of a more detailed study on the radiative properties of aerosol in the Netherlands in a separate project in the NRP-2-program.

Table 1.1 Overview of days with measurements, screened for absence of cirrus by visual inspection.

	Date	Status	Balloon sounding	BL Lidar	Tropos Lidar	Criteria*)
1993	5-11-93	Ref 1	x	x	-	OK
	17-11-93	Ref 2	x	x	-	OK
	18-11-93	Ref 2	x	x	-	OK
	19-11-93	Ref 2	x	x	-	OK
	24-11-93	Ref 1	x	x	-	OK
	29-11-93	Ref 1	x	x	-	OK
1994	26-6-94			-	-	
	27-8-94			-	-	
	28-6-94			-	-	
	29-6-94			-	-	
	30-6-94			-	-	
	1-7-94			-	-	
1995	22-5-95		x	x		OK
	24-5-95		x	x		-RH
	26-5-95		x	x		-RH
	25-6-95	Selected	x	+/-		-L
	26-6-95	Selected	x	X		OK
	27-6-95	Selected	x	X		OK
	28-6-95	Selected	x	X		OK
	29-6-95	Selected	x	X		OK
	30-6-95	Selected	x	X		OK
	10-7-95		18	X	x	-DNSI
	11-7-95		12	X	x	-DNSI
	20-7-95		x	X	x	-wind
	25-7-95	Selected	X	X	X	OK

Table 1.1 (Continuation) Overview of days with measurements

	Date	Status	Balloon sounding	BL Lidar	Tropos Lidar	Criteria*)
	26-7-95	Selected	x	X	x	OK
	1-8-95		x	X	x	-RH
	14-9-95		x	X	x	-RH
	18-9-95		x	X		-RH
1996	16-1-96		x	X		-RH
	29-1-96		--	X	x	-RH
	1-2-96		x	X	x	-RH
	9-3-96		x	X	o	-Wd
	14-3-96		x	X	o	-Wd
	1-4-96		x	X	x	-Wd
	3-4-96		x	X	o	-RH
	4-4-96		x	X	o	-RH
	10-6-96		x	X	x	-Wd
	19-8-96	Selected	x	X	x	OK
	20-8-96	Selected	x	X	x	-RH
	Date	Status	Balloon sounding	BL Lidar	Tropos Lidar	Criteria*)
1997**)	16-1-97		x	x	x	OK
	2-6-97		x	x	o	
	3-7-97		x	x	x	OK
	6-8-97		x	x	o	
	7-8-97		x	x	o	
	11-8-97		x	x	x	OK
	20-8-97		x	x	o	
	27-10-97	Selected	x	x	o	
1998**)	11-5-98		o	x	o	
	13-5-98	Selected	x	x	x	
	18-5-98		o	x	x	OK
	23-11-98	Selected	x	x	x	

*) Criteria to be met for proper closure test, as discussed in section 1.2.3; see also comments in last row of table. OK = All criteria met. -RH = the balloon-sounding showed regions with RH > 80% or: difference between the RH at Petten and center-site Bilt considered too large. -L = boundary Lidar data missing. -DNSI =only single radiation measurement made or difference between center site and Petten is too large. -Wd = wind came from wrong direction: north or west.

**) For 1997 and 1998 a different tabulation applies on days with troposphere-Lidar information are shown.

Closure experiment of 25 July 1995

General meteorological aspects and mixing state of the boundary layer

The first part of the day was cloud-free, with a gentle air flow from the east, thus a typical day for a closure study. Because of the cloud-free conditions, temperatures were rather high.

As indicated before, a closure test is only meaningful when the boundary layer air is completely mixed. Therefore the first step in the evaluation process is assessment of the state of mixing of the boundary layer. Analysis of the boundary layer Lidar signal showed that before 11:00 UTC an initial nocturnal surface inversion layer existed which vanished at the mentioned time, leaving a well-mixed boundary layer extending up to 1000 m.

Solar radiation measurements and AOD

The intensity of the direct solar radiation as measured at the two sites is shown in fig. 1.3 and indicated by I(ECN) and I(KNMI). The data from the site in the center of the country (KNMI, de Bilt) were used in the analysis because of clouds setting in early in the afternoon at the other site (ECN, Petten). Measurements after 16:00 were disregarded.

Figure 1.3 Measured and modeled intensity, I, in W m^{-2}, of the direct solar radiation (actually DNSI) at the two measuring sites. Io is the calculated intensity in the absence of aerosols. Shown is also the fit obtained assuming an aerosol optical depth of 0.12 and 0.15 and α (Angstrom coefficient) equal to 1.45, see text for further explanation.

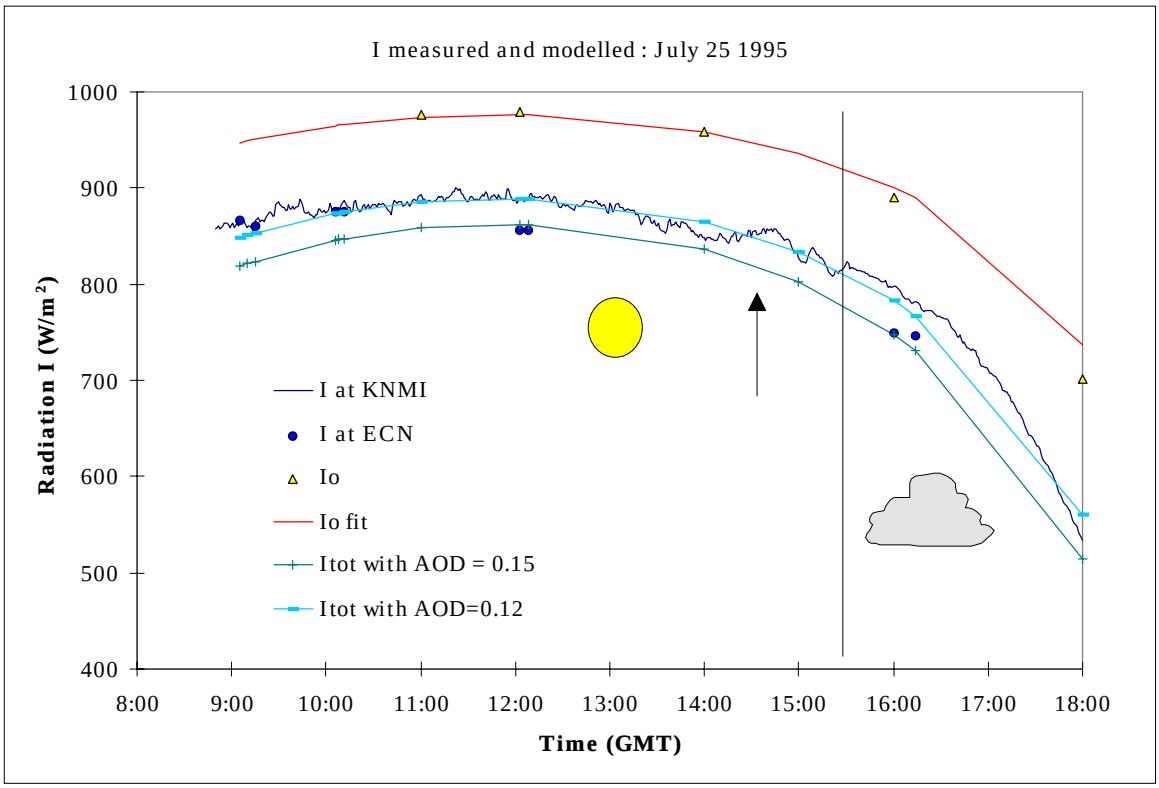

Table 1.2 Measured direct solar radiation intensity I and intensity calculated for an aerosol-free atmosphere Io on July 25 1996 at the measuring sites at the given time; also tabulated is the aerosol optical depth (at 525 nm) calculated from the difference in I and Io.

UT	Solar Elev Degrees	Io W m^{-2}	I W m^{-2} Petten	I W m^{-2} De Bilt	AOD Petten	AOD de Bilt
12:00	57.5	978	856	889	0.15	0.12
16:00	32.6	890	749	798	N.A.	0.12

Fig. 1.4 Sketch of the extrapolation of the boundary-layer AOD from ground-level Bsp, right panel, using the RH-profile from soundings (left) and the measured RH-dependence of the Bsp, mid-panel. The RH-dependence is expressed in the standard enhancement factor F(RH), which is the ratio of Bsp at a given RH to that at the "dry" reference RH, of 40%.

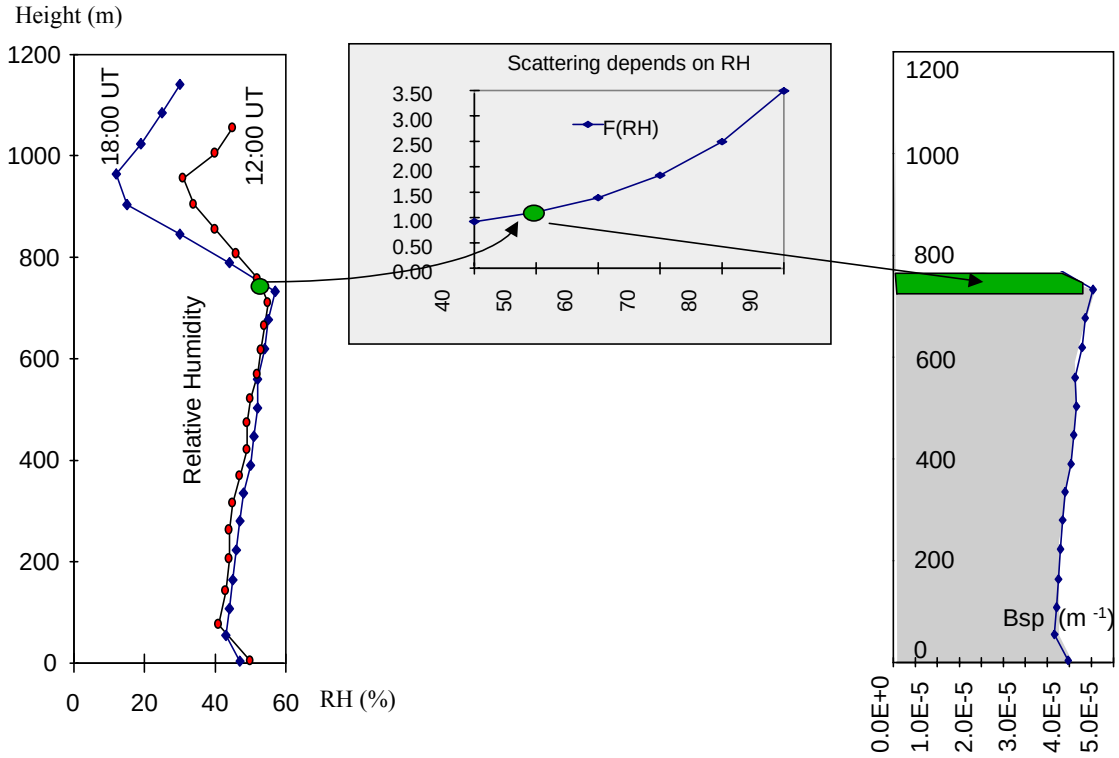

Boundary layer height and RH profile

Boundary-layer AOD

The boundary-layer AOD is obtained by integration of the light-scattering coefficient (Bsp), as measured at ground level, over the height of the boundary layer. The dry Bsp was rather constant over the afternoon. Its RH-dependence is shown in figure 1.4.

The balloon soundings at 12:00 and 18:00 UTC (fig. 1.4 upper left panel) were quite similar indicating a constant profile over the afternoon. Combining the RH-dependence of Bsp with the vertical RH-profile the actual vertical aerosol light-scattering coefficient profile is obtained, which is presented in the right panel of fig. 1.4. Summation (integration) of the Bsp values as a function of height up to the top of the boundary layer leads to the total scattering of

light by the aerosol in the boundary layer, the boundary-layer AOD. This value is listed in table 1.3.

Table 1.3 Bsp at ground level, boundary layer height and boundary-layer AOD (at 525 nm)

25-7-1995	Bsp (10^{-4} m-1)	Boundary layer Height	Boundary-layer AOD
base case	0.25	1000	0.028
RH +5%	,,	,,	0.031
RH –5%	,,	,,	0.025
mix layer hght	,,	1055	0.029
mix layer hght	,,	950	0.027

In the lower part of the table results of a sensitivity analysis are given. RH and the boundary-layer height were varied with the indicated amounts, representing the most probable value for their uncertainty. It is seen that the resulting relative uncertainty in the boundary-layer AOD is 25% for this day.

Closure between total and boundary-layer AOD

The boundary-layer AOD of 0.03 is much less than the total AOD of 0.15 even taking into account the uncertainty in the two values. It must therefore be concluded that closure was not applicable on this day. The absence of closure is in part due to aerosol absorption but the conservative estimate for its contribution to the AOD is less than 0.01 based on the concentration of black carbon [Berner et al, 1997]. The presence of aerosol above the boundary layer is supported by the (boundary layer) Lidar which clearly showed a residual layer of aerosol extending from 1000m to approximately 1500 m.

AOD of residual aerosol layers

The AOD of the aerosol above the boundary, extending up into the free troposphere has been analyzed from the troposphere Lidar returns, as discussed above. This analysis indicates some AOD in the residual layer. The results are presented in table 1.3 and fig. 1.5. As discussed in the experimental section the uncertainty in this AOD is rather large. Nonetheless even when

the maximum value for the residual-layer AOD is added to the boundary-layer AOD this (total) AOD is low compared to the total AOD from the radiation measurements.

Satellite AOD

For the day analyzed here the AOD was also evaluated with satellite retrieval. In such a retrieval, the solar light which is reflected by the aerosol into the direction of the satellite, is translated to AOD, see thesis of Veefkind [1999] for full details. The "retrieved" AOD for the Netherlands for 10:00 UT was 0.15, at a wavelength of 555 nm. This AOD_{555} is translated to an AOD that at reference wavelength of 525 via equation (3). Using α= 1.5 the average satellite AOD_{525} for the Netherlands is 0.14. This compares well with an AOD of 0.12 and 0.15, at the two radiation measurement sites, see table 1.2.

Interpretation and discussion

Both the radiation measurements and the satellite retrieval indicate a much higher AOD than that of the boundary layer alone. The Lidar returns cannot account for the "missing" AOD. This mismatch might be real or the result of an experimental error in the boundary-layer AOD. A possible potential explanation for the large mismatch is severe evaporation of ammonium nitrate in the integrating nephelometer. The additional heating might raise the temperature in the instrument to well above the temperature at which the mentioned compound evaporates [Dougle et al., 1998]. On a cloudless closure day in summer the air temperature is high and the RH as discussed above is low so that extra heating is not necessary.

It appears that this day, which was the most intensively studied because maximum information was available, is actually the most unsatisfactory example of closure. The reason for better closure on other days is presumably that the contribution of ammonium nitrate to the total the was smaller, so that relatively less of the light-scattering material evaporates, see for more details also Dougle et al. [1998].

July 26 1995

General meteorological conditions

The meteorological situation was quite similar to that on the day before. At 15:00 UTC cloud-cover was reported and therefore only data at the time of break up of the nocturnal inversion at 12:00 were used in the evaluation.

Total AOD

Only data of the solar radiation measurements in Petten are available. The AOD derived from the measurements is shown in fig. 1.5 and table 1.5.

Boundary-layer AOD

Bsp is rather constant over the period of interest with an average value of 0,82 10^{-4} m^{-1}. This, incidentally, is almost three times higher than the value on the day before. The mixing layer height as derived from Lidar, was 883 m.

Table 1.4 Bsp and calculated boundary-layer AOD (at 525 nm) on 7-26-1995

	Bsp in 10^{-4} m^{-1}	Boundary height	Boundary AOD
Standard	0.82	883	0.076
RH +10 %	idem	idem	0.093

Whereas the relative humidity at ground level in the center of the Netherlands was around 50%, it was higher at the measuring site. We used the vertical RH-sounding from the site in the center of the Netherlands, assuming an RH vertical profile shifted by 10% RH units to construct the vertical Bsp-profile at the measuring site, see table 1.4.

Closure between total AOD and boundary-layer AOD

As seen from table 1.5 the total AOD is a factor of two larger than the boundary-layer AOD. As mentioned, the RH at the measuring site was higher than that at the site of the vertical RH-sounding. We made the assumption that the RH in the boundary layer was even more increased at the measuring site and used an increased RH for the whole boundary layer of an additional 10%, see table. This would increase the boundary-layer AOD to 0.1. In that case still a substantial fraction of the total AOD should be caused by aerosol above the mixing

layer. This idea is supported by the tropospheric Lidar returns from which an AOD of aerosol above the boundary layer is derived of 0.13, see table 1.5.

Conclusion

The higher Bsp on this day, compared to the day before, is associated with a higher aerosol concentration advected from a southern direction; a more detailed discussion on the possible origin of this aerosol is given in the modeling chapter, section 2.5.2.

June 29 1995

AOD

The AOD was close to 0.1 in de Bilt; in Petten it was 0.165. The higher AOD at Petten as compared to de Bilt is presumably related to the higher RH there.

Boundary-layer AOD

Bsp was 0.4 10^{-4} m^{-1} on average. As mentioned, the RH was rather high. The boundary-layer AOD was 0.04, see table 1.5. Lidar indicated a significant amount of aerosol in a residual layer at a height between 750 m and 1700 m.

Other days

Other days evaluated so far are August 19 and 20 1996, October 27 1997, May 13 and November 23 1998. The results are tabulated in table 1.5 and graphically represented in fig. 1.5.

Fig. 1.5 Overview of Aerosol Optical Depth (AOD) values on the given days

Left: Boundary-layer AOD
Mid: Total AOD
Right: Sum of boundary-layer AOD and AOD in the layers above it

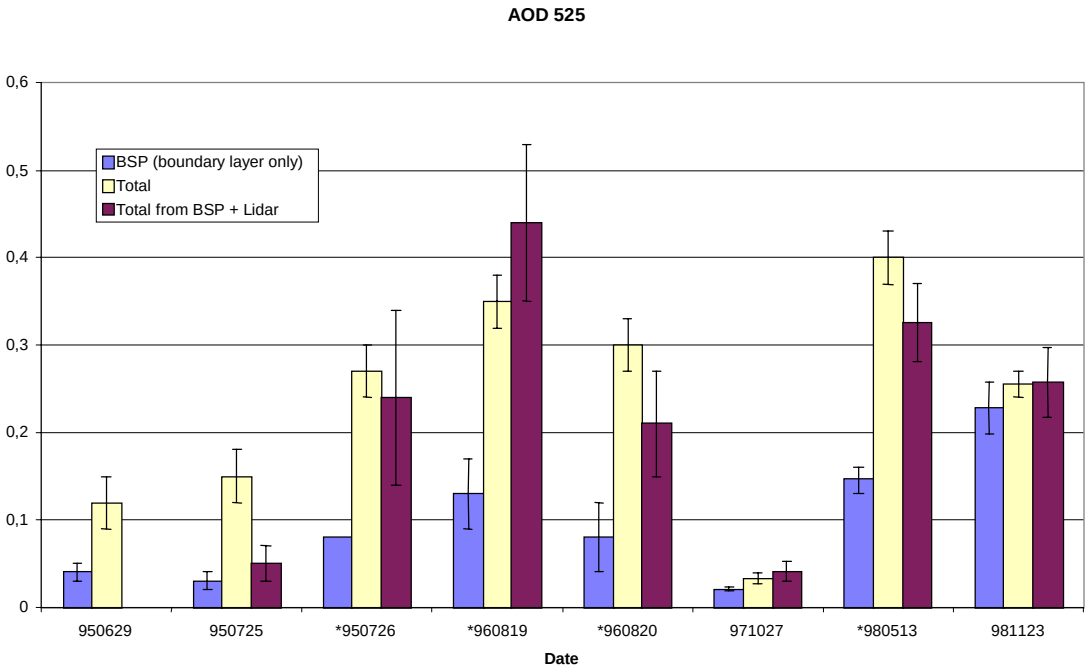

Table 1.5 Overview of AOD levels on closure days analyzed so far; the combined uncertainty in total AOD and boundary-layer AOD is around 20-30%, the other AOD's values are indicative, as described in the text; notice deviation for 27 October 1997.

date	boundary layer height (m)	total AOD	boundary AOD		residual AOD		free trop AOD
950629	700	0,12	0,04		n.a.		
950725	900	0,15	0,03		absent		0,02
950726	880	0,27	0,08		0,16		n.a.
960819	900	0,35	0,13		0,31		
960820	900	0.30	0,08		0,13		
971027	980	0,03**	0,02**		absent		0,02
980513	920*	0,41	0,15		0,18*		
981123	740	0,26	0,23		absent		0,03

Table 1.5 continued; older data.

931105	340	0.17	0.09				
931117	1010	0.11	0.10				
931118	690	0.15	0.135				
931119	400	0.12	0.11				
931124	270	0.18	0.10				
931129	760	0.19	0.11				

*) top of boundary layer ill-defined; residue layer extends to 1800 m
**) the low AOD values lead to higher combined uncertainty (40%)
in bold the examples of successful radiative column closure are indicated

In addition to the data in the present study, results from 1993 [Veefkind et al., 1996; Veefkind MS-thesis 1994] were reevaluated here using MODTRAN, instead of the cruder module used then. It turned out that the new results are not significantly different from the older data. Three days are excellent examples of radiative column closure, see table 1.5.

In the table also the, provisional, AOD for aerosol in residual layers and in upper ("free") troposphere is presented. Though the AOD of the free troposphere is the most difficult to quantify the table shows it is presumably of minor importance.

1.2.6 Discussion and preliminary conclusions

The conclusions given here are based on the data of the fourteen days analyzed so far. Closure, within the mentioned uncertainty limits, was found on four of those days. This was, apart from the November days in 1993, 21 November 1998. It is possible that closure also applied on 27 October 1997, but the large uncertainties in AOD does not allow a definite conclusion.

The number of days with closure seems small, but the good agreement between total AOD and boundary-layer AOD on those days gives confidence that column closure is attained when the aerosol is confined to the boundary layer.

In the other cases, on average half of the total AOD is contributed by aerosol above the boundary layer.

There is a very strong indication that the upper level AOD is confined to layer(s) directly adjacent to the boundary layer. Most of the upper layer aerosol is confined to a height of 3000 m. This has important implications for aerosol modeling, like that in section 3.1, since information on air transport is most reliable for levels up to 3000m.

Meteorological note: the height of the boundary layer on the summer days seems rather small. The strong surface heating on cloudless days result into very strong buoyancy. Adiabatic cooling in the associated rising airparcels leads to a continuous increase of RH with height, very often to the extent that cumuli develop. The requirement in closure studies that the RH should not approach saturation, is equivalent to the criterion that the vertical extent of the convections should be limited. On the closure days the convections are therefore suppressed: we speculate that they are counteracted from above by strong subsidence motions. The strong subsidence motions occur in the center of high pressure systems. It thus seems that column closure days are characterized by a synoptic situation with a strong anticyclone in the region. More definite conclusions with respect to this aspect can only be made when all of the days and also additional data from 1999 and the year 200 have been analyzed. This is done in the framework of another, ongoing, project.

References

ref 1 in table 1.1

J.P. Veefkind

"Scattering of solar radiation by aerosol in the Netherlands" June 1994

MS-thesis, ECN-R-94-013

ref 2 in table 1.1

J.P. Veefkind, J.C.H. van der Hage and H.M. ten Brink (1996)

"Nephelometry-derived and measured optical depth of the boundary layer"

Atmos. Research. **41**, 217-228.

E. Visser, A. Apituley, J.B. Bergwerff, J.A. Bordewijk, H.M. ten Brink, A.C.A.P. van Lammeren, H.A.J.M. Reinen and D.P.J. Swart (1996)
"RIVM's automated lidar system for climate research"
In: 'proc. EOS/SPIE European Symposium for Environmental and Public Safety' SPIE, volume 2505, 21-28.

A. Apituley, E.P. Visser, J.B. Bergwerff, J.M. de Winter, H. de Backer and M.A.F. Allaart (1997)
"RIVM Tropospheric Ozone LIDAR Routine Measurements, Validation and
Analysis",
In: "Advances in Atmospheric Remote Sensing with Lidar", A. Ansmann, R. Neuber, P. Rairoux and U. Wandinger(eds.), pp. 375--378, Springer-Verlag, Berlin,

Pauline G. Dougle, J. Pepijn Veefkind and Harry M. ten Brink (1998)
"Crystallisation of mixtures of ammonium nitrate, ammonium sulfate and soot"
J. Aerosol Sci. 29, 375-386

1.3 Comparison of Model-Estimated and Measured Solar Irradiance

H.M. ten Brink

The AOD at the reference wavelength for the column closure tests discussed in section 1.2 is obtained from the total reduction in solar radiation. Reduction in total solar radiation is caused by interception of solar light by aerosol but also by absorption of light by atmospheric trace gases like ozone and water vapor. In a co-operation with FEL-TNO (J.P. Veefkind) the amount of solar radiation intercepted by the gases was calculated using the radiative transfer model Modtran and standard data on the mentioned gases for the respective days. In a study performed as part of an agreement for co-operation with Brookhaven National Laboratory to share knowledge the opposite was investigated. In that study the direct solar irradicance, known as Direct Normal Solar Irradiance (DNSI) to the experts was deduced from AOD measurements and additional information on atmospheric trace gas loadings. DNSI was modeled with the same code and compared with measured DNSI. The agreement between

measured and model calculated values of DNSI was within 1% and the most important conclusion was that this agreement is nearly independent of airmass and water-vapor path. These results thus establish the accuracy of the current knowledge of the atmospheric extinction, especially that of water vapor as a function of wavelength as represented in MODTRAN-3 within that margin.

Adapted from:
"Comparison of model estimated and measured Direct-Normal Solar Irradiance"
Rangasayi N. Halthore, Stephen E. Schwartz, Joseph J. Michalski, Gail P. Anderson, Richard A. Ferrare, Brent N. Holben and **Harry M. ten Brink**
J. Geophysical Res (1997) **102**, 29991-3002

1.4 Trend in summer sulfate in Europe

B. Arends, H.M. ten Brink

North-West Europe is the only region on the globe with a large number of sulphate monitoring stations and therefore a search was made of its trend.

1.4.1 Approach

The trend analysis of the sulphate concentration was made for the summer half-year. The reason for this was that most solar radiation is received in this period and the influence of aerosols on a possible radiation trend is thus also most pronounced in that season. 1978 served as the reference year for the trend analysis, because then most stations started operation.

1.4.2 Results and discussion

The relative decrease in summer-sulphate at the densest network in Belgium was 3.3% per year, corresponding to an absolute decrease of 0.42 ug.m-3 per year. In The Netherlands the average yearly decrease in summer-sulphate at two stations, 80 km apart, was 3.5%. In nearby Northwestern Germany, a region with several monitoring stations, a yearly averaged decrease of 3.0% occurred. A similar decrease was found in southern Scandinavia.

The decrease in sulphate should have resulted in an estimated 3% increase in solar flux over the trend period, which is equivalent to an average increase in irradiance of 4 W m^{-2}. In Germany, the direct solar radiation, which is more sensitive to aerosols than the total radiation, did not show an increase over the years.

The reduction in atmospheric sulphate concentrations is the result of a reduction in emissions of sulphur dioxide, from which compound sulphate is formed in the atmosphere. The regional decrease in emissions is more than a factor of five over the trend period, whereas the decrease in sulfate is only a factor of two. It shows the non-linearity between the emission of the precursor sulphur dioxide and the product sulphate and is warning for those making scenario's for future sulphate concentrations assuming linearity, in IPCC-95 for instance. A more detailed discussion of the non-linearity is beyond the scope of the present report which focuses on assessing the present-day forcing but can be found in the first reference, of which the present section is a short summary.

References

B.G. Arends, J.H. Baard and H.M. ten Brink (1996): "Trends in summer sulphate in Europe" *Atmos. Environ.* **31**, 4063-4072

B.G. Arends, J.H. Baard and H.M. ten Brink (1997): "Trends in summer sulphate in NW-Europe". *J. Aerosol Sci.* **28**, S119-120

1.5 Associated more general publications on aerosol and radiative forcing

References

H.M. ten Brink (1996): "Reduction of solar radiation by aerosols in Europe". *Change* **30**, 13-14.

H.M. ten Brink (1997): "Antropogene aërosolen en de stralingsbalans van de aarde". *LUCHT* **13**, 121-125 (in Dutch; English abstract pg. 132)

H.M. ten Brink and A. Khlystov (1997): "Aerosol particles have a non-linear effect on climate". *Change* **38**, 11-13.

H.M. ten Brink (1999): “Aerosol, size and composition determine their effects”. . Proceedings Eurotrac Symposium 1998, pp 425-428

J. Slanina, H.M. ten Brink, and A.Y. Khlystov (1999): Policy Implications of Emissions Resulting in the Formation, Transport and Deposition of Aerosols. Proceedings of Eurotrac Symposium 1998, pp16-19.

2. RADIATION FORCING OF TROPOSPHERIC AEROSOLS

Rob van Dorland, KNMI

2.1 Introduction

The aerosol burden has increased considerably since preindustrial times due to anthropogenic emissions of SO_x and NO_x leading to the formation of sulphate and nitrate aerosols, respectively, via both gas and aqueous-phase chemistry. These gases and particles have relative small atmospheric lifetimes of the order of a few days in the troposphere. As a consequence, changes predominantly occur downwind of the industrial regions. The complexity of atmospheric chemistry, often critically depending on a variety of atmospheric conditions, also leads to a large variability in space and time of the concentration fields. Therefore, uncertainties are largely associated with estimates of the emissions of precursors and with the parameterizations of atmospheric chemical processes as well as the modeled transports. In addition, uncertainties in the microphysical properties of the sulfate aerosol such as size distribution, which influence the radiative properties, hamper accurate estimates of their radiative effects. In this respect, the relative humidity is an important parameter, since affects both the size distribution and the refractive index [*Nemesure et al.,* 1995*; Boucher and Anderson,* 1995*; Pilinis et al.,* 1995; *Veefkind et al.,* 1996]. Therefore, the direct radiative forcing due to anthropogenic sulfate and nitrate aerosols is poorly known, especially if compared to the forcing due uniformly mixed greenhouse gases [*IPCC,* 1995]. Since the cooling effects of aerosols are expected to compensate the enhanced greenhouse effect to a large extent on a global scale [*Van Dorland,* 1999], more accurate estimates are needed to calculate the total anthropogenic influence on climate and to make future projections of climate change.

In this chapter we discuss the work performed within the framework of the NRP-project MEMORA on the implementation of aerosol optical parameters in the radiation code. In addition we present radiative forcing calculations using either this radiation code or a derived analytical approach.

2.2 Global Aerosol Modelling

2.2.1 Aerosols in the ECHAM General Circulation Model

In the first phase of the NRP-II project, the radiation code of the European Centre HAMburg climate model (ECHAM, MPI, Hamburg) has been extended with the optical parameters of 11 aerosol components, derived from narrow band Mie calculations (Global Aerosol Data Set, *d'Almeida et al.,* 1991). The original optical parameters in ECHAM have been derived from *Tanré et al*. [1984]. They describe a mixture of aerosol components converted into five aerosol types, namely urban, maritime, continental, stratospheric and volcanic aerosol. Since the global aerosol fields from GADS have not been validated explicitly, the control climate of ECHAM has been determined using the geographycally and seasonally dependent optical thickness of the five aerosol types to account for the general extinction of solar radiation. In climate models it is important to include such kind of extinction in order to get the surface as well as top of atmosphere energy balance in approximate agreement with the satellite and ground based observations. In order to perform perturbation runs with ECHAM, such as the determination of the anthropogenic climate effects of sulfate as well as soot aerosols, it was decided to incorporate the optical parameters of GADS on top of the existing Tanré types.

The radiative effects of aerosols can be determined from three optical parameters: the extinction coefficient, the single scattering albedo, which is the ratio of scattered radiation and extinction, and the asymmetry parameter, giving the relative amounts of forward and backward scattered radiation. These optical parameters have been calculated for eight classes of relative humidity to account for the deliquescence properties of the aerosol components.

2.3 Radiative forcing due to tropospheric sulfate and nitrate aerosols

An off-line version of the ECHAM4 radiation code (KRCM: KNMI Radiative-Convective Model) has been used for the determination of the contemporary and future radiative forcing due to tropospheric ozone and sulfate aerosol increases as calculated with the MOGUNTIA transport-chemistry model [*Van Dorland et al.,* 1997]. We find global and annual average radiative forcings over the industrial period (1850-1990) of 0.38 Wm^{-2} and -0.36 Wm^{-2} for tropospheric ozone and sulfate changes, respectively. The calculated potential effects of nitrate aerosol are an order of magnitude smaller than of sulfate aerosols, at least on global

scale. Regionally, significant forcings up to -0.8 Wm^{-2} are found. New results are presented for the ozone and sulfate toward 2050. It is expected that the climate effects of ozone increase by another 70%, while the direct cooling effects of sulfate aerosols are estimated to increase with 150% as compared to the industrial period. Maximum changes of both constituents are shifting southward in the northern hemisphere as a result of the increasing industrial activities in countries with emerging economies. In this study, we derived an analytical expression for the direct (shortwave) forcing of sulfate aerosols as a function of surface albedo and cosine of solar zenith angle.

2.3.1 Sulfate aerosol radiative forcing

The sulfate burden of the atmosphere has increased considerably since preindustrial times due to anthropogenic SO_x emissions. As the residence time of sulfate aerosols in the troposphere is about 6 days due to the fast removal by dry and wet deposition, the strongest concentration increases are found in the vicinity of industrial areas. In MOGUNTIA the sulfur oxidation has been calculated using explicit oxidation chemistry, which is in between the slow and fast oxidation case described by *Langner and Rodhe* [1991]. For radii between 0.1 and 1 micron the particles are radiatively most active. Sulfate particles are hygroscopic and hence they accrete water vapor, especially above the so-called deliquescence point. The uptake of water implies that both the size distribution and the refractive index change, thereby modifying the optical parameters. For the tropospheric sulfate aerosol model experiments, we adopted the optical parameters of the water-soluble aerosol component (WASO) of GADS [*d'Almeida et al.*, 1991].

In this study we determine the anthropogenic sulfate effect in two ways. First, we fix the size distribution at a relative humidity of 80% for all locations and altitudes. Second, we repeat the experiments for the prescribed relative humidities up to a pressure level of 350 hPa. In the upper troposphere we assume a relative humidity of 50%.

The zonal average maximum change in optical depth (at 0.55 micron) of about 0.07 is found around 35ºN in February/March. The southeast Asia region shows the largest sulfate changes over the industrial period, amounting to 0.25 in optical depth. A second but much lower maximum of about 0.03 is found in the tropics in the southern hemisphere in

September/October and is associated with biomass burning. The sulfate increases over Europe are relatively small due to the effect of wintertime oxidant limitations. There are indications that our model underestimates European wintertime sulfate concentrations, possibly due to the neglect of an unknown oxidation mechanism. In contrast, a strong increase of sulfate is calculated over Europe in July.

The computed radiative forcing in the northern hemisphere is largest in March and amounts to -0.82 Wm^{-2} and -0.86 Wm^{-2} with the fixed RH of 80% and the RH dependent calculation, respectively. For the annual average the fixed RH run shows somewhat larger values of -0.60 Wm^{-2} against -0.54 Wm^{-2} for the RH dependent simulation. For the global and annual average radiative forcing we find -0.36 Wm^{-2} and -0.32 Wm^{-2}, respectively. Hence, on a global scale the difference between the fixed RH (80%) and the RH dependent run is small. However, differences of more than 0.2 Wm^{-2} are found in the zonal (annual) averages. Figure 2.1 shows the impact of the relatively dry subtropics and humid mid-latitudes on the radiative forcing when including the relative humidity dependencies of the sulfate optical parameters. The largest annual mean negative forcing due to sulfate changes occurs at 35ºN and at 55ºN for the fixed and the variable RH runs and amounts to -1.04 Wm^{-2} and -0.87 Wm^{-2}, respectively. In July the air is drier than 80% over large parts of the northern hemispheric continents. Consequently, the variable RH-run shows a smaller (negative) forcing up to 1 Wm^{-2} over southeast Europe. In January, the midlatitudes are much wetter than 80%, resulting in a much higher (negative) forcing up to 5 Wm^{-2} over east Asia.

Global or even zonal averages (Figure 2.2) are not very representative for the sometimes large regional radiative forcings. We find peak values of -4 Wm^{-2} over the southeast Asian region and about -2 Wm^{-2} over the United States and more than -1 Wm^{-2} over large parts of Europe in January. In July the largest (negative) forcing of about -5.5 Wm^{-2} is found over Europe and the United States, while the peak value over southeast Asia is reduced to -2.7 Wm^{-2}. This implies that, regionally, the positive forcing greenhouse gases can be completely offset by the direct effect of increasing sulfate aerosols. The very large sulfate burden and consequent radiative forcing over the southeast Asian region as compared to other regions in January is in fact a new result, mostly due to the updated emissions inventory [*Benkovitz et al.,* 1996] that puts more emphasis on this region and to the oxidant-limited sulfur oxidation scheme.

2.3.2 Nitrate aerosol radiative forcing

The effects of ammonium nitrate aerosols have also been investigated briefly. The main reason for this is that measurements in the Netherlands over the last two decades indicate that about half of the lightscattering is caused by material other than sulfate aerosols, namely, nitrate and to some extent carbonaceous aerosol as became evident from direct composition measurements [*Ten Brink et al.,* 1996].

As a first-order estimate we assumed that 50% of all boundary layer HNO3 over continents occurs as accumulation range ammonium nitrate. In the free troposphere this fraction is only 25%. It is implicitly assumed that nitrate in the marine mixed boundary layer is entirely present in sea-salt aerosol. *Dentener et al.* [1996] have shown that in mineral-dust-rich areas most nitrate may in fact be associated with dust, which would reduce the forcing of nitrate in these regions significantly. The latter aspect has not yet been considered. Further, we adopted the optical parameters of sulfates at 80% relative humidity for the radiative forcing calculations (H.M. Ten Brink, personal communication, 1996).

The change in nitrate optical depth as calculated by the MOGUNTIA model over the period 1850-1990 reaches its maximum value of about 0.04 over the United States in July (Figure 2.3a). For the same month secondary peaks are found over Europe (0.03), over southeast Asia (0.015), and over the central African region (0.02). The consequent calculated radiative forcing reaches its maximum value of -0.8 Wm^{-2} over western Europe and is larger than the peak of -0.6 Wm^{-2}, reached over the United States in July (Figure 2.3b). The largest forcing in January of -0.4 Wm^{-2} is found over southeast Asia. In fact, we found that the pattern of nitrate aerosol change is quite similar to the sulfate aerosol change. Nitrate aerosol changes in the southern hemisphere are negligible.

Annually averaged, the zonal mean radiative forcing is largest at 45ºN, and amounts to -0.11 Wm^{-2}. The calculated northern hemispheric mean forcing is about one tenth of the sulfate forcing, namely, -0.06 Wm^{-2}, varying from -0.05 Wm^{-2} in June to -0.07 Wm^{-2} in March. Hence, (ammonium) nitrate aerosol forcing can be significant in a few locations, but it appears to be of minor importance on hemispheric and global scales. It must be emphasized that the values of ammonium nitrate change and the consequent radiative forcing are very speculative.

Modelling efforts of the chemical cycle, as well as in situ measurements, are therefore strongly recommended.

2.4. Analytical fit for the sulfate (nitrate) shortwave forcing

Some effort has been devoted to investigate the sensitivity of the clear sky shortwave forcing to surface and atmospheric parameters for sulfate aerosol. The rationale for this is twofold. First, several studies on the direct sulfate aerosol forcing have been performed using a simple shortwave multiple-reflection model to estimate the dependencies on surface albedo, cloud cover, and solar zenith angle [*Charlson et al.,*1991; *Taylor and Penner,* 1994; *Pilinis et al.,* 1995] or using surface albedo changes so as to simulate the optical thickness of sulfates with GCMs [e.g., *Mitchell et al.,* 1995]. Second, a parameterization in which the solar zenith angle is taken into account creates the possibility for an analytical calculation of the error which is introduced by taking the daily average parameters as compared to accounting for the diurnal cycle. Our fits have been tested using the clear sky shortwave forcing over the period 1850-1990 for January as well as July, computed with a sophisticated radiation model. Each monthly average contains 648 points covering the globe with surface albedos ranging from 0.06 to 0.75, $\mu 0$ ranging from 0 to about 0.8, and day fractions ranging from 0 to 1. The shortwave forcings are normalized at an optical depth of 0.01 for sulfate.

First-order estimates of the sulfate aerosol shortwave forcing are commonly obtained using an analytical expression based on a simple one-layer multiple reflection model of the atmosphere, yielding a $(1-R_s)^2$ dependency [*Charlson et al.,* 1991]. We examined this relationship by plotting the normalized clear sky forcing in Wm^{-2} per 0.01 optical depth versus the day fraction (as solar fluxes are linearly weighted with this parameter) multiplied with the one minus surface albedo squared dependency (Figure 2.4a). It is evident from the scatter in this plot that large anomalies from this expression can occur. Also, the *Charlson et al.* expression does not generate positive sulfate radiative forcings at any location. Although it must be emphasized that *Charlson et al.* used this expression as a first-order estimate for the aerosol effect, it has been adopted in GCM studies as it helps avoid the difficulties associated with radiative transfer calculations.

In order to find an improved analytical expression for the sulfate forcing, we have performed radiation computations for the sulfate change profile at 45°N and 55°E in July over the period 1850-1990, varying the surface albedo and μ0 in steps of 0.1. The plotted values of the normalized forcing, ΔF/ΔSO4, at 0.01 optical depth (Figure 2.5) match best with the analytical expression

$$\frac{\Delta F}{\Delta SO_4} = S_0 \cdot f_d \cdot k \cdot [4xy(y-x)-r] \qquad (1)$$

where

S_0 is the solar constant (=1370 Wm^{-2}),

f_d is the day fraction (=1 in Figure 2.5),

$x = \mu_0^{0.5}$,

$y = (1-R_s)^{0.5}$,

$k = 5.8 \times 10^{-2}$ per unity optical depth, and

r = 0.05.

For high values of $R_s+\mu_0$ the shortwave sulfate forcing is found to be positive due to the fact that additional aerosol scattering is mainly absorbed by the surface and by other atmospheric constituents. In the real atmosphere, most values of R_s and μ_0 occur in the negative forcing region. In a cloudless atmosphere the backscattered fraction of the shortwave radiation is a function of the solar zenith angle and increases for more oblique incident radiation in case of mainly forward scattering media such as sulfate aerosols. This yields an increase of the normalized shortwave forcing towards the poles (equinox situation). Simultaneously, the absolute amount of solar insolation decreases from equator to poles and so does the forcing. These two opposing effects result in a maximum of the (negative) normalized forcing for some value of μ_0 , slightly depending on the surface albedo (Figure 2.5).

It must be emphasized that the computations have been performed with a two-spectral-interval shortwave model, which can introduce inaccuracies because of the wavelength dependence of Rayleigh scattering. Also, we have used the optical parameters of the water-soluble (WASO) aerosol [*Koepke et al.,* 1997], which is slightly absorbing in the near-infrared spectral region. This causes positive forcing to occur for smaller values of μ_0 as compared to calculations with high spectral resolution models for increases of purely scattering aerosols. For purely

scattering aerosols we find a zero forcing on a slightly curved line through μ_0=0.6, R_s=0.75 and μ_0=1, R_s=0.10 (Figure 2.5).

By evaluating other sulfate change profiles in a similar way as described above, we have investigated the sensitivity of the normalized forcing to the vertical profile of sulfate aerosol change. The largest differences, about 0.2 Wm^{-2} per 0.01 optical depth, are found for low surface albedos between the forcing due to upper and lower troposphere changes. The sensitivity to changes in relative humidity is quite small, because accreted water vapor changes the optical depth, which is normalized in the expression, rather than changing the characteristics of the water-soluble aerosol. The usefulness of this expression (Eq.1) can be obtained from actual radiation computations (at fixed relative humidity of 80%). In Figure 2.4b we plotted the normalized shortwave forcing per 0.01 optical depth versus the forcing expression using the actual day fraction. The scatter in this plot is caused either by the vertical profile of sulfate aerosol change or by normalizing very low values of optical depth changes to 0.01, yielding an enhancement of the deviation from the fit. Positive sulfate forcing is found over Antarctica in January and over Greenland in July due to relatively high values of both the surface albedo and μ0.

If we compare our analytical expression with the relationship between normalized forcing and surface albedo based on *Charlson et al.* [1991], we find large differences. If we assume the same forcing for the global and annual average, that is, μ_0=0.5 and R_s=0.114 then our calculations result in a forcing which is up to a factor of 1.6 larger for large solar zenith angles and high surface albedos and substantially smaller for small zenith angles and low surface albedos. Especially if the focus is on the regional effects of sulfate changes, the more sophisticated fit (Eq.1) should be used.

Differences between computations of the radiative forcing using daily average parameters and integrating the diurnal cycle can occur because our analytical fit (Eq.1) is not linearly proportional to μ_0. The largest differences of up to 0.06 Wm^{-2} per 0.01 optical depth are found at low latitudes over oceans, where μ_0 varies most during daytime and the surface is relatively dark. When adopting daily averages, the computed radiative forcing is more negative or less positive than the forcing evaluated with the inclusion of the diurnal cycle.

2.5 Radiative forcing due to sulfate aerosols in Europe

2.5.1 Sensitivity

The clear sky radiative forcing sensitivity, i.e. the forcing for a fixed change of sulfate aerosols (see section 3), is applied for Europe. In winter (Figure 2.6a) high latitudes are insensitive to aerosol changes caused by the polar night (f_d=0). We find the largest sensitivities over the subtropical Atlantic Ocean and the Mediterranean Sea of about 25 Wm^{-2} per unity optical depth. Oceans possessing low surface albedos show a larger sensitivity as compared to land surfaces with high surface albedos at the same latitude. In summer, we find sensitivities up to 60 Wm^{-2} per unity optical depth (OD) at high latitudes, where f_d=1 (Figure 2.6b). The seasonal cycle of the sulfate (nitrate) aerosol forcing is therefore strongest at high latitides.

The seasonal cycle of the sensitivity over the Netherlands is plotted for several values of the surface albedo (Figure 2.7). Over dark surfaces the sensitivity is largest in June (35 Wm^{-2} per OD) and smallest in December (21 Wm^{-2} per OD). For high surface albedos the situation is reversed. On average, the surface albedo over Dutch soils is between 15% and 25%. This implies that the combined effects of surface albedo, solar zenith angle and dayfraction on the sulfate (nitrate) aerosol forcing results in an almost constant daily average clear-sky forcing sensitivity in the Netherlands. However, cloud cover has a strong seasonal cycle in the Netherlands. As a first order approximation, cloud effects can be included by using the factor $(1-C_{cld})$ in Eq.1 (where C_{cld} is the cloud fraction, ranging from 0 to 1), implying no direct forcing for total cloudiness.

2.5.2 Case Studies

Within the NRP project several cases have been selected for a detailed investigation, i.e. a comparison between measurements and model results. In this study, we evaluate the modelled fields of sulfate aerosol burden using TM3 in terms of the direct radiative forcing. Hereto, a translation has to be made from aerosol mass into optical depth. This conversion factor depends strongly on the aerosol size distribution and therefore on relative humidity. Following the approach of *Kiehl and Briegleb* [1993], the aerosol optical depth (OD) is expressed as:

$$OD = f(RH) \cdot \alpha_{SO4} \cdot B_{SO4+NO3} \quad (2)$$

where α_{SO4} is the dry mass scattering coefficient of sulfate aerosols, i.e. extinction coefficient per unit of mass SO_4 at low relative humidity (RH) < 40% and is about 5 m^2g^{-1} at 0.55 μm [*Veefkind et al.,* 1996]; $B_{SO4+NO3}$ is the column burden of sulfate and nitrate aerosols; and f(RH) is the relative increase of the scatttering coefficient at given RH to the scattering at low relative humidity (*see section Ad Jeuken*). The relative humidity fields are calculated in TM3 from the water vapor and temperature fields. On line computations of the radiative forcing using the analytical expression (Eq.1) are performed by substracting the aerosol radiative effects in the control run from that of the perturbation run.

Three days were chosen for a first exercise modeling effort, which were cloudless days on which also successful column closure experiments were performed, see section 1.2: the 29th June 1995, the 25th of July 1995 and the 19th of August 1996. The latter day serves as an example for the modeling effort and outcome. The area covering the North Sea up to Italy is highly polluted with sulfate aerosols with peak values of more than 30 mgm^{-2} (Figure 2.8). The strong gradients in sulfate burden over Spain, Ireland and northern Europe coincide with the polar frontal zone (Figure 2.9). The nitrate aerosol burden shows peak values up to 2 mgm^{-2} over large parts of the United Kingdom, northern France, Belgium and The Netherlands. Both, the sulfates and nitrates result in an optical depth of 0.20 in The Netherlands (Figure 2.10). This implies a value of the mass scattering coefficient (in our region) of about 6.3 m^2g^{-1}. The subsequent radiative forcing is shown in Figure 2.11. Although aerosol optical depths are very high in front of the Norwegian coast (Figure 2.10), the radiative forcing is strongly reduced by the presence of clouds (Figure 2.9). For the Dutch grid we computed a radiative forcing of -2 to -3 Wm^{-2} (Figure 2.11). For the three investigated cases, we find daily average forcings of –0.8 Wm^{-2}, -1.5 Wm^{-2}, and –2.5 Wm^{-2} on the 29th of June 1995, the 25th of July 1995 and the 19th of August 1996, respectively. This indicates that on the regional scale increases of the sulfate and nitrate burden can act to (over)compensate the positive forcing due to greenhouse gases.

2.6 Conclusions

The global patterns of radiative forcing due to tropospheric sulfate and nitrate aerosol changes since preindustrial times, as well as for the future, based on the IS92a emission scenario [*IPCC,* 1992], has been assessed using a wide band radiation scheme. The aerosol fields have been computed with the MOGUNTIA transport/chemistry model using monthly averaged climatological data. We found global and annual averaged forcings of –0.36 Wm^{-2} and –0.04 Wm^{-2} for sulfate and nitrate aerosols over the industrial period, respectively. For the future (1990 to 2050) we calculated an additional radiative forcing of –0.59 Wm^{-2} due to sulfate aerosol changes, showing a southward shift associated with increasing industrial activities in countries with emerging economies in the near future.

The effect of relative humidity on the aerosol optical parameters, and on the sulfate forcing, has been studied for the given distribution of change. It appears that globally and annually averaged differences between the forcing computed with fixed relative humidity (at 80%) and that with a dependence is quite small, -032 Wm^{-2} against –0.36 Wm^{-2}. Zonal averages show larger differences up to –0.2 Wm^{-2}, especially in the dry subtropics and the humid mid-latitudes. Regionally, differences up to 5 Wm^{-2} are found. Hence, if the focus is on regional forcing, relative humidity effects should be included.

We developed an analytical fit for the clear sky sulfate (nitrate) shortwave forcing as a function of the surface albedo, the solar zenith angle and the day fraction. This parameterization have been tested for a wide range of occurring situations. We demonstrate that our analytical expression for the quantification of the sulfate forcing matches the radiation computations much better than the commonly used f_d x (1 – surface albedo)^2 relationship [*Charlson et al.,* 1991]. It also accounts for conditions of high surface albedo in combination with sufficiently small solar zenith angles, when the sulfate forcing can be positive.

We focus further on the changes of sulfate and nitrate aerosols over Europe, using the TM3 transport/chemistry model in which actual meteorology is updated every six hours. On line computations of the radiative forcing are performed using the above-mentioned analytical expression. The vertical distribution of sulfate (nitrate) aerosols is found to be of utmost importance due to the fact that the optical depth is strongly dependent on the relative humidity

and therefore on altitude (the boundary layer is usually much more humid than the free troposphere). For the three investigated cases, we find a daily averaged forcing of –1.6 Wm^{-2}. This indicates that on the regional scale increases of the sulfate and nitrate burden can act to (over)compensate the positive forcing due to greenhouse gases.

References

d'Almeida, G.A., P. Koepke and E.P. Shettle, *Atmospheric Aerosols Global Climatology and Radiative Characteristics,* 562 pp., A. Deepak Publ., Hampton, Va., USA, 1991.

Benkovitz, C.M., M.T. Scholtz, J. Pacyna, L. Tarrason, J. Dignon, E.C. Voldner, P.A. Spiro, J.A. Logan, and T.E. Graedel, Global gridded inventories of anthropogenic emissions of sulfur and nitrogen*, J. Geophys. Res., 101*, 29239-29253, 1996.

Boucher, O., and T.L. Anderson, General circulation model assessment of the sensitivity of direct climate forcing by anthropogenic sulfate aerosols to aerosol size and chemistry*, J. Geophys. Res., 100*, 26117-26134, 1995.

Charlson, R.J., J. Langner, H. Rodhe, C.B. Leovy, and S.G. Warren, Perturbation of the northern hemisphere radiative balance by backscattering from anthropogenic sulfate aerosols, *Tellus, 43AB*, 152-163, 1991.

Dentener, F.J., G.R. Carmichael, Y. Zhang, J. Lelieveld, and P.J. Crutzen, The role of mineral aerosol as a reactive surface in the global troposphere, *J. Geophys. Res., 101*, 22869-22889, 1996.

Intergovernmental Panel on Climate Change, *Climate Change 1992: The Supplementary Report to the IPCC Scientific Assessment,* edited by J.T. Houghton, B.A. Callander, and S.K. Varney, 200 pp.,WMO/UNEP, Cambridge Univ. Press, Cambridge, UK, 1992.

Intergovernmental Panel on Climate Change, IPCC *Second Scientific Assessment of Climate Change,* edited by J.T. Houghton, L.G. Meira Filho, B.A. Callander, N. Harris, A. Kattenberg and K. Maskell, 572 pp., Cambridge Univ. Press, Cambridge, UK, 1995.

Kiehl, J.T., and B.P. Briegleb, The relative roles of sulfate aerosols and greenhouse gases in climate forcing, *Science, 260*, 311-314, 1993.

Koepke, P., M. Hess, I. Schult, and E.P. Shettle, Global aerosol data set, *Report, 243*, MPI, Hamburg, Germany, 1997.

Langner, J., and H. Rodhe, A global three-dimensional model of the tropospheric sulfur cycle, *J. Atmos. Chem., 13*, 225-263, 1991.

Mitchell, J.F.B., R.A. Davis, W.J. Ingram, and C.A. Senior, On surface temperature, greenhouse gases and aerosols: Models and observations, *J. Clim., 8*, 2364-2386, 1995.

Nemesure, S., R. Wagener, and S.E. Schwartz, Direct shortwave forcing of climate by the anthropogenic sulfate aerosol: Sensitivity to particle size, composition and relative humidity, *J. Geophys. Res., 100*, 26105-26116, 1995.

Pilinis, C., S.N. Pandis, and J.H. Seinfeld, Sensitivity of direct climate forcing by atmospheric aerosols to aerosol size and composition, *J. Geophys. Res., 100*, 18739-18754, 1995.

Tanre, D., J.F. Geleyn, and J. Slingo, First results of the introduction of an advanced aerosol-radiation interaction in the ECMWF low resolution global model, in *Aerosols and their climatic effects,* H.E. Gerber, and A. Deepak (Eds.), 133-177, 1984.

Taylor, K.E., and J.E. Penner, Response of the climate system to atmospheric aerosols and greenhouse gases, *Nature, 369*, 734-737, 1994.

Ten Brink, H.M., J.P. Veefkind, A. Waijers-IJpenlaan, and J.C. van der Hage, Aerosol light-scattering in the Netherlands, *Atmos. Environ., 30*, 4251-4261, 1996.

Van Dorland, R., F.J. Dentener, and J. Lelieveld, Radiative forcing due to tropospheric ozone and sulfate aerosols, *J. Geophys. Res., 102*, 28079-28100, 1997.

Van Dorland, R., Radiation and Climate: from radiative transfer modelling to global temperature response, *thesis,* 148 pp, ISBN 90-646-4032-7, 1999.

Veefkind, J.P., J.C.H. van der Hage, and H.M. ten Brink, Nephelometer derived and direct measured aerosol optical depth of the atmospheric boundary layer, *Atmos. Res., 41*, 217-228, 1996.

Figure 2.1
Annual mean zonal averaged radiative forcing (in Wm^{-2}) due to sulfate aerosol changes over the period 1850-1990 as well as the period 1990-2050, using the fixed RH (80%) and the explicitly calculated RH dependency.

Figure 2.2
Hovmüller diagram of the zonal mean total radiative forcing (in Wm^{-2}) due to tropospheric sulfate aerosol changes for the period 1850-1990 as computed with the radiative transfer scheme (KRCM) using the calculated fields of MOGUNTIA.

Figure 2.3a:
July average optical depth (OD) change (in 0.01 OD) of tropospheric nitrate aerosol since preindustrial times (1850-1990) as calculated by the MOGUNTIA model.

Figure 2.3b:
July average total radiative forcing (in Wm^{-2}) due to tropospheric nitrate aerosol since preindustrial times (1850-1990).

Figure 2.4a:
Normalized sulfate shortwave forcing (in Wm^{-2} per 0.01 increase in optical depth (visible region)) versus day fraction x $(1 - \text{surface albedo})^2$ for January and July over the period 1850-1990.

Figure 2.4b:
Normalized sulfate shortwave forcing (in Wm^{-2} per 0.01 increase in optical depth (visible region)) versus forcing expression (Eq.1) for January and July over the period 1850-1990.

Figure 2.5:
Comparison of the normalized sulfate shortwave forcing (in Wm^{-2}) per 0.01 increase in optical depth (visible region) between radiation computations (shaded) for the change at 45ºN and 55ºE over the industrial period and the analytical expression (Eq.1) for the sulfate forcing (contours).

Figure 2.6:
Daily averaged sulfate shortwave forcing sensitivity (in Wm^{-2} per unity optical depth (OD)) for typical values of the surface albedo, solar zenith angle and day fraction over Europe at the 1st of January **(a)** and at the 29th of June **(b)**.

Figure 2.7:
Daily averaged sulfate shortwave forcing sensitivity (in Wm^{-2} per unity optical depth (OD)) for four values of the surface albedo as a function of the day number.

Figure 2.8:
Sulfate aerosol burden (in mgm^{-2}) over Europe at the 19^{th} of August 1996 as calculated with TM3.

Figure 2.9:
NOAA satellite image (visible channel) of Europe at the 19th of August 1996 (12.31 UT).

Figure 2.10:

Sulfate and nitrate aerosol optical depth (at 555 nm) over Europe at the 19th of August 1996 as calculated with TM3, using relative humidity to correct the dry mass scattering coefficient.

Figure 2.11:

Radiative forcing due to sulfate and nitrate aerosols (in Wm^{-2}) over Europe at the 19^{th} of August 1996 as calculated with TM3, using the analytical expression (Eq.1).

3. AEROSOL CYCLE IN EUROPE

GENERAL INTRODUCTION

Sulfate, nitrate and a better part of the carbonaceous aerosol material are not the result of direct emissions and projection of future aerosol loadings and forcing must therefore be based on reliable models of their cycle of formation and removal in the atmophere. Models like MOGUNTIA use monthly averaged aerosol fields and corresponding average values of the aerosol properties. However, actual aerosol-concentration fields change from day to day, depending on synoptic conditions. Thus more detailed models are needed which describe the fields on a day to day basis using actual meteorological data. Since nitrate obviously is of importance regionally the model should also calculate the nitrate cycle. For this purpose the resolution of an existing model TM3 was improved and a nitrate module included. To be able to compare modeled and measured value, the actual mechanism of formation of sulfate and nitrate should be incorporated in models. This aspect was also addressed in the study.

3.1 Modelling the ammonium sulphate and nitrate aerosol distributions over Europe with the chemical tracer transport model tm3

Ad Jeuken, Peter van Velthoven KNMI

3.1.1 Introduction

In this chapter the development of the chemical tracer transport model TM3 with respect to the modelling of the sulphate and nitrate aerosol cycle is described and model results are evaluated using measurements available from ECN and RIVM as well as from other European institutions.

The TM3 offline chemical tracer transport model has gradually evolved from the TM2 model as developed by Heimann [1995] at the end of the eighties. Throughout the years the applications for the model have shifted from studies of long-term trends of long-lived species like carbon dioxide and methane via tropospheric ozone to studies of the chemistry and transport of shorter-lived species like nitrogen oxides, isoprene, sulfur dioxide and ammonia.

These short lived species require a better model description of transport and source and sink processes, since the variability on time scales larger or equal to the chemical lifetime should be captured. Within the MEMORA project we have therefore worked on model improvements necessary to perform simulations of highly variable aerosol species with an accuracy higher than before.

Ammonium-sulphate and -nitrate aerosols vary strongly both spatially and temporarily. The main reasons for this are the irregularly spaced sources of the precursor gases SO_2, NO_2 and NH_3, the strong dependence of SO_2 oxidation and aerosol scavenging on cloud and precipitation processes and the strong dependence of nitrate aerosol concentrations on relative humidity and temperature. The concentration distribution of SO_2 and NH_3, in addition, strongly depends on dry deposition at the surface, since the deposition velocities vary considerably depending on surface characteristics and local meteorology.
Vertical mixing in the boundary layer in addition plays a key role in the life cycle of aerosols since it serves to ventilate the boundary layer where the major emissions occur. In this way vertical mixing contributes to the supply of oxidants and the rapid transport of SO_2 and NH_3 to the clouds.
Due to a limited resolution and due to rather crude parameterisations of the before mentioned processes current models have difficulties to simulate the observed variability in aerosol concentrations correctly. Therefore, the boundary layer diffusion, the wet scavenging, dry deposition and cloud- and aerosol chemistry in TM3 have been adapted and improved to be better able to simulate the variability of aerosols and its precursors correctly and obtain more accurate estimates of aerosol radiative forcing.

To evaluate the model, we compare its results with various measurements. Here we present a selection of these results. For a complete overview we refer to Jeuken [2000]. First we will focus on the global scale and compare the TM3 model results with monthly averaged measurements at the background sites used in the COSAM (Comparison of large scale atmospheric sulphate aerosol models) workshop [Barrie et al., 2000] in which we have participated with TM3. To assess the model's ability to represent free tropospheric sulphate,

we will consider profiles measured during a few aircraft measurement campaigns. Finally we look more specifically at model results for Europe. Day to day variations and daily cycles are compared to ground based measurements. We will especially focus on the selected days for MEMORA with complete measurements in Petten and Bilthoven. In addition model results for Europe will be looked upon from quite a different perspective by comparing model calculated aerosol optical depths derived from aerosol sulphate, nitrate and associated water with satellite retrieved optical depths from ATSR-2 and GOME.

3.1.2 Model description

In TM3 the chemical continuity equation is solved:

$$\frac{\partial \mu}{\partial t} = -\vec{v} \cdot \vec{\nabla} \mu + \left\{ \frac{\partial \mu}{\partial t} \right\}_{conv} + \left\{ \frac{\partial \mu}{\partial t} \right\}_{diff} + S$$

with μ the tracer mixing ratio which is advected by the three-dimensional wind field *v* and transported by parameterised convection (*conv*) and turbulent diffusion (*diff*). *S* is the net source term which can be subdivided in emissions, chemical production or destruction, the loss of a tracer by precipitation scavenging processes and the loss of a tracer by dry deposition at the surface,

$$S = S_{emis} + S_{chem} + S_{scav} + S_{depo}$$

Three-dimensional tracer transport in the model is accounted for by advection for the resolved motions and by convection and vertical diffusion for the unresolved motions (the sub-grid scale). The advection of tracers in the model is calculated with the slopes scheme of Russell and Lerner [1981] . The sub-grid scale convection fluxes are calculated using the scheme of Tiedtke [1989]. The other model parts will be discussed in more detail below.

Photo-chemistry

The sulfur cycle is coupled to the chemistry version of TM3 as described by Houweling [1998]. This chemistry model describes the background tropospheric CH_4-O_3-HO_x-NO_x chemistry and the chemistry of Non Methane Hydro Carbons (NMHC's) lumped in groups, using a modified version of the widely used Carbon Bond mechanism [Gery et al., 1989].

Compared to the current TM3 version we use the photolysis scheme adapted from Krol and van Weele [1997] consistently with local cloud cover and ozone columns.

We have added the gas and cloud phase reactions of SO_2, DMS, NH_3, SO_4^{2-} and NH_4^+ [Dentener and Crutzen, 1994]. SO_2 is oxidised in the gas phase by the OH radical, ultimately producing sulphate. The reaction of DMS with OH has several pathways, which are not completely understood yet. Besides SO_2 Methyl Sulphonic Acid (MSA) is a major product of this reaction. Two major steps can be identified, one leading to SO_2 only and one leading to 75 % SO_2 and 25 % MSA.

Aqueous phase chemistry

We also included the aqueous phase reaction of the sulphur species in TM3. SO2 and its oxidants H_2O_2 and O_3 are dissolved into the cloud droplet according to their Henry's Law equilibrium. For SO_2 an effective Henry's law constant is used, taking into account dissociation into HSO_3^- and SO_3^{2-}, effectively allowing more SO_2 to dissolve. Dissolved SO_2 and its dissociation products can be denoted as *S(IV)* i.e. total sulphur in oxidation state 4 and consists of $[SO_2 \cdot H_2O]$, $[HSO_3^-]$ and $[SO_3^{2-}]$ [Seinfeld, 1986]. Both the dissociation equilibrium and rate coefficients are pH dependent. Ignoring the contribution of weak acids and bases the pH ($-\log[H^+]$) is calculated from the strong acids and bases as:

$$[H^+]=2[SO_4]_a+[MSA]_a-[NH_4]_a+[HNO_3]_g+[NO_3]_a$$

where subscripts a and b stand for dissolved aerosol and gaseous species respectively. For pH>4.3 also the dissociation of the weak acids SO_2 and CO_2 as well as the base NH_3 is taken into account. With the concentration H^+ known, the effective Henry's law coefficient for *S(IV)* can be calculated.

The reaction of *S(IV)* with ozone can be written as 2 independent reactions of which one increases strongly with increasing pH. This pH dependency of the O_3 reaction is stronger than that of the H_2O_2 reaction. This means that with increasing pH the O_3 reaction will become more important.

Aerosol equilibrium model

Recent measurements [ten Brink et al., 1997] indicate that nitrate may constitute an important mass fraction of the aerosol, and that therefore simulations of the sulfur cycle alone may not always be sufficient to obtain the aerosol optical properties such as the radiative forcing. However, the aerosol optical properties also strongly depend on the hygroscopicity (=aerosol associated water), which in turn depends on the composition of the aerosol. The latter is difficult to model in a global model, since species such as nitrate, are volatile and partition between gas and aerosol phase. Furthermore, the gas-aerosol partitioning strongly depends on the ambient relative humidity and temperature, in addition to the aerosol precursor gases (HNO_3, NH_3) and pre-existing aerosol particles. Therefore, we have accounted for the gas-aerosol partitioning of the ammonia-sulphate-nitrate system, by adding a simplified thermo-dynamical equilibrium model [Metzger, 2000]. An EQM describes the equilibrium partitioning between aerosol precursor gases (NH_3, H_2SO_4, HNO_3, and HCl) and liquid and solid aerosol phases for major inorganic aerosols compounds (ammonium, sulphate, nitrate, sea salt, mineral dust).

Based on fundamental physical properties, a new method has been introduced, which allows to calculate the gas-aerosol partitioning for global modelling rapidly and accurately.

The method is based on the fact that, for atmospheric aerosols in thermodynamical equilibrium with the ambient air, the solute activity, and hence the activity coefficient calculation, is governed by the aerosol associated water. The latter depends only on the relative humidity and the type and number of moles of dissolved matter. Central in the method is the use of concentration domains, which are based on the mole ratio of the solute concentrations. For instance the aerosol can be in the “sulphate rich” domain (i.e. $2NH_4^+ < SO_4^{2-}$) or in the sulphate poor case (i.e. $NH_4^+ > SO_4^{2-}$). Based on the domain and the relative humidity the aerosol associated water amount can be calculated and from this it is possible to directly derive the activity coefficients using a generalization of Raoult's law. The activity coefficients calculated non-iteratively with the new method, compare well with those obtained with common iterative methods of various EQMs. Since the new method is an inexpensive and straightforward alternative to the explicit and more expensive thermodynamic calculations, it is suited for large scale aerosol chemistry transport models.

In TM3 the above described EQM is implemented to calculate the gas-aerosol partitioning of NH_3, NH_4^+, HNO_3, NO_3^- and SO_4^{2-}. Removal of ammonium nitrate by wet scavenging and by dry deposition is treated the same as for sulphate aerosol, thus implicitly assuming similar physical properties as sulphate.

Emissions

Anthropogenic emissions of NO_x, NH_3, SO_2 have been taken from the historical Emission Database for Global Atmospheric Research (EDGAR) [Olivier, 1996] calculated on a grid of 1^o by 1^o. Van Aardenne et al. [1999] have estimated trends in these emissions, based upon demographical, economical, agricultural and technological developments during the past century. The time resolution of the database is 10 years until 1970 and 5 years hereafter unto 1990. After 1990 we have extrapolated the 1990 emission data based on the increase of energy consumption. The seasonal variation in NO_x and SO_2 is based upon the Global Emission Inventory Activity (GEIA) database valid for 1985 [Benkovitz et al. 1996]. The GEIA database distributes the emissions between two layers, below and above 100m height. Data per grid cell have been normalised in such way that the annual and two level total equals one. These seasonal and vertical weight factors have been applied to the EDGAR annual totals. Volcanic sulfur emissions are estimated by Andres and Kasgnoc [1998] . They distinguish between continuously and sporadically erupting volcanoes. DMS emissions are obtained by combining the oceanic surface concentrations compiled by Kettle et al. [1998] with turbulent air-sea exchange coefficient calculated by using the parameterization by Liss and Merlivat [1986] . For DMS land-emissions and SO_2 natural emissions we use the estimates of Spiro et al. [1992]. All other emissions are described in Houweling et al. [1998].

For Europe we use SO_2 emissions from the CORINAIR (COre INventory AIR) project. In contrast with the global EDGAR data after 1990, reported CORINAIR emissions take into account the changes in emission factors, e.g. changes in the conversion factors from fossil fuel use by electric power generation to SO_2 emissions. While the total of SO_2 emissions for Europe in the extrapolated EDGAR database is 22 Tg S, it is only 12 Tg S in the CORINAIR database. This remarkable difference naturally must lead to differences in model results depending on which emission data are taken.

Wet scavenging

Instead of using a climatology of the vertical distribution of precipitation rates, in the new proposed scavenging scheme the generation of precipitation is calculated in TM3 itself from the cloud liquid and ice content obtained from ECMWF. In this way a three-dimensional distribution of precipitation was obtained which was applied to remove gases and aerosol by large-scale precipitation. The removal of tracers in convective clouds has been parameterised as a function of the updraft mass flux [Balkanski et al., 1993].

The radio active decay daughter of radon ^{210}Pb was used to test the new scheme [Jeuken, 2000]. Since ^{210}Pb attaches indiscriminately to aerosol particles and has no other sinks than wet and dry deposition it is a good tracer to validate the removal of aerosols by precipitation scavenging. It was concluded that in comparison with the old scavenging scheme used in TM3, ^{210}Pb was removed by precipitation much more effectively, especially at high latitudes. In comparison with measurements the new scheme appeared to be superior. However, in wintertime there seems to be a slight over estimation of observed ^{210}Pb surface concentrations.

In TM3 we use HNO_3 as the reference for a completely soluble gas. The scavenging rate for any other gaseous specie is scaled to the scavenging rate of HNO_3 according to its Henry equilibrium constant [Dentener and Crutzen, 1993]. The Henry coefficient of SO_2 is with 1.24 M atm^{-1} at 298 K about 2. 10^5 times lower than for HNO_3. This means that most SO_2 would reside in the gas phase and that it would hardly be scavenged by rain. We have seen that due to dissociation of SO_2 in the water droplet the effective Henry coefficient is much higher. This effective Henry coefficient is used in the cloud chemistry to describe the dissolution and reaction of SO_2. So the in-cloud scavenging of SO_2 is already accounted for via the cloud chemistry. For below-cloud scavenging we assume that the amount of SO_2 scavenged is only limited by the amount of H2O2 in the falling rain with a pH below 5 assuming fast reaction of H_2O_2 and *S(IV)*. Above pH=5 the below-cloud scavenging rate of SO_2 is equal to the rate of HNO_3, assuming that oxidation by O_3 effectively removes *S(IV)*. By keeping track of the amount of H_2O_2 and H+ scavenged in the grid cells above, the below cloud scavenging rate of SO_2 is calculated. This simplified method probably presents an upper limit for the below

cloud scavenging of SO_2 since it assumes that the reactions and dissociation processes are fast compared to the time scales of existence of rain droplets.

Boundary layer vertical diffusion

For short-lived components like SO_2 and NH_3 with large and heterogeneous emission sources within the boundary layer, vertical mixing should be well represented in the model. Therefore we have implemented a new boundary layer scheme similar to the scheme used in the ECMWF model [Beljaars and Viterbo, 1998].

For stable atmospheric conditions we use a local formulation based on the work of Louis [1979] and for unstable conditions a non-local formulation based on the work of Holtslag and Boville [1993]. In addition we have increased the time resolution from 6 to 3 hours.

To exclude effects of chemistry, deposition and wet scavenging, the radio nuclide radon (^{222}Rn) has been used to test the influence of the new vertical diffusion scheme in TM3 [Jeuken, 2000]. Simulated radon concentrations from a model run with and one without the new parameterisation were compared with measurements. It was concluded that mainly due to the better temporal resolution of 3 hours instead of 6 used for the new scheme the diurnal cycle in radon surface concentrations is much better resolved by the model. In addition also the absolute concentrations were better simulated with the new diffusion scheme but were still somewhat overestimated by the model indicating that mixing remains underestimated. It was suggested that the parameterisation of vertical diffusion is sensitive to the resolution of the meteorological input data, which is lower than the original resolution of the ECMWF model. Due to interpolation of the ECMWF wind and temperature fields to the input resolution of TM3, profiles become smoother and more stable resulting in less mixing. It is therefore recommended that diffusion coefficient are calculated at a resolution as close as possible to the original ECMWF resolution.

Dry deposition

Dry deposition is the major sink for soluble or reactive trace gases like SO_2 and NH_3. Especially in wintertime when low H_2O_2 concentrations limit SO_2 oxidation it will be the dominant sink for SO_2. Therefore we use the "resistance in series" dry deposition scheme as described by Ganzeveld [1998], which contains a fairly detailed description of surface characteristics. The deposition velocity can be written as the reciproke of the aerodynamic resistance, the quasi-laminar boundary layer resistance and the surface resistance. The surface resistance of SO_2 strongly depends on snow cover and surface wetness. For sulphate aerosol the deposition velocity is dependent on two parameterised size distributions, one for land and one for oceans, and further depends on the wind velocity which may increase the contact surface area over ocean when the sea becomes rough. Most meteorological surface fields like for example the aerodynamic resistance are obtained from the ECMWF archive. Vegetation descriptions are derived from a global ecosystem database [Olson, 1983]. Variables like snow cover and surface wetness are prescribed by ECHAM4 climatological data [Claussen, 1994].

3.1.3 Results

In this section results from different model simulations are presented. Simulation A1 is done with the TM3-model with the old vertical diffusion parameterisation, A3 with the above-described new parameterisation. Simulations A1 and A3 are performed at a resolution of 4^o by 5^o and 19 vertical levels A4 and A5 at 2.5^o by 2.5^o and 31 levels. Except for the resolution A4 is similar to A3. Simulation A5 is done with CORINAIR SO_2 emissions for Europe.

We compare model output with measurements selected for the COSAM model inter comparison workshop [Barrie et al., 2000]. In order to utilise consistent measurements, with similar collection and analysis techniques, data from the large-scale networks were preferred. The sites are chosen based upon their location on the periphery of source regions and in more remote areas downwind of source regions. Results

For a few sites for sulphate are shown in Figure 3.1. Statistics for different regions for SO_2 and sulphate are shown in figure 3.2.

Figure 3.1
Monthly averaged concentrations for sulphate at selected stations with standard deviation of daily measurements (vertical bars) for 1993. A3 is model simulation with new and A1 with the old scheme for vertical diffusion.

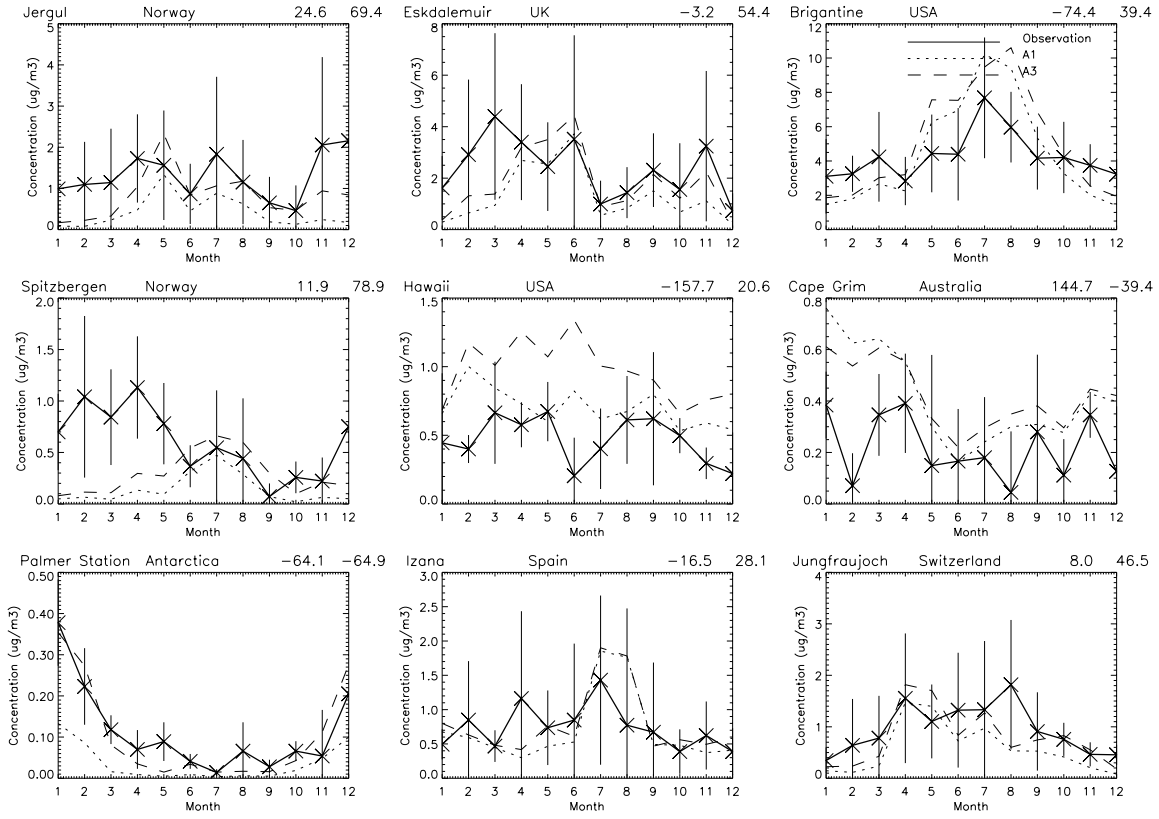

For sulphate, winter concentrations are clearly underestimated by TM3 and SO_2 concentrations (not shown) are highly overestimated. Including the new vertical diffusion parameterisation yields a small improvement, except for Hawaii. Figure 3.2 confirms this. In this figure the average difference model - observation for all COSAM sites is presented. In addition sites have been subdivided per area. Especially for SO_2 the TM3 model strongly overestimates the measurements. As was also reported by other researchers, the bias is larger for Europe than for North America, e.g. Koch et al. [1999]. The underestimation of sulphate concentrations is similar for Europe and North America. Remarkably, the underestimation of sulphate concentration is relatively smaller than the overestimation of SO_2.

We also compared TM3 model results with profile measurements over North America (not shown) and the Pacific ocean. The Pacific Exploratory missions PEM West A and B took

place over the northern and central West Pacific Ocean, in September/October 1991 and February/March 1994 respectively [Dibb et al.,1996]. Aircraft measurements of aerosol composition and various trace gases were made to estimate the impact of anthropogenic emissions from China and Japan in this pristine oceanic region. Reported accuracy's for the measurements are 10% for sulphate, SO_2 and H_2O_2. For PEM-West A little outflow of polluted air from Asia was measured while for PEM-West B considerable amounts of pollution were transported over the ocean in a well mixed boundary layer below 4 kilometre.

Figure 3.2
Mean (symbols), median (lines) and standard deviation (vertical lines) for the difference between observed and modeled SO_2 and sulphate. Definition of regions: North America (140W-35W,25N-90N), Europe (35W-80E,30N-90N), Oceania (80E-180E,60S-0S).N denotes number of monthly averages in plot.

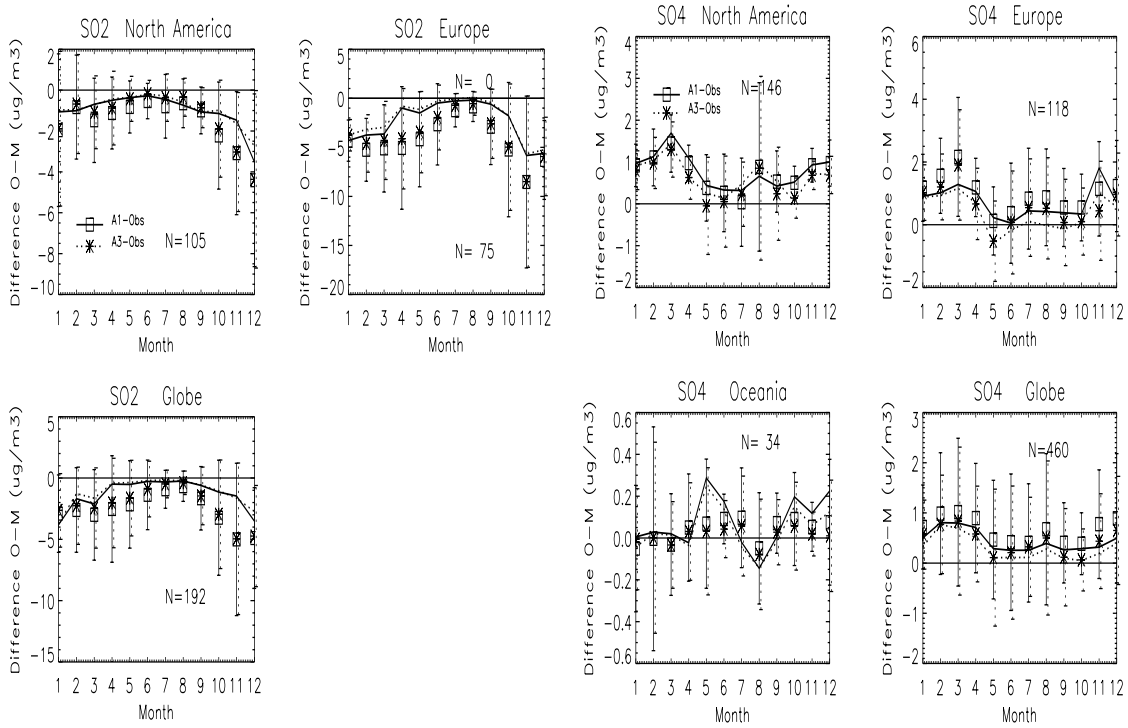

Figure 3.3
Average SO_2, sulphate and H_2O_2 profiles for PEMW-A October 1991 (upper panels) and PEMW-B February 1994 (lower panels) + 1 σ. Observations are represented by the solid and the model by dashed line.

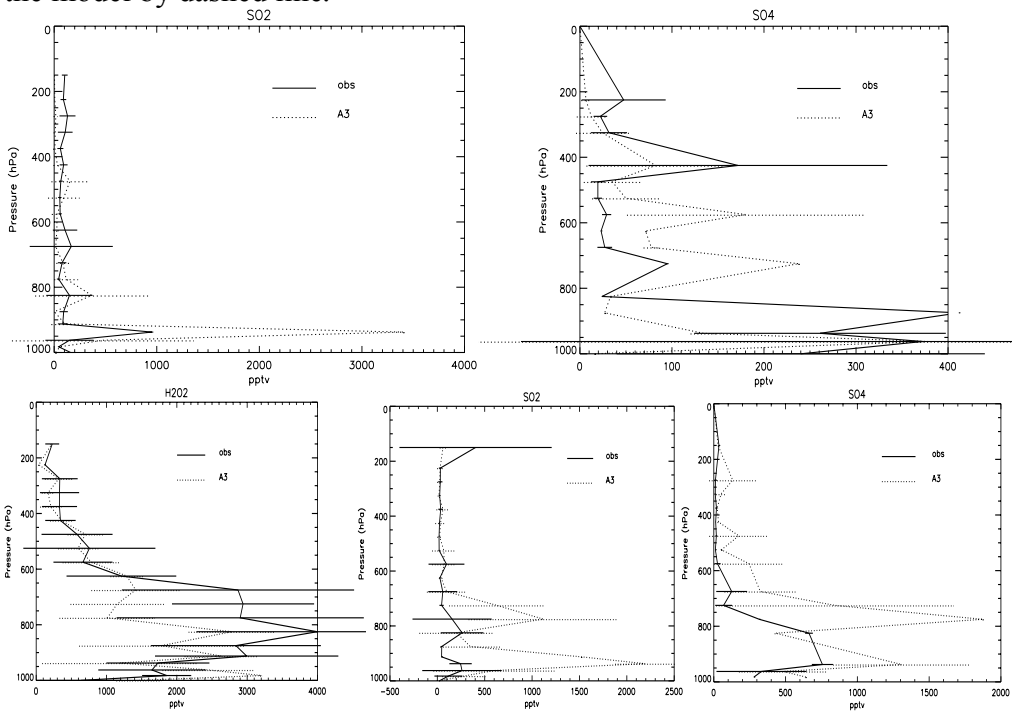

As sulphate is not continuously measured we have averaged all available aircraft measurements over 20 vertical levels between the surface and 10 hPa. Model simulated values were interpolated to the time and location of the aircraft measurements and averaged in the same way.

Figure 3.3 shows that for all components the agreement between model and measurements is good. The model overestimates the observed peak concentrations of sulphate, especially for the PEM-west B campaign. It should be noted, however, that at some levels there is only one observation available. H_2O_2 seems to be underestimated by the model in the free troposphere. Due to the fact that measurements have been taken at various locations with different pollution characteristics, the scatter in the data is large. The model also represents the variability in the measured profiles.

It should be realised that these aircraft campaigns merely present a detailed snapshot for a certain period and area. Model simulated profiles have been compared to profiles from three distinctly different regions. For the coastal location of Nova Scotia, Canada (not shown) the model seems to have difficulties to simulate the long-range transport of pollution plumes. For the continental location just North of the Toronto urban area boundary layer concentrations of SO_2 are overestimated which, in this case, could be an indication of oxidant limitation [Jeuken, 2000]. For both locations sulphate is underestimated. For the remote area of PEM West A and B the model below 600 hPa overestimates both sulphate and SO_2. For the moment it is not clear what are the causes of these discrepancies as there are many model uncertainties.

Figure 3.4
Comparison between model and EMEP measurements for sulphate for August 1997.

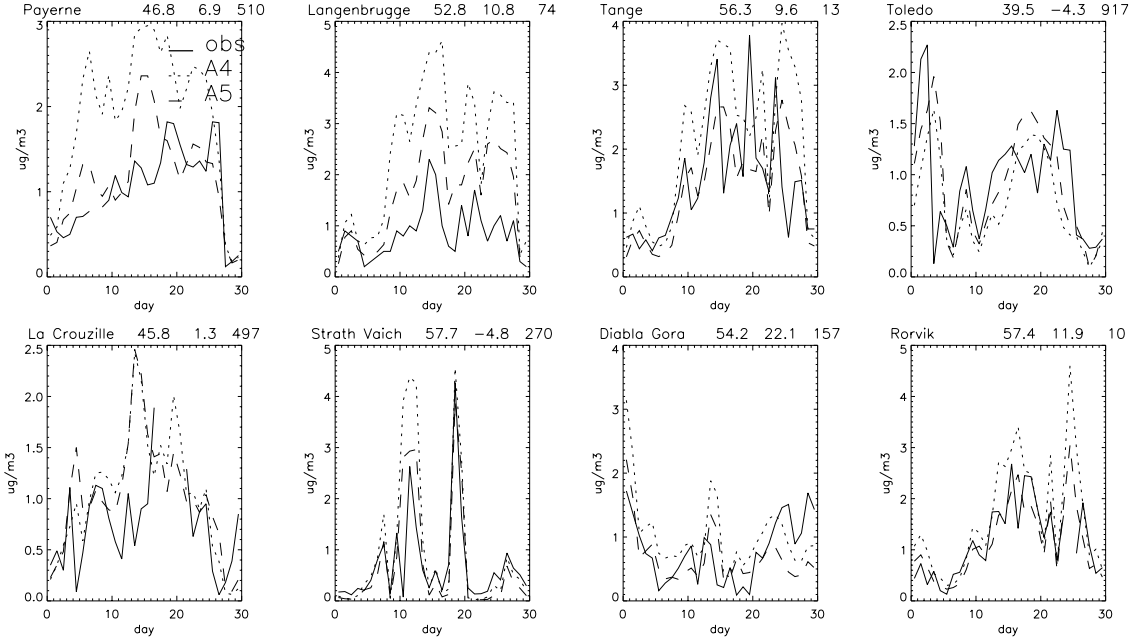

Figure 3.5

Comparison between model and EMEP measurements for NH_x for August 1997.

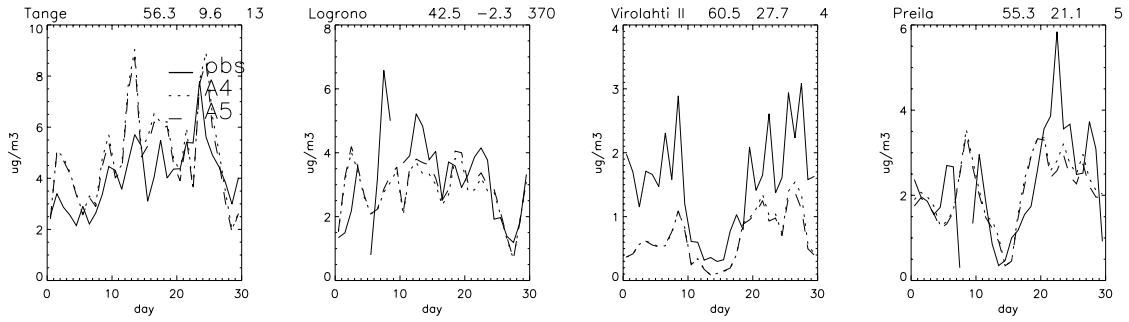

Finally we will focus on the day to day variability and daily cycle of SO_2 and the aerosol components represented by the model. For this purpose we use measurements from the EMEP network for August 1997 and measurements performed at the Dutch Energy Research Center (ECN) at Petten (53^{o}N, 5^{o}E) and at a few other measurement sites in the Netherlands from the "Landelijk Meetnet Luchtverontreiniging" . To be able to represent variability on time scales of a day or less, model simulations have been done at the, currently, highest possible resolution of TM3, which is 2.5^o by 2.5^o and 31 layers in the vertical. Model concentrations of SO_4, NO_3, NH_4, NH_3, SO_2 and HNO_3 have been saved every two hours at the locations of the measurement sites. This includes 6 sites for the Netherlands and additional 200 sites from the EMEP network. It must be noted that not all sites measured all species over the whole time period. Especially for NH_3 and NO_3 only a few measurements are available.

For SO_2 (not shown) in general, episodic peak values are reasonably well captured by both model simulations. However, the absolute values are in most cases much too high. At the eastern end of the European domain we obtain good agreement between model simulation A5 and the measurements. Over the British islands the model strongly overestimates the observations but there is a good correlation between model and measurements. Over central Europe observed concentrations are almost constantly very low, whereas the model simulations show rather high values. In general, model concentrations agree better with observations for the model simulation with the CORINAIR emissions. We also get the

impression that concentrations are most severely overestimated over the western European countries and that there is better agreement for Eastern and Northern European sites.

Table 3.1 Correlations and average differences observation-model (μg m^{-3}) based on daily averages for all available EMEP stations for August 1997. XNO_3 is the sum of NO_3 and HNO_3 and NH_x of NH_3 and NH_4.

		Correlation		*Average difference (O-M)*	
	N	**A4**	**A5**	**A4**	**A5**
SO_2	1868	0.36	0.39	-4.2±5.4	-2.7±4.3
SO_4	2059	0.56	0.58	-0.3±1.8	0.0±0.8
NH_x	956	0.66	0.66	-0.5±1.7	-0.4±1.7
XNO_3	884	0.60	0.61	-0.5±0.9	-0.5±0.9
NO_3	401	0.66	0.66	0.3±0.3	0.3±0.3

The average difference observation - model and the correlation between model and observation for all available EMEP measurements is shown in Table 3.1. Also these numbers clearly indicate that the agreement with observations becomes better when the CORINAIR emissions are used. The correlation between model and measurements improves considerably when using the CORINAIR emissions, but is with a value of 0.39 still rather low.

Figure 3.6
Monthly averaged mole fraction NO3/(SO4+NO3) for August 1997 at surface level.

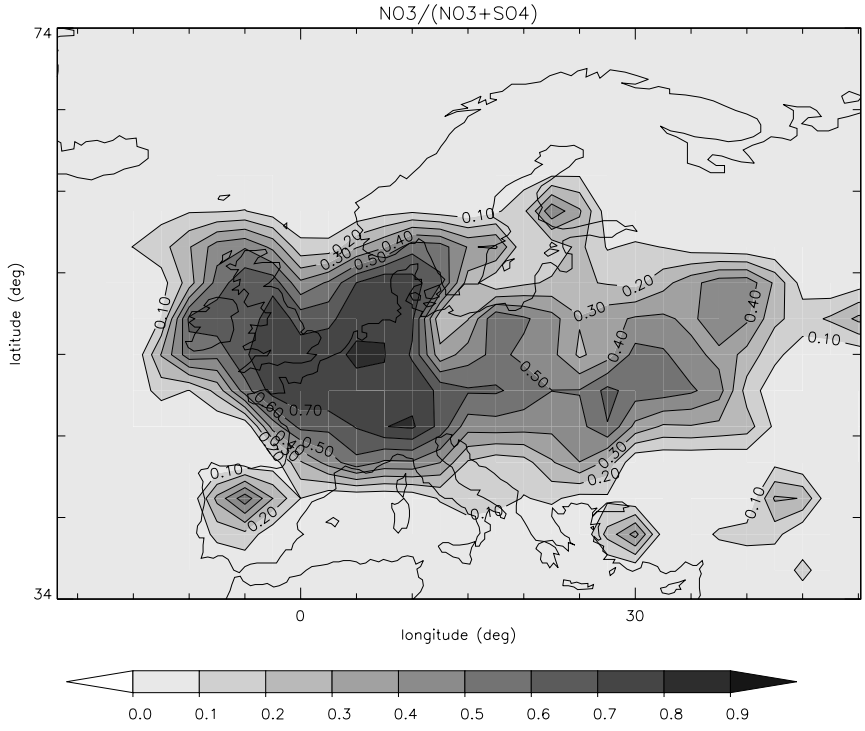

Agreement between model and observations is much better for sulphate, the reaction product of SO_2. As is shown in Figure 3.4, both model runs simulate the day to day variability as well as the absolute magnitude of the concentrations well. At the sites where SO_2 was overestimated by a factor 5 to 10 (e.g. Langenbrugge, Tange), sulphate is within 10 to 20% of the observations. Best agreement is clearly obtained with simulation A5. This is also confirmed by the improved statistics in Table 3.1.

Figure 3.6 shows that nitrate (in the model), may constitute a large fraction of the TM3 aerosol surface concentration (nitrate + sulphate) over large parts of Europe. In comparison with measurements of EMEP (not shown) modelled nitrate is in general too low at the surface. Nitrate is difficult to model since its

formation strongly depends on humidity, temperature and the concentrations of sulphate and ammonia. If the ammonia concentrations do not exceed the sulphate concentrations, no nitrate can partition to the aerosol. For Ispra in Italy, Kollummerwaard in the Netherlands and Leba in Poland, model values get close to the observations. At Liesek in Slowakia the model generates no particulate nitrate.

While, particulate nitrate is on average too low, the sum of nitrate plus nitric acid is too high compared to the observations at the 8 sites that measure the sum of these components. This indicates, that the availability of HNO_3 is not limiting the formation of nitrate aerosol.

The sum of ammonium and ammonia is measured at about 24 sites. Ammonium concentrations are strongly correlated with sulphate (e.g. Tange, Denmark). As was the case for sulphate, agreement between model and observations is very good (see also Table 3.1). Ammonia is a difficult component to model due to its short lifetime and heterogeneous sources. However based on this result, there seems to be no reason to doubt about the quality of the NH_3 emissions in TM3. The fraction ammonia in NH_x is on average 50% over the European continent at surface level. Co-located ammonia measurements would however be needed to find out about the fraction ammonia in measured NH_x.

Figure 3.7

Comparison between model and LML measurements for SO_2 for August 1997.

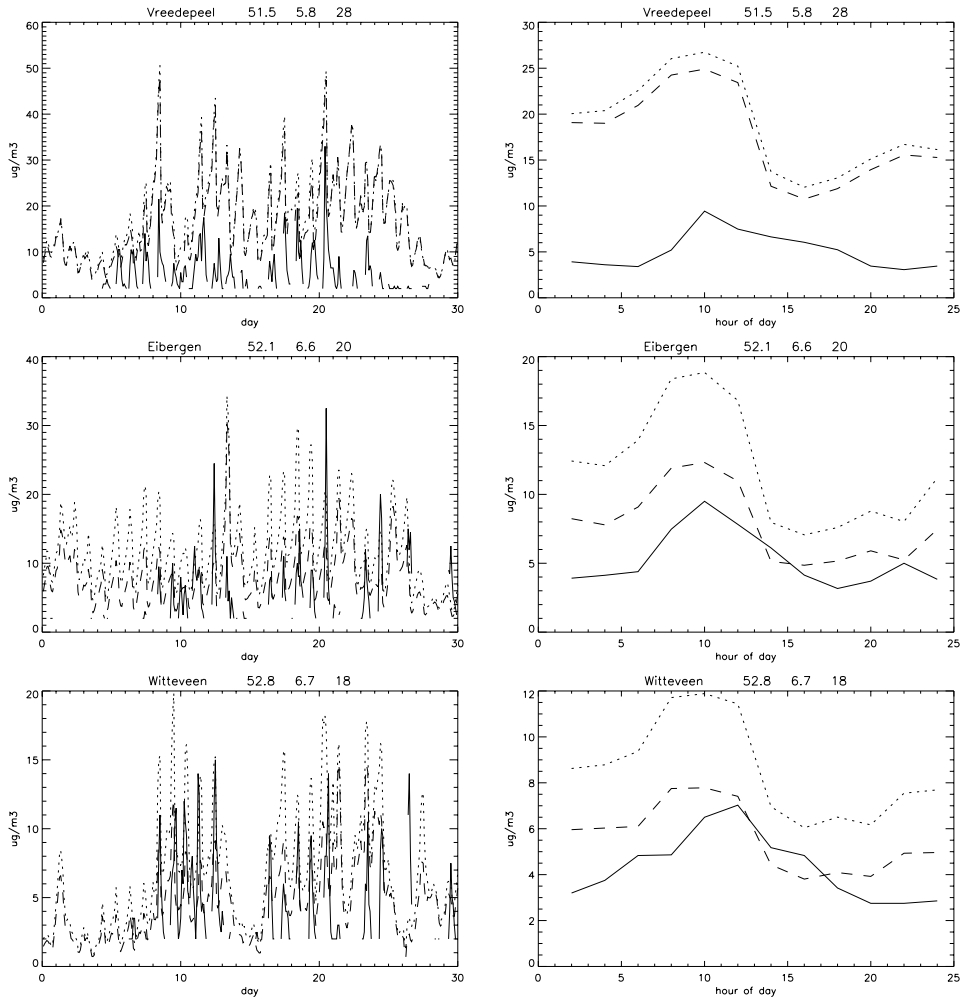

We also compared the simulated daily variability of sulphate, nitrate and SO_2 with sites in the Netherlands, for which we have a detailed set of measurements. Results are shown in Figure 3.7 to 3.9. Modelled SO_2 concentrations exhibit a similar daily cycle as radon (not shown) [Jeuken, 2000] with accumulation of SO_2 in the stable boundary layer during the night and a steady decrease during the day. The measurements however show a rather different diurnal cycle. Modelled radon concentrations agreed well with measurements indicating a good representation of the diurnal cycle in the boundary layer mixing. For SO_2 the situation is much more complicated. Therefore there is an indication, that there is a diurnal cycle in the emissions, which is not accounted for in the model.

Observational sites are usually at rural sites away from major sources and therefore advective transport processes rather than local vertical mixing determines the daily cycle in observed SO_2. In the model, however, the emissions are grid box averages. Nevertheless, the variability over the whole month is well captured by the model with both simulations generally overestimating the concentrations.

Sulphate does not show such a strong diurnal cycle (see Figure 3.9). However, the correlation between both model runs and the observations is high. Both simulations A4 and A5 underestimate the sulphate levels for Petten by 25 and 50% respectively. The episodic nature of elevated sulphate concentrations is well simulated by the model. The daily cycle of nitrate seems to be too strong in the model (see Figure 3.8). Especially in the afternoon nitrate concentrations are too low. Although there must be ammonia in excess in the Netherlands nitrate concentrations are about 50% underestimated.

The simulation of the day to day and diurnal variation of aerosol species provide a severe test for the model. Given the highly variable nature of aerosols and the limited resolution of the model (e.g. The Netherlands covers a little more than one grid cell only), model simulated aerosol concentrations agree surprisingly well with the measurements.

SO_2 is difficult to simulate by the model due to its short lifetime and strong dependence on emissions. Using the CORINAIR emissions instead of the EDGAR emissions results in a clear improvement of not only SO_2 but also of sulphate and ammonium. As was the case for the comparison of monthly averages also for August 1997 simulated SO_2 concentrations are too high even with reduced emissions. However, because of the ever-present emission sources within a coarse resolution grid cell, measurements that are usually performed at "regionally" remote sites might systematically underestimate the grid cell average.

Clearly more attention needs to be given to modelling and validation of SO_2 emissions.

Figure 3.8
Comparison between model and ECN measurements for NO_3 for August 1997.

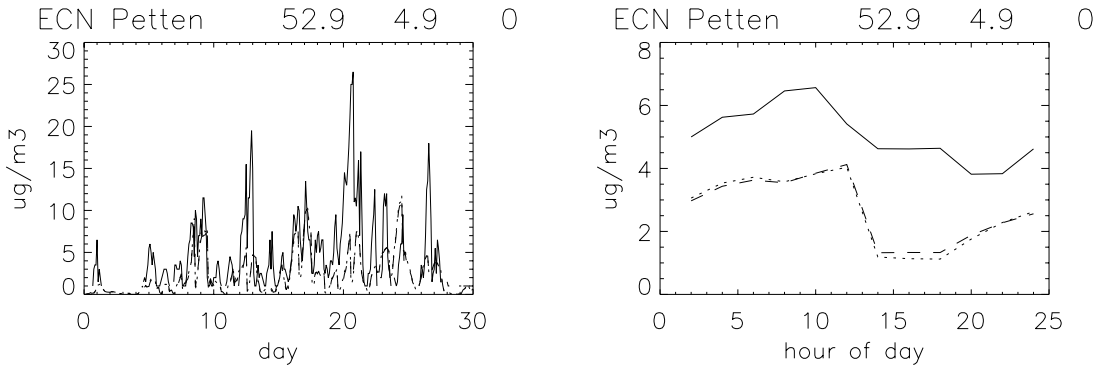

Figure 3.9
Comparison between model and ECN measurements for SO_4 for August 1997.

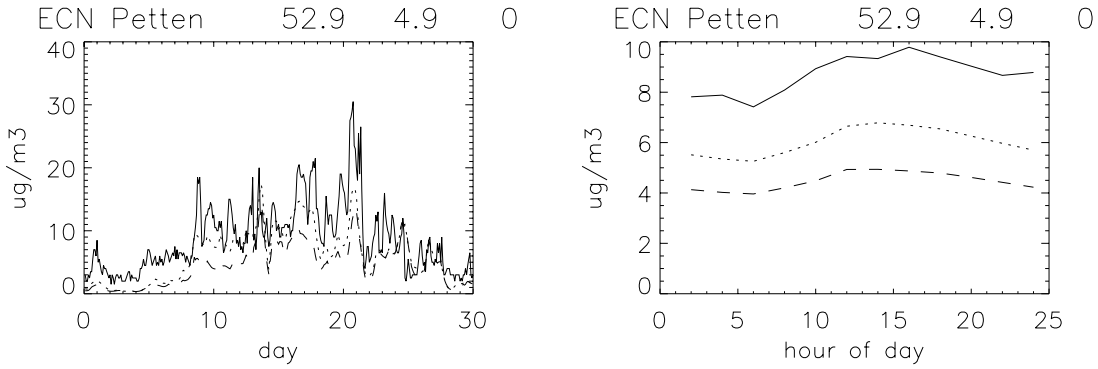

To derive the AOD of the sulphate/nitrate aerosol, assumptions are made on the aerosol size distribution. Other aerosol species, such as organic aerosols contribute significantly to the total AOD. Additional assumptions could be made to account for the contribution of these "missing" aerosol species.

Studies in the Netherlands in the 1980s and 1990s for instance showed that the contributions of sulfates and nitrates to aerosol scattering are comparable [ten Brink et al., 1996]. Large parts of the fine particle mass could not be identified, and were presumed to be carbonaceous material. Ten Brink et al. [1996] speculated that the contribution of sulphate to particle scattering was between 30 and 40%. This fraction which pertains to the Netherlands may be

significantly different elsewhere. A complication is that the optical properties of especially organic aerosols are not well known. We therefore ignore this unknown aerosol fraction from the calculation of the AOD and focus on spatial patterns in the AOD field.

Following the approach of Kiehl and Briegleb [1993], the AOD is expressed as:

$$AOD(\lambda) = f(RH,\lambda) \cdot \alpha_{SO4}(\lambda) \cdot B_{SO4+NO3}$$

where α_{SO4} is the mass extinction efficiency of ammonium-sulphate; i.e. extinction coefficient per unit of mass SO_4 at relative humidity < 40%;

$B_{SO4+NO3}$ is the column burden of ammonium sulphate and nitrate; and $f(RH,\lambda)$ is the relative increase of the scattering coefficient at given RH to the scattering at low (<40%) relative humidity. α_{SO4} and $f(RH,\lambda)$ depend on the aerosol size distribution and chemical composition of the particles. The aerosol size distribution was assumed to be lognormal, with a geometric mean radius of 0.05 μm and a geometric standard deviation of 2.0. The dry density of the particles was taken as 1.7 g cm^{-3}.

α_{SO4} was evaluated using a Mie code.

Using the above assumptions, the AOD by sulphate/nitrate aerosol at low RH is calculated from the model-predicted sulphate, nitrate and ammonium mass and the sulphate mass extinction efficiency. This implies that for nitrate aerosol the same mass extinction efficiency is assumed as for sulphate aerosol.

Most aerosol particles absorb water vapour when exposed to increasing RH. The particle growth results in more scattering by the aerosol particles, and consequently a higher AOD. To account for the increase of aerosol extinction with increasing RH, the factor $f(RH,\lambda)$ is used. This factor is the ratio between aerosol extinction at given RH to aerosol extinction at low RH (<40%). The increase of the scattering coefficient with increasing RH can be measured by humidity controlled nephelometry. Veefkind et al. [1996] have measured *f(RH)* in the Netherlands in November 1993, for days with a continental air mass. A polynomial fit to these experimental data is used to describe *f(RH)*. Mie calculations showed that the wavelength dependence of *f(RH)* can be ignored. To compute the humidity effect on the AOD in TM3 the polynomial fit is used together with 3-dimensional relative humidity fields, which are calculated every 6 hours based on ECMWF temperature and specific humidity fields.

Figure 3.10
Simulated timeseries of the AOD at Petten and Bilthoven for the months, which contain the selected measurement days for MEMORA.

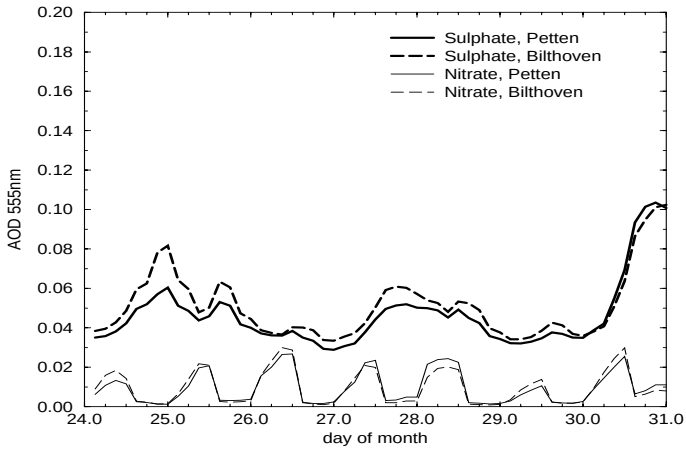

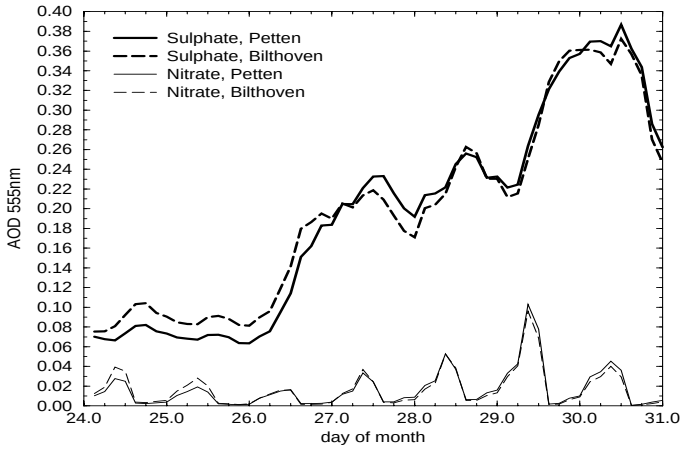

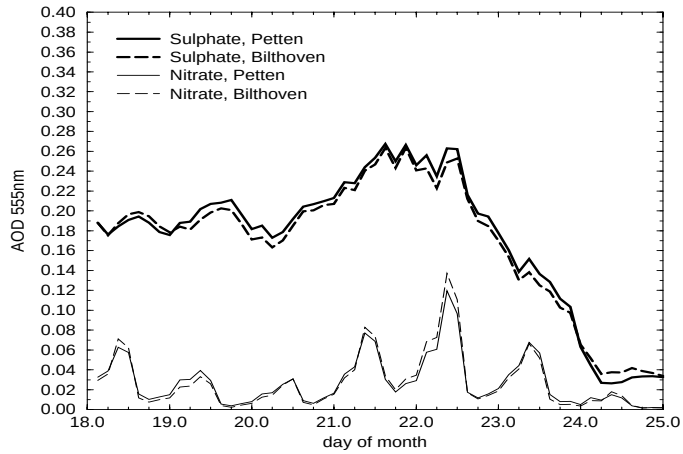

The calculation of the AOD is done every timestep (=40 minutes) online in TM3 for the spatial resolution of 2.5^{o} by 2.5^{o} and 31 levels used in this inter-comparison study. By using the derivative of the tracer mass field in all spatial directions, which is calculated and stored in the advection module of TM3, we output the model AOD on a higher resolution of 1.25^{o} by 1.25^{o}. Note that the higher resolution structures obtained in this way are a result of advective transport processes only.

Figure 3.10 shows the contributions to the aerosol optical depth of ammonium nitrate and sulphate respectively both for Bilthoven and Petten. There is a strong diurnal cycle in nitrate and due to its lower mass it contributes less to the AOD than sulphate.

In figure 3.11 a comparison between the AOD of the TM3 aerosol field with the AOD of ATSR-2 at 0.555 μm. For this purpose all available cloud free ATSR-2 pixels for August 1997 are combined into a monthly averaged composite field for Europe. Such a composite field presents a rather biased view of the monthly averaged aerosol field. For instance over England and Scotland the average consist of a few points in time only, while for other more sunny areas each overpass might be included. Figure 3.11 shows that model captures the main features observed by ATSR-2, like the maxima over the Po valley and the south of Italy, the Barcelona area, the maximum over the Netherlands and the urban areas along the Scandinavian coast. Especially noteworthy are the well-simulated peak values over England ,as they are an average of one or two overpasses only. Also the low AOD values over North Scandinavia is simulated well.
The variability in the satellite data is not quite reproduced by the model simulations. Of course it can not be expected that the small scale variability is resolved by the relatively coarse grid model, however at large scales also some important sources of aerosols seem to be missing, especially over Southern France, Spain, Eastern Europe and the Balkan. Possible explanation for these missing aerosol sources could be the production of large amounts of secondary organic aerosols resulting from biogenic and anthropogenic sources [Kanakidou et al., 2000]. This secondary production might be enhanced under photo-chemical smog conditions with

high ozone levels [Griffin et al., 1999]. For the South of Europe in addition dust aerosol originating from the Sahara or locally produced may play a role.

Figure 3.11
Composite (only data for cloud free pixels have been used) monthly averaged field of the AOD at 555nm for Europe August 1997. Upper panel is ATSR-2, lower panel is TM3 simulation A5.

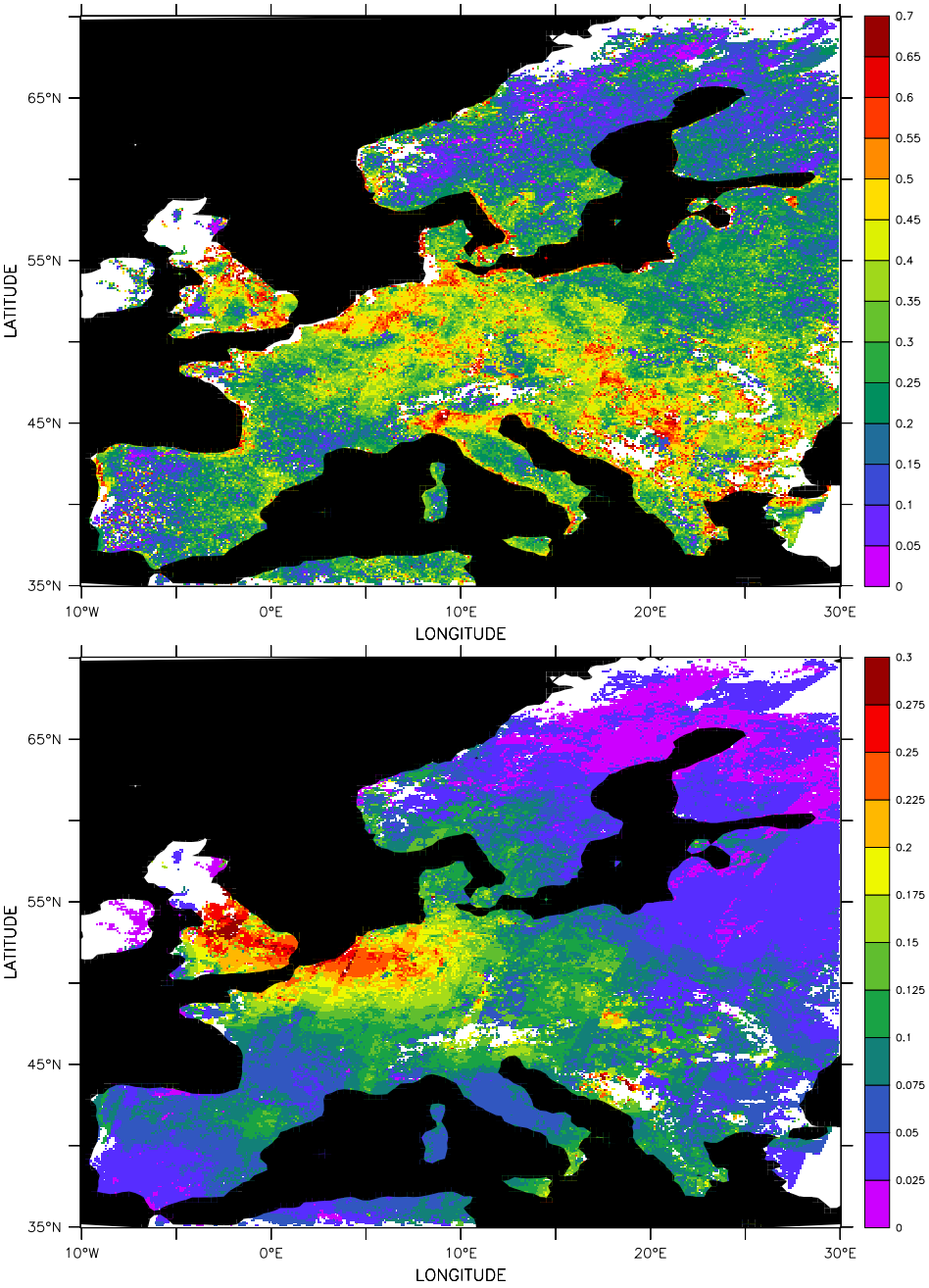

The model does not represent the narrow coloured borders at the land-sea boundaries that are clearly visible in the ATSR-2 image. Sea salt aerosol, which is also not simulated by the model, may explain this difference. Also the retrieval algorithm is expected to experience problems in simulating land sea changes.

On average there is a difference between model simulations and ATSR-2 in the AOD of 0.2. This is demonstrated in Figure 12, which shows the zonal and meridional averages of Figure 3.11. We simply added 0.2 to the model AOD values, which results in a surprisingly good agreement between model and satellite. The question is how this offset of 0.2 should be interpreted.

We should not forget that the TM3 model with its coarse resolution only simulates the water soluble aerosol species SO_4 and NO_3 and the complex mix of various other aerosol species is not included. The ATSR-2, on the other hand observes the whole aerosol burden. Particularly in the East-West direction the model simulations correlate well with the ATSR-2 AOD. The apparently constant offset suggests that the missing part in AOD is some sort of background aerosol, which is well mixed. However, the North-South gradient in AOD from 60^o to 70^oN is not so well simulated by the model. Apparently a constant offset of 0.2 is not appropriate for this part of Europe. Emission and formation of organic aerosol are temperature dependent processes. It seems therefore reasonable to assume that there is a North-South gradient in organic aerosol production. In addition desert dust influences over Europe strongly decrease from South to North. Also Figure 11 does not really support the suggestion of an additional well mixed layer.

3.1.4 Conclusions

Changes in vertical diffusion and precipitation scavenging were included in the tropospheric chemistry version of TM3. In addition the chemistry of sulfur and reduced nitrogen species and a thermodynamical equilibrium parameterisation, describing the partioning of ammonia and nitric acid between aerosol and gas phase, were added to TM3. With this model version various simulations were performed and model output was compared with measurements on different temporal and spatial scales. The main conclusion is that sulphate aerosol

distributions are well simulated by the model. Both the absolute magnitude and the seasonal and day to day variability agree well with observations. SO_2 emissions appeared to be the most uncertain factor in the modelling of the sulphur cycle. The sum of all emission in the CORINAIR data set for Europe is a factor two lower than that of the default data set in TM3. By applying this CORINAIR data set in TM3, SO_2 surface concentrations for August 1997 were reduced by almost a factor two but appeared to be still much too high. Therefore more attention should be directed towards more accurate estimates of emissions. However, too high SO_2 surface concentrations also seem to be a more fundamental problem in TM3 as well as in most global sulphur models. In winter, in addition this also leads to too low sulphate levels. Also based on the findings of the radon simulations, it is concluded that an increase in vertical mixing under stable conditions in combination with an extra oxidation mechanism would be the most likely solution to reduce the systematic overestimation of SO_2 [Jeuken, 2000]. With surface measurements alone, the complex mechanisms and feedbacks within the sulphur cycle can not be fully understood. A clear lack of profile measurements has been pointed out. These profiles are necessary to understand what is happening above the boundary layer where, according to the model and a few measured profiles, a major fraction of sulphate and SO_2 resides. It has been shown that with satellite measurements of the aerosol optical depth (AOD), patterns in the modelled aerosol column burden can be analysed. TM3 simulated aerosol patterns correlate well with the patterns observed by the ATSR-2 instrument. About 40% of the measured AOD could be explained by the aerosol and associated water simulated by the model. However, large uncertainties remain in the modelling and retrieval of the AOD. Additional aerosol species should be included in the model and the model and retrieval algorithm should use the same assumption about the optical properties of the aerosol. To understand discrepancies better, additionally profiles at representative locations should be measured.

References:

A. Jeuken, Ph.D. Thesis, Utrecht, May 2000; "Evaluation of chemistry and climate models using measurements and data assimilation.

The input of Swen Metzger (IMAU) and the co-operation with J. Pepijn Veefkind (FEL-TNO) is gratefully acknowledged

Figure 3.12
Composite zonally and monthly average for August 1997 for Europe (upper panel and meridian average (lower panel) for model runs A4 and A5 (+0.2) and ATSR-2.

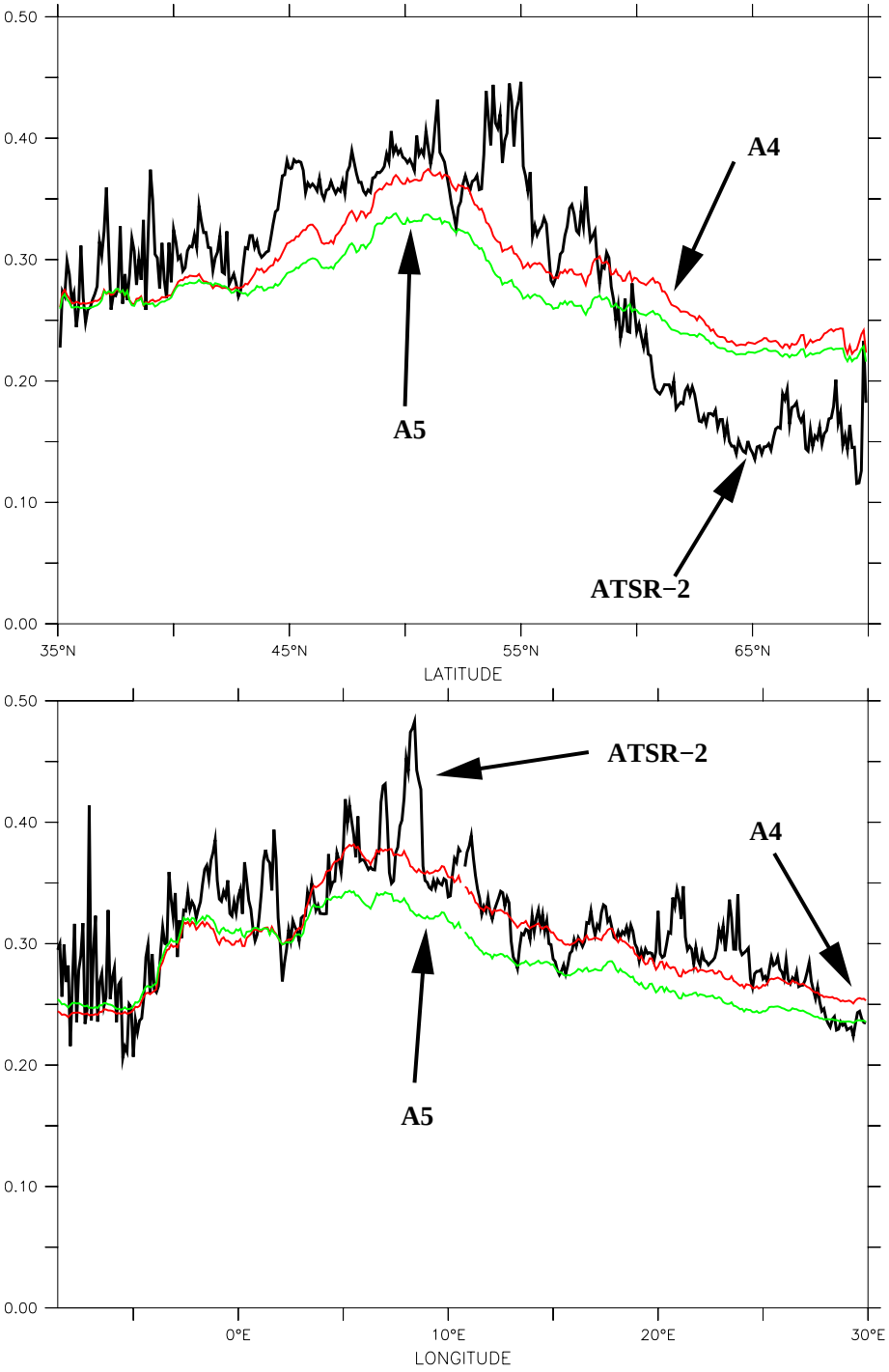

3.2 Aerosol formation mechanisms

Aerosol-cloud interactions and heterogeneous chemistry

A. van den Berg, J. Lelieveld; IMAU

3.2.1 Introduction

Clouds play an important role, both in the direct aerosol forcing, studied in this project and in the indirect effect. Aerosol particles act as cloud condensation nuclei (CCN). The number of available CCN regulates the number of cloud droplets and thus, indirectly, effects the radii of the cloud droplets, the albedo, the formation of precipitation and the lifetime of a cloud. Sulfate production in the cloud droplets will increase the aerosol mass and possibly alter the radiative properties of the aerosol particles after the cloud is evaporated and the aerosol particles are released into the atmosphere. Furthermore, rain-out and wash-out processes in and under the cloud will alter the aerosol number- and mass concentration.

The objective of this study is to develop parameterizations which describe the chemical change of aerosol particles in clouds and the aerosol-cloud interactions reasonably accurate with limited consumption of CPU time, so that they can be used in General Circulation Models. A boundary layer model (Duynkerke, 1987) is extended with a microphysics module, which describes the aerosol-cloud interactions, and a chemistry module, which describes the production of sulfate in both the liquid phase and the gas phase.

3.2.2 Approach

Aerosol-cloud interactions.

The cloud droplet spectrum is prescribed according to Cotton (1972) by a Gamma distribution function. Necessary input parameters are the width of the distribution function, the liquid water content and the activated aerosol concentration. The width of the distribution is prescribed and constant in time. The liquid water content is calculated diagnostically by the MBL model. The activated aerosol concentration is a function of the critical radius of the aerosol particle and the critical supersaturation in the cloud. Supersaturation is taken place at such a small scale (both temporal and spatial) that it is not resolved by the MBL model.

Therefore, two parameterizations are implemented, which can be switched on or off. In the first parameterization the supersaturation is prescribed and constant in time. In the second parameterization the cloud droplet number concentration (and thus the activated aerosol concentration) is a function of the sulfate mass (Boucher and Lohmann, 1995). Autoconversion-, accretion-, and selfcollection processes as parameterized by Beheng (1994) are implemented in the model. These processes influence not only the cloud droplet number concentration, the liquid water content and the radiative properties of the cloud, but also the aerosol number concentration. Furthermore, it is now possible to model the rain-out effect.

Gas phase chemistry

The standard CH_4-O_3 (photo-)chemistry and the DMS-SO_2-H_2SO_4 chemistry is implemented. The photolysis rates are a function of the actinic flux and calculated according to the model of Krol and van Weele (1997). Initial profiles of the gases are prescribed. For some gases (e.g. DMS, NH_3) emissions at the surface are prescribed as well. The CO_2, CO and CH_4 concentrations remain constant in time. The radical species are assumed to be instantaneously in chemical equilibrium with the gases. The vertical turbulent transfer is parameterized using the eddy diffusion coefficient from the meteorological model. Dry deposition is parameterized according to the scheme of Ganzeveld and Lelieveld (1995) and is a function of surface type and turbulent state of the boundary layer.

Liquid phase chemistry.

The S(iv)-H2O2-O3 chemistry is extended with CH4-O3 (photo-)chemistry. The CH4-O3 reaction scheme may significantly reduce the formation of HOx radicals in the gas phase by an enhanced breakdown of CH2O in the liquid phase. As a consequence, the gas phase SO2 oxidation by the OH radical may be reduced too. A monodisperse cloud is assumed in the liquid phase chemistry calculations. The cloud droplet radius being the geometric mean radius of the cloud droplet distribution. Transport between the gas- and liquid phase is based on the method of Schwartz (1986). The vertical turbulent transfer for the liquid phase is parameterized in the same way as for the gas phase. When a cloud droplet evaporates all the

dissolved gases and their ions are released to the gas phase. All the S(vi) produced by H2O2 and O3 remain on the aerosol particle where the droplet condensed on.

Aerosol chemistry.

Emphasis is put on the change in aerosol number- and mass concentration by aerosol-cloud interactions and by production of sulfate in the gas- and liquid phase. The aerosol distribution is assumed to be log-normally distributed with a fixed width parameter. Initial aerosol number- and mass concentrations are prescribed for each aerosol type (max 10 types). The vertical turbulent transfer is calculated in the same way as for the gases. Dry deposition of aerosols is parameterized according to Ganzeveld et al. (1998). All Svi formed in the liquid phase remain on the aerosol particle when the droplet evaporates. All Svi formed in the gas phase will condense immediately onto the aerosol particles. NH3 will react heterogeneously with aerosol particles to form NH4HSO4 or (NH4)2SO4 aerosol. The accommodation coefficient of this reaction is a function of the ratio of non-neutralized sulfate to total sulfate.

3.2.4 Results and discussion

The performance of the model has been tested against observations from ASTEX/MAGE and several sensitivity tests were performed, showing that. Preliminary results indicate good agreement with observations. S(vi) production in seasalt aerosols will be implemented in a future version of the model. It was found that this must have been the dominant route for formation of sulfate from sulfur dioxide in the NW-European region. The model was evaluated with data from field campaigns over the ocean, a situation which is the simplest to evaluate with such a highly complex model. Implementation of the module in the TM3 transport model for description of the formation of sulfate overt the European continent is foreseen.

References:

Beheng, K.D., 1994 A parameterization of warm cloud microphysical conversion processes. Atmospheric Research, 33, 193-206, 1994.

Boucher , O., and U. Lohmann, 1995 The sulfate-CCN-cloud albedo effect: A sensitivity study with two general circulation models. Tellus, 47B, 281-300, 1995.

Cotton, W.R., 1972 Numerical simulation of precipitation development in supercooled cumuli: Parts I and II. Monthly Weather Review, 100, 757-784, 1972.

Duynkerke, P.G., and A.G.M. Driedonks A model for the turbulent structure of the Stratocumulus-topped atmospheric boundary layer. Journal of the Atmospheric Sciences, 44 (1), 43-64, 1987.

Ganzeveld, L., and J. Lelieveld, 1995 Dry deposition parameterization in a chemistry general circulation model and its influence on the distribution of reactive trace gases. Journal of Geophysical Research, 100 (D10), 20999-21012, 1995.

Ganzeveld, L., J. Lelieveld, and G.J. Roelofs, 1998 A dry deposition parameterization for sulfur oxides in a chemistry and general circulation model. Journal of Geophysical Research, in press.

Krol, M.C., and M. Van Weele, 1997 Implications of variations in photodissociation rates for global tropospheric chemistry. Atmospheric Environment, 31 (9), 1257-1273, 1997.

Schwartz, S.E., 1986 Mass transport considerations pertinent to aqueous phase reactions of gases in liquid-water clouds. In: Chemistry of multiphase atmospheric systems. Jaeschke (ed.), Springer Verlag, Berlin, 415-471.

APPENDIX 1 PROJECT DESCRIPTION

Project abstract

The study is a combined experimental/modeling program in which "closure" is pursued between measured and calculated aerosol properties for an estimate of the direct radiative forcing of climate by anthropogenic aerosols in Western Europe, using the Netherlands as the reference site. In ***measuring-campaigns***, properties properties of the aerosol and vertical burden of the aerosol will be determined and radiation measurements will be performed; the amount of anthropogenic versus natural aerosol will be assessed. These data will provide a first measure of the local aerosol radiative forcing. An existing ***radiative transfer*** model will use the measured aerosol characteristics to calculate the reduction in solar radiative flux. The model results will be validated against the measured reduction in radiation. The new aerosol parameters must replace the outdated "GADS" aerosol used in climate models for our region. An ***aerosol-model*** will be developed which will use ***real-time*** meteorology and a detailed description of the aerosol life-***cycle***. The model will provide the origin of the anthropogenic aerosol in The Netherlands, with emphasis on the aerosol which is most effective in the interception of solar radiation. The model will be validated against the aerosol measurements.

A. RATIONALE

Anthropogenic aerosols reflect solar radiation and the resulting negative radiative forcing of climate (cooling tendency) is estimated to be larger than the longwave forcing by the greenhouse gases in Europe in a recent IPCC report [1, figure 12]. The IPCC-report gives as uncertainty in the global shortwave forcing by aerosol +-1.5 W.m^{-2}, a range of 3 W.m$^{-2.}$ This uncertainty range exceeds the magnitude of the enhanced longwave forcing by the greenhouse gases. Aerosols therefore present the single largest uncertainty factor in climate change over the industrial period. Of national interest is the fact that the aerosol forcing is of a ***local/regional*** *nature because of the limited residence time of aerosols in the atmosphere.*

Very recent own measurements [2] showed that the local instantaneous **reduction** of solar radiation in the Netherlands by anthropogenic aerosol is of order **-20** W.m^{-2}. The measurements

were a "closure" experiment, defined as a test of the consistency of directly measured reduction of radiation by anthropogenic aerosol and the reduction modeled/extrapolated on the basis of aerosol characterisation at the ground. Such closure tests are one of the central suggestions in a recent paper on the uncertainties in the radiative forcing by aerosol and the path to minimize these [3].

Empirical global models with which the aerosol forcing is estimated use **sulfate** as the representative anthropogenic aerosol species. However, measurements in NOP-1 show that **nitrate** together with **carbonaceous** material are **more important** for the light-scattering by aerosol in Western Europe. On the other hand, Global Circulation Models, such as ECHAM, use aerosol parameters which are far too general for a specific region. Furthermore "GADS" (the Global Aerosol Data Set) used in ECHAM does not discriminate between anthropogenic and natural aerosol. One of the aims of the present project is to provide aerosol-characteristics specific for the anthropogenic aerosol in the West-European region.

Sulfate, nitrate and most carbonaceous aerosol are not the result of direct emissions, and projection of future aerosol loadings and forcing must therefore be based on reliable modeling. Such a model will be developed, with emphasis on assessing the origin of the aerosol occurring in the Netherlands, where it is validated against the detailed aerosol measurements. An aerosol chemistry/transport-model is needed which extends on existing models, in the following sense. The existing models use monthly averaged aerosol fields and corresponding average values of the aerosol properties. However, actual aerosol-fields have orders of magnitude changes from day to day depending on synoptic conditions. The synoptic conditions most relevant for radiative forcing by anthropogenic aerosols at our latitude are at midday in summer under clear-skies and thus modeling and measurements should focus on these conditions.

Long-term aerosol data for generalisation are not available from existing networks, since these operate on a 24 hour basis whereas data for the relevant midday hours are required. These data will be obtained from a recently established station where aerosol measurements are made on a two-hour basis.

An appreciable fraction (as high as 50%) of the aerosols may be carbonaceous. Part of this carbonaceous material is soot, black carbon, of special importance since it absorbs rather than scatters light; its fraction thus requires quantification. The amount of non-absorbing

carbonaceous aerosol and its optical properties have not been studied in Western Europe. For this reason a start will be made to do so here.

Natural tropospheric aerosol does not exert a forcing effect since it is part of the natural global system. However, in order to assess the anthropogenic aerosol forcing the contribution of the natural aerosol must be quantified. The working hypothesis is that in Europe the natural aerosol is only a small fraction of the total aerosol and thus not significant. For Western Europe, with its long coast-line, the contribution of marine aerosol might be substantial and will be quantified.

Partial cloud cover is a problem in assessing the reflection of the anthropogenic aerosols in-between the clouds. It is as yet not possible to calculate this effect. We propose an empirical approach by making optimal use of radiation/cloud-cover data from NOP-2 project ***98*** ("Clouds and Radiation"). In exchange, the aerosol-data pertinent for cloud microphysics will be delivered to that project.

Note:

1. The aerosol transport model not only calculates the import of aerosol into Netherlands but can also quantify the export of "nitrogen"-species (in the form of ammonium sulfate and ammonium nitrate) which contribute to the eutrophication of the remote terrestrial biosphere.
2. Modelling of the important carbonaceous aerosol fraction will not be possible within the time-frame of the present project since first sufficient experimental data must have been gathered.

B. REFERENCES

[1] "Radiative Forcing of Climate Change". 1994 Report of the Scientific Assessment Working Group of IPCC. Summary for Policymakers.

[2] J.P. Veefkind, J.C.H. van der Hage and H.M. ten Brink "Scattering of solar radiation by aerosol in the Netherlands" manuscript accepted for Atmos. Research; based on: Master Thesis, J.P. Veefkind, June 1994, ECN-report R-94--013.

[3] J.E. Penner et al. "Quantifying and Minimizing Uncertainty of Climate Forcing by anthropogenic Aerosols" Bull. Americ. Meteorol. Soc. 75 (1994), 375 ef.

C. OBJECTIVES AND EXPECTED RESULTS/PRODUCTS

-Development of a detailed transport/chemistry model describing the sources, sinks and loadings of aerosol in Europe and surrounding areas, in combination with a radiative transfer model which will be validated by measurements.

-Quantification of the current direct radiative forcing of climate by anthropogenic aerosol in the Western European domain, approximately five times more accurate than the present estimates.

-As an interim result the reduction of solar radiation by anthropogenic aerosols in the Netherlands will have been assessed, to serve as a reference for Europe.

D. RELEVANCE AND USE

Science

The results of the project are to be incorporated in the ECHAM climate-model with which the total impact of manmade emissions in Europe on radiation/climate will be assessed.

The aerosol-characterisation will be used as a basis to assess the increase of cloud number and cloud optical density by manmade aerosols.

Measured aerosol characteristics and fields can be used in the quantification of the amount of UV-radiation intercepted by manmade aerosol in the Netherlands.

The improved knowledge of the aerosol-fields will be used in modeling studies of heterogeneous chemical reactions at the particle surfaces.

Policy

Quantification of the radiative forcing by the anthropogenic aerosol will allow a comparison of its importance as a perturbation of the radiation balance relative to that of the greenhouse gases

and appreciation of the effect of expected future emission changes of aerosols and aerosol precursors on the radiative budget.

The approach followed here will allow assessment of the aerosol forcing in regions in which aerosol concentrations are expected to drastically increase in the coming years, such as Southeastern-Asia.

The detailed model developed here will allow reliable assessment of the contribution of West-Europe to the global biosphere eutrophication by nitrate and ammonium-aerosol.

Interim results will be made available as soon as possible for coming new updates of the IPCC assessment.

D. INTERNATIONAL RELEVANCE

IPCC. Ten Brink and Lelieveld have contributed to chapter 3 "Aerosols" of the update of the IPCC-report which is currently under preparation; it is our intention that the interim-results of the present project will be used in coming updates.

European programmes: Glomac, Sindicate. The TM2 model is used for studies of the transport and chemistry of the troposphere and stratosphere. Addition of aerosols in the TM2 model will strongly improve the tropospheric chemistry scheme of the model.

IGAC. It has been agreed that we will provide our routine data on aerosol to the European Data Bank Center at Ispra on request.

ECHAM/GADS. The radiation module is part of ECHAM. It will implement the new GADS-aerosol of ECHAM.

ARM. There is an official cooperation with Brookhaven National Laboratory (one of the leading institutes in the "ARM"-Atmospheric Radiation Measurement program of the US-DoE) with exchange of data prior to publication.

E. OTHER PROGRAMS

European:

Glomac/Sindicate. Global chemistry and climate modeling using the TM2 and ECHAM models.

Project "Reduction of solar radiation in Europe by anthropogenic aerosol" will finish in February 1995. The institutes in Austria and Munich will continue activities in national programs and our cooperation will be continued on a bilateral basis.

National:

Relation to other projects in **NOP-2**:

Proposal **98**: "Clouds and radiation": Aerosols are the nuclei for clouds and thus determine their microstructure.

F. RELEVANT EXPERTISE

Ten Brink is program manager at ECN. He has over fifteen years of experience in atmospheric science. He is the coordinator of the cluster-project "The reduction of solar radiation in Europe by anthropogenic aerosol" in the Climate-Change Program of the European Union.

Key Publications

H.M. ten Brink. "Influence of anthropogenic aerosol on solar radiation in Europe". Proceedings of the Conference on Atmospheric Chemistry, Nashville TN, USA, January 1994, pg 42-46.

H.M. ten Brink J.F. van de Vate. "Sources of Aerosols in The Netherlands". in: Aerosols; Research, Risk Assessment and Control Strategies. S.D. Lee, T. Schneider et al. eds., Lewis Publ., Chelsea MI, USA (1986), pg 3 e.v.

J. Lelieveld and J. Heintzenberg. "Sulfate cooling effect on climate through in-cloud oxidation of anthropogenic SO_2". Science 258 (1992), 117-120.

R.J. Charlson and J. Lelieveld "Multiphase atmospheric chemistry: implications for climate". in: Global Atmospheric-Biospheric Chemistry, R.G. Prinn (ed.), Plenum Press, New York (1994), 57-69.

J.P.F. Fortuin, R. van Dorland, W.M.F. Wauben and H. Kelder. "Greenhouse effects of aircraft emissions as calculated by a radiative transfer model", Ann.Geophys., in press, 1994.

R. van Dorland. "A radiative-convective model study into the direct effects of aerosols" (in preparation). Presentation at the EGS conference, Grenoble, April 1994.

P.F.J. van Velthoven, W.M.F. Wauben, H. Kelder, I. Kohler, R. Sausen, F.Rohrer, and A.B. Kraus. "A comparative study of global 3-D transport of NOx emitted by aircraft", Proc. of the International Scientific Colloquium on the Impact of Emissions from Aircraft upon the Atmosphere, Koln,Germany, April 18-20, (1994), 174-179 (available from Deutsche Forschungsanstalt fur Luft- und Raumfahrt, DLR Mitteilung 94-06)

W.M.F. Wauben, P.F.J. van Velthoven, and H. Kelder. "Chemistry and transport of NOx aircraft emissions in a global 3-D chemical transportmodel". idem, pg 241-246.

G. LONG TERM STRATEGY OF THE INSTITUTES

ECN: active in aerosol research for over twenty years. ECN is the coordinator of a current EU-project on reduction of solar flux by aerosol. Manmade aerosols are mainly a product of energy

production and coming levels of manmade aerosol are a central subject in the energy scenarios generated at ECN as a support for energy policy.

KNMI: the national meteorological institute has long-time expertise in transport modeling and in radiation measurements and radiative transfer modeling. Long term policy includes assessment of the effect of global change of trace constituents on climate.

LUW: the Air Quality department has a long tradition in air pollution assessment. Its long-term policy includes studies of the effect of manmade atmospheric components on regional to global scales.

RIVM: in the Air Research Laboratory atmospheric processes are studied in both the troposphere using various measuring techniques and models. An important goal now and in the future is to understand the effects of changes in atmospheric parameters on the global environment.

H. RESEARCH PLAN

The project centers on quantification of the aerosol forcing at a site in the Netherlands which will serve as a reference point for the forcing by anthropogenic aerosol Europe. For this quantification, a combined set of activities will be undertaken in three subprojects. Central in the study is the concept of "closure", ***in which consistency of measured and modeled/extrapolated parameters is pursued. The closure experiments increase in complexity with time.***

First, the reduction in solar influx will be measured and compared to the reduction extrapolated from the scattering coefficient of the aerosol at ground level. Secondly, the transfer of solar radiation through the atmosphere will be calculated on the basis of measured aerosol characteristics. These detailed aerosol characteristics will be determined in measurement-campaigns. Finally, the origin of the anthropogenic aerosol during these campaigns days will be calculated with an aerosol model to be developed in the project.

The increase in complexity is shown in the time schedule.
In the first year measurements of the local optical properties of the aerosol as measured at ground level will be extrapolated to obtain a first good estimate of the local radiative forcing.
In the second year the radiative transfer module with the aerosol will be ready and aerosol characteristics as measured in the campaigns will be used to calculate the forcing. The model results will be compared with the measured forcing. Also the contribution of the natural aerosol on the reduction of the solar flux will be quantified. The forcing over longer time periods will be extrapolted from these findings.
A crude version of the aerosol-transport model is expected to be ready at the end of the second year allowing first calculations of the **aerosol burden** in the Netherlands to be compared with measured burdens in **year three**.
At the ***end of year two*** an ***evaluation*** will be made which could result in modifications of the research to be discussed with NOP. The project is thus divided into 2 phases of two years.

Phase 1

2 years

Measurements. size-distributions with mass, nitrate and sulfate; radiative flux;

Development of measurement of "carbon"

Radiative transfer calculations with parametrized aerosol

Assessment of amount of natural aerosol

Implementation and testing of regional "zoom" version of transport model

First modeling of aerosol chemistry

Evaluation:

Choice on method for speciation of carbonaceous aerosol.

Phase 2

2 years

Continuation measurements, similar to 1st phase

Comparison with other sites in Europe

Development speciation of "carbonaceous" aerosol

Radiative transfer calculations with measured aerosol characteristics

Modeling of aerosol sources, transport and sinks; comparison with measurements

The division of the project in subprojects with subproject leaders is as follows:

Subproject 1 *Measurements* (ECN, RIVM) Ten Brink

Three campaigns of two weeks of intensive measurements are planned in 1996 which will take place at the same location and time as those in another ***NOP-2 project.*** We will have a test-campaign in the summer of 1995. In 1997 and 1998 campaigns will focus on quantification of the carbonaceous aerosol. The number concentration, and hygroscopic properties of the aerosol will be measured. Also the (spectrally resolved) solar flux and the reduction of radiation will be determined. The composition of the aerosol as a function of size will be measured with special impactors by the University of Vienna (prof. Berner). Nitrate in the West-European atmosphere is present as ammonium nitrate, which is semi-volatile. It requires the development of special techniques for representative size-classified sampling and preservation of the samples.

RIVM will provide height and vertical profile of the aerosol for the days of the campaigns from the existing (1064 nm) LIDAR-instrument. These data will be used in the comparison of the extinction of the solar radiation as extrapolated from the ground-level measurements and the measured extinction ("column closure").

The fraction of the aerosol that is assumed to be ***carbonaceous*** will be quantified and a start will be made to speciate it as far as it is relevant for the radiative properties of the aerosol. Its refractive index and the amount of light-absorption by soot will be quantified in the second phase of the project. Also the hygroscopicity of the carbonaceous material will be investigated then.

The two-hour measurements of the "dry" aerosol light-scattering and the concentration of sulfate and nitrate will be continued for the period of the project. These are performed at a site in the NW of the Netherlands (Schagerbrug). Sulfate and nitrate are measured with novel "thermodenuders". Quality of the data is assured by continuous attention and calibration of the

instruments with the appropriate procedures. The data provide the average correlation between optical and compositional properties of the aerosol. During the campaigns the relation between light-scattering at the reference low relative humidity ("dry") and the ambient relative humidity will be assessed.

The contribution of the (natural) marine aerosol to the light-scattering in the Netherlands will be deduced from existing ECN-data on composition/size of the seasalt aerosol using sodium (chloride) and magnesium as the reference elements. The size-distribution of these elements will also be measured during the projected campaigns. The continuous measurements of the light-scattering at the measuring station will provide the longer-term average of the aerosol extinction in marine air.

NOTE: The measuring ***campaigns*** in 1996 will be at the same location and time as that in another ***project in NOP-2***: ***98*** "Clouds (and Radiation)". Data will be exchanged within six months after the campaigns.

Data provided by our "Aerosol" project are:

To "Clouds": Number concentrations, size/composition

Data to be obtained:

From "Clouds": radiation/cloud-cover during partial overcast

Subproject 2 *Radiation modeling* (KNMI) Van Dorland

Objectives and activities

In order to quantify regional (and global) climate forcing by anthropogenic aerosol particles, we aim to utilize the ECHAM (MPI, Hamburg) radiation scheme as an off-line model. In this scheme, which has been based on the Morcrette radiation code (ECMWF), extensions have been made for several trace gases and aerosol components. The optical parameters of 11 aerosol components within each of the 2 shortwave and 6 longwave frequency intervals have been obtained from Mie calculations in 60 wavelength regions, assuming fixed size distributions. For computational efficiency the relative humidity or deliquescence has also been fixed. The optical

parameters like extinction, single scattering albedo and factor of asymmetry of the anthropogenic sulphur species have been incorporated in the radiation model. For the nitrogen species, which seems to be of particular interest in the European and regions, a new parameterization has to be developed.

Aerosol fields computed with the regional "zoom" version of the global transport/chemistry model TM2 enables us to compare the model's shortwave surface fluxes with in-situ measurements. This tool, among others Lidar measurements (RIVM), can be used for validating the transport model and for estimating the aerosol optical depth in the free troposphere as well. By partitioning the aerosol optical depth in natural/background and anthropogenic, future projections can be made for sulphur and nitrogen species. With the help of the ECHAM radiative transfer model an estimate of the climate forcing can be obtained.

Rationale

As the result of the geographical distribution of aerosol emissions and the relatively short residence time as compared to the greenhouse gases, strong variations exist in the atmospheric aerosol densities. Even when considering the annual average, the anthropogenic aerosol loading is unequally distributed over the globe. In addition, direct climate forcing of sulphur and nitrogen species is strongly dependent on a variety of parameters such as cloud fraction, surface albedo, solar insolation and solar zenith angle. As a consequence of enhanced backscattering, anthropogenic aerosols act to cool the climate system directly, thereby reducing the greenhouse effect due to trends in trace gas concentrations.

As gradients in direct radiative forcing due to the geographical distribution of anthropogenic aerosol loading influence the climate feedbacks, it is necessary to assess the causes and effects of the regional climate forcing due to sulphur and nitrogen species.

Subproject 3 ***Modeling of the aerosol-cycle*** (LUW,KNMI) Lelieveld

Objectives and transport-model

We intend to assess the contributions of Dutch and West-European anthropogenic SO_2, NOx and NH_3 emissions to aerosol formation on regional and global scales. The main objective is to quantify the processes that control aerosol abundances in western Europe by including

descriptions of these processes into a regional model that is nested within a global model of the troposphere. The model is the global transport/chemistry model TM2 that has been developed at the Max-Planck-Institutes for Meteorology (Hamburg) and Chemistry (Mainz), and that has been adopted and further developed by the LUW and the KNMI. Special emphasis will be devoted to the role of clouds in the formation, processing and removal of aerosol species. Realistic representation of in-cloud oxidation of sulphur dioxide into sulphate will be pursued.

The horizontal resolution of the global model is 10x8 degrees, which will be used to provide the boundary conditions for the regional model of western Europe, which has a 1x1 degree grid resolution. The global and the regional "zoom" versions of the model use ECMWF analyzed meteorology, made available by the KNMI, to simulate tracer transports. The current ECWMF model has T213 resolution (of the order of 50 km) and in the preprocessing phase for the TM2 model subgrid scale parameters, like eg. convective mass fluxes, are computed at this fine horizontal resolution and subsequently averaged over the cells of the TM2 model. Meteorological input parameters are available only every 6 hours , but the time-step for dynamics in the TM2 model is much smaller and depends upon the resolution since the Courant-Friedrichsen-Levy-criterion needs to be satisfied.

Validation of the model will be performed by comparing its results with available measurements of aerosols and chemical composition of precipitation (e.g., from EMEP) and measurements from other ground based monitoring stations. A main objective is to pursue "closure" between modeled physicochemical and optical aerosol properties and detailed measurements of these quantities at ECN. This means that model results of one grid cell (location Petten and environment) will be extensively analyzed, e.g., looking at diurnal and seasonal variations, on the basis of high quality measurements on this location. Ultimately, the model will be used to evaluate emission control scenarios. The coupling of the model to a radiative transfer model will, in addition, enable assessment of the climate forcing that result from emission changes.

Sources, sinks and physicochemical processes

Trace gas source inventories of sulfur and nitrogen species will be adopted from the EDGAR project, which has been carried out within the NOP-I program. The relevant processes that control aerosol size distributions and their chemical compositions include chemical transformations, aerosol nucleation, coagulation, "cloud processing" and wet and dry deposition processes. We will develop model parameterizations as much as possible based on first principles, i.e., we aim to explicitly describe these processes in the regional model rather than to prescribe empirical relations based on measurements, which has been common practice in the past. The initial and boundary conditions for the model will be based on the Global Aerosol Data Set (GADS) that has been developed at the Max-Planck-Institute for Meteorology in Hamburg. In the second phase the aerosol-set as determined in subproject 1 will replace the GADS aerosol. Once the aerosol physico-chemical properties are described satisfactorily, as based on comparison of the results with measurements, the model will be coupled to the radiative transfer scheme to assess direct aerosol climate forcing by anthropogenic emissions in The Netherlands. These modeling tasks will be performed in a collaboration between LUW and KNMI, in which the LUW focuses on chemical and aerosol processes and the KNMI on transport and cloud processes.

APPENDIX 2 LIST OF REVIEWED PUBLICATIONS AND PAPERS IN PREPARATION

In this list are the three PhD theses prepared in the course of this project.

H.M. ten Brink, C. Kruisz, G.P.A. Kos and A. Berner "Size/composition of the light-scattering aerosol in the Netherlands". *Atmos. Environ.* **31**, 3955-3962.

Van Dorland, R., F.J. Dentener, and J. Lelieveld: "Radiative forcing due to tropospheric ozone and sulfate aerosols". *J. Geophys. Res., 102*, 28079-28100, 1997.

Van Dorland, R., Radiation and Climate: from radiative transfer modeling to global temperature response, *thesis,* 148 pp, ISBN 90-646-4032-7, 1999.

A. Jeuken, Ph.D. Thesis, Utrecht, May 2000; "Evaluation of chemistry and climate models using measuremtns and data assimilation.

Pauline G. Dougle, J. Pepijn Veefkind and Harry M. ten Brink*): "Crystallisation of mixtures of ammonium nitrate, ammonium sulfate and soot". *J. Aerosol Sci.* **29**, 375-386

E. Visser, A. Apituley, J.B. Bergwerff, J.A. Bordewijk, H.M. ten Brink, A.C.A.P. van Lammeren, H.A.J.M. Reinen and D.P.J. Swart 1996: "RIVM's automated lidar system for climate research". In: 'proc. EOS/SPIE Eueopean Symposium for Environmental and Public Safety' SPIE, volume 2505, 21-28.

A. Apituley, E.P. Visser, J.B. Bergwerff, J.M. de Winter, H. de Backer and M.A.F. Allaart, “RIVM Tropospheric Ozone LIDAR Routine Measurements, Validation and Analysis”. In: "Advances in Atmospheric Remote Sensing with Lidar", A. Ansmann, R. Neuber, P. Rairoux and U. Wandinger(eds.), pp. 375--378, Springer-Verlag, Berlin, 1997.

Khlystov, A., Thesis, Wageningen University. March 1998.

Khlystov , A., P. Dougle, R. Otjes, P. Jongejan, A. Waijers-IJpelaan and H.M. ten Brink: "Comparison of four techniques for measurement of aerosol ammonium nitrate content". *J. Aerosol Sci.* **29**, S151-152.

A. Even, A. Khlystov and H.M. ten Brink: "Performance of two ambient carbon particulate monitors in background air". *J. Aerosol Sci.* **29**, S873-S874.

H.M. ten Brink, C. Kruisz, A. Khlystov and A. Berner "Size of the light-scattering aerosol in the Netherlands". In: 'proceedings Eurotrac Symposium' Garmisch-Partenkirchen Germany, March 1996; P. Borrell et al. eds., Springer.

ten Brink, H.M., J.P. Veefkind, A. Waijers-IJpenlaan, and J.C. van der Hage: "Aerosol light-scattering in the Netherlands". *Atmos. Environ.*, **30**, 4251-4261.

Harry ten Brink, Anita Waijers-IJpelaan and Sjaak Slanina: "Performance of an automated thermodenuder for ammonium nitrate measurements". *J. Aerosol Sci.* **29**, S633-S634.

Harry M. ten Brink and Arjan Hensen: "Light-scattering data relevant for aerosol radiative forcing". *Aerosol Sci.* **29**, S675-S676.

J.P. Veefkind, J.C.H. van der Hage and H.M. ten Brink 1996 "Nephelometry-derived and measured optical depth of the boundary layer". *Atmos. Research.* **41**, 217-228.

Rangasayi N. Halthore, Stephen E. Schwartz, Joseph J. Michalski, Gail P. Anderson, Richard A. Ferrare, Brent N. Holben and Harry M. Ten Brink. "Comparison of model estimated and measured Direct-Normal Solar Irradiance". *J. Geophysical Res* (1997) **102**, 29991-3002

B.G. Arends, J.H. Baard and H.M. ten Brink 1996: “Trends in summer sulphate in Europe”. *Atmos. Environ.* **31**, 4063-4072

J. Slanina, H.M. ten Brink and Yuhua Bai: “The analysis of ‘bulk-elements in aerosols; an underdeveloped area”. In: Measurements and modelling in environmental pollution, R. San Jose and C.A. Brebbia eds, CMP publish. Boston USA, 343-357.

A. Khlystov, A. Even and H.M. ten Brink: "Effect of temperature, ammonia concentration and flow rate on under-sizing of ammonium nitrate aerosol in DMPS/SMPS". *J. Aerosol Sci.* **28**, S59-S60.

Mikuska P., A. Even, A. Khlystov, H.M. ten Brink and J. Slanina: “Artifact-free method for size-resolved chemical analysis of ambient aerosols”. *J. Aerosol Sci.,* **28**, S443-S444.

Mikuska P., A. Khlystov, H.M. ten Brink and J. Slanina: “A system for on-line chemical analysis of aerosol species”. *J. Aerosol Sci.,* **28**, S445-S446.

B.G. Arends, J.H. Baard and H.M. ten Brink 1997: “Trends in summer sulphate in NW-Europe”. *J. Aerosol Sci.* **28**, S119-120.

H.M. ten Brink 1996: "Reduction of solar radiation by aerosols in Europe". *Change* **30**, 13-14.

H.M. ten Brink 1997: "Antropogene aërosolen en de stralingsbalans van de aarde". *LUCHT* **13**, 121-125 (in Dutch; English abstract pg. 132)

H.M. ten Brink and A. Khlystov 1997: "Aersosol particles have a non-linear effect on climate". *Change* **38**, 11-13.

H.M. ten Brink and A. Even: *Hysteresis in the water uptake by real and simulated ambient aerosol particles.* Invited lecture at the annual meeting of the American Geophysical Union, 11-15 December 1999; abstract in December volume of *EOS*.

APPENDIX 3 RELATION WITH OTHER PROJECTS AND PROGRAMS

IGBP

Within this international framework for cooperative studies in two subprograms aersosl feature as key compnenets:

IGAC

Within IGAC several campaigns have been performed in scientists of MEMORA participated.

ACE-2

Two of the groups were present as participants in this large aerosol-radiation closure experiment off the coast of Africa over the Atlantic Ocean. Data from this program provide background values for the aerosol and radiation interception on the mainland. The measuring campaign was in the summer of 1997.

ACE-3

Planing meetings in 1997 and 1998 were attended by the coordinator of MEMORA

There is a new IGBP-Focus on Aerosol. We participate in DARF: Direct Aerosol Radiative Forcing.

ARM

There is an official co-operation with Brookhaven National Laboratory (one of the leading institutes in "ARM"-Atmospheric Radiation Measurement program of the US-DoE). As shown above, this led to a joint publication.

ECHAM/GADS.

The radiation module is part of ECHAM.

GERMANY

The AFS-group (Aerosol Forschungs Schwerpunkt) performed a concerted clear air closure experiment in Berlin in the summer of 1998, LACE. The coordinator of MEMORA was consultant for this effort.

NATIONAL RESEARCH

Partial cloud cover is a problem in assessing the reflection of the anthropogenic aerosols in-between the clouds. It is as yet not possible to calculate this effect. We make use of radiation/cloud-cover data and expertise from the NOP-2 project ("Clouds and Radiation"). Aerosol-data pertinent for cloud microphysics were delivered to that project.

Aerosol characteristics for relevant days were provided to those quantifying the amount of UV-radiation intercepted by (manmade) aerosol in the Netherlands and there was direct co-operation with scenitists working in the framework of the national research (BCRS and SRON) on satellite retrieval of aerosol, as indicated in the text.

APPENDIX 4 PRESENTATIONS AT INTERNATIONAL CONFERENCES

Annual European Aerosol Conference:
1995 1996 1997 2000.

5th International Aerosol Conference:
1998.

Annual American Aerosol Meeting:
1995 1997 2000.

AGU fall meeting Invited lecture
1999.

Eurotrac Symposium:
1996 1998 2000.

IGAC Symposium:
1999.

Of the mentioned presentations extended abstracts are available; these are documented in the reference list in appendix 2.